REMARKS

In the action, the examiner rejected claims 17-18 and 58-62 under 35 USC §112, first paragraph, as assertedly lacking written description; and rejected claims 17-19, 21 and 58-62 under 35 U.S.C. §103(a) as obvious in view of Pardridge (*Nature Rev. Drug Disc.* 1:131-39, 2002, hereinafter "Pardridge"), in view of Fillebeen, (*J Biol Chem*, 274:7011-17, 1999, hereinafter "Fillebeen"), Neels et al. (*J Biol Chem* 274:31305-311, 1999, hereinafter "Neels") and Saenko, WO00/71714, (hereinafter "Saenko"). Reconsideration is requested in view of the amendments and arguments herein.

I. Support for the Amendment to the Claims

Support for the new claims 63 and 64 is found throughout the application. For example, page 8, lines 2-6, discloses that a RAP polypeptide for use in the method is contemplated to be at least 85% or at least 90% identical to the native RAP sequence or a fragment thereof.

II. The rejection of claims 17-18 and 58-62 under 35 U.S.C. §112, first paragraph, as lacking written description should be withdrawn

The Examiner rejected claims 17-18 and 58-62 as allegedly lacking written description on the basis that the disclosure does not adequately support the scope of the fragments recited in the claims, i.e, RAP polypeptides at least 80% identical to residues 221-323 of SEQ ID NO: 1. The Examiner asserts that the claims are not described because Applicant has not shown actual reduction to practice variants at lest 80% identical to residues 221-323 of SEQ ID NO: 1. Applicants respectfully disagree.

A written description rejection of method claims is not appropriate where a primary argument with respect to patentability is the process step. Applicants are not claiming to have been the first to discover RAP; rather, Applicants are claiming a novel method of using a specific portion of RAP that has unexpected properties. The present case is thus analogous to Example 16 of the Written Description Guidelines published March 25, 2008, which concludes that there is written description of a broad process claim where novelty resides in the process step.

Nevertheless, written description is satisfied even if the conjugates are considered *per se* without reference to the method. The test for determining compliance with the written

description requirement is whether the disclosure of the application as originally filed reasonably conveys to the artisan that the inventor has possession at the time of the later claimed subject matter. See Chiron v Genentech, 363 F3d 1247 (Fed Cir 2004) and In re Alton, 76 F.3d 1168, 1172 (Fed. Cir. 1996). Additionally, written description for each of the new claims must be considered separately. The Examiner himself states that written description may be demonstrated by actual reduction to practice, description of complete of partial structure and identifying characteristics (page 3 of the Action). Applicants submit that the application describes a compete or partial structure of the polypeptide recited in the claims and discloses identifying characteristics, thereby demonstrating to one of ordinary skill that the inventor was in possession of the invention.

The Examiner cites Example 11 of the Written Description Guidelines published March 25, 2008, (hereinafter "the Guidelines") (Submitted herewith as Exhibit A), as evidence of the alleged lack of written description of the claims in the specification. Example 11 relates to claims for a polynucleotide encoding a polypeptide having a recited percent identity to a known polypeptide sequence, further wherein the polypeptide has a recited activity. Example 11A discusses a claim for a polynucleotide encoding a polypeptide having 85% identity to a polypeptide and having a recited activity. The *polypeptide in Example 11A has no known sequence identity to any other polypeptide or polypeptide family*. The Guidelines state that one of ordinary skill can readily obtain sequences that are 85% identical to the known sequence due to the high level of skill in the art, but states that because there is no known correlation between the structure of the polypeptide sequence and its function there is no written description for a polypeptide having 85% identity to the identified polypeptide and having a recited activity. The Examiner asserts that the present situation is analogous to Example 11A and therefore the claim lacks written description in the specification.

Applicants submit that the claims are akin to Example 11B in the Guidelines. Example 11B relates to a polynucleotide encoding a polypeptide *at least 85% identical to a known polypeptide sequence and having a recited activity*. In this Example, the specification does not disclose which of the nucleic acid (or amino acid) residues that encode a polypeptide having 85% identity to the known sequence can be changed and the polypeptide still retain the stated activity Y. The specification in the Example identifies two domains of the polypeptide responsible for activity Y, i.e., a binding domain and a catalytic domain. In the Example, the

specification states that it is expected that a polypeptide having a conservative substitution should retain the stated activity, but the Example goes on to note that "all conservative substitutions in these domains will not necessarily result in a protein having activity Y, but one of ordinary skill in the art would expect that many of these conservative substitution s would result in a protein having the required activity." Based on this analysis, the Guidelines consider that there is an adequate structure-function correlation since particular domains of the polypeptide are disclosed in the specification, and those of ordinary skill would conclude that the applicant would have been in possession of the claimed genus of polynucleotides and polypeptides. Thus, the claims directed to a polynucleotide encoding a polypeptide having at least 85% identity to a known sequence and retaining a recited activity is adequately described.

Similar to Example 11B of the Guidelines, the claims are directed to a method of using a polypeptide having a recited % identity to a known polypeptide sequence and having a domain with a particular function. It so happens that in the present case, the polypeptide recited in claims 17-19 is the activity domain and not part of a larger polypeptide as exemplified in Example 11B, i.e., the polypeptide recited in the claim (a polypeptide sequence at least 80% identical to acids 221-323 of RAP) is equivalent to the binding domain as described in Example 11B. The fact that the polypeptide in the claims is the functional domain and not a larger polypeptide having a functional domain should not, however, alter the treatment of a "polypeptide" with a known activity discussed in Example 11B.

The Examiner, however, appears to be requiring Applicants to describe more than what is recited in the Written Description Guidelines by necessitating knowledge of the amino acid sequence of subdomains or residues of activity within the already identified functional domain. Example 11B states that because the polypeptide activity and knowledge of the structure of the catalytic and binding domains are correlated, one of ordinary skill could determine if a variant of the catalytic and/or binding domain in Example 11B could maintain polypeptide activity. The Applicants in Example 11 of the Guidelines were not required to determine which residues within the catalytic or binding domain are actually responsible for catalytic activity, it was sufficient to know that the domains were responsible for the activity and have available methods to determine if a variant maintained the required activity. Similarly, in the present case, the d3 domain of RAP is associated with receptor binding function, thereby establishing the required structure-function correlation, as evidence by the art (see below), and

therefore one of ordinary skill can readily determine if variants of this domain maintain activity, such as receptor binding. The polypeptide in the claims is a variant of the d3 domain and Applicants have adequately described the full structure of the RAP polypeptide and one of ordinary skill can readily determine the structure of the variants based on the high level of skill in the art. Applicants should not be required by the Examiner to further divide and define the domain with known function into subdomains with more discrete function when the Guidelines make no requirement to this effect.

As noted above, the structural features of the fragments recited in the claims, i.e., the 102 amino acid sequence of residues 221-323 of RAP, are known, the function that correlates to this sequence is known, and therefore a polypeptide having a particular percent identity to the sequence are known and effectively disclosed in the specification. The Guidelines state that it is well within the ability of one of ordinary skill to take the amino acid sequence of SEQ ID NO: 1 and envisage the chemical structure of any polypeptide having a recited percent identity, e.g., 80%, to the polypeptide. Methods for manipulating the genetic code are well-known in the art and described in the specification (see page 50, line 1, to page 52, line 27). Thus, based on the description in the specification and knowledge in the art, it is clear that one of ordinary skill is in possession of the chemical structure of a polypeptide 80% identical to residues 221-323 of SEQ ID NO: 1 and would understand that the inventors were in possession of said polypeptides at the time of filing.

Additionally, the art provides guidance to one of ordinary skill as to the general secondary structure of RAP d3. For example, Melman et al. (J Biol Chem 276:29338-346, 2001, cited at page 39, line 8) teaches that certain residues within the 221-323 fragment (e.g., residues 282-289 and 311-319 of RAP) contribute to binding of RAP to LRP and heparin(see Melman, Figure 8 and page 29344). Additionally, Rall et al. (J Biol Chem 273:24152-57, 1998, cited at page 39, line 4) teaches that residues 223-323 of RAP are highly protease resistant, exhibit a coiled structure, are similar in structure and activity to regions of the ApoJ protein (page 24156) an LRP2 ligand, and that residues 301-323 are likely a heparin binding domain (page 24157).

The LRP2-binding functional characteristics of the d3 fragment have been described previously [see Declaration of Zankel submitted Feb. 28, 2007 which teaches that the d3 region (residues 201-319) confers binding to LRP2]. It is standard in the art to make fragments and

variants of a peptide to determine the minimum protein fragment size that will retain protein function (see, e.g., Melman et al. *supra*), and methods to determine receptor binding of a fragment of RAP are well-known in the art and described in the specification (see Example 2, page 86, and Melman, *supra*) and to determine the ability of the RAP fragment to traverse the BBB (see Example 3, pages 87-88). Thus, using techniques well-known in the art and described in the specification, a person of ordinary skill could readily obtain the chemical structure of a RAP polypeptide at least 80% identical to residues 221-323 that binds LRP2 and is transcytosed across the BBB into the central nervous system. Therefore, the structure-function correlation between the RAP and the binding activity was disclosed in the specification and art (see Melman and Rall et al.), as were many other binding domain characteristics of the RAP protein. Although not all amino acid substitutions or deletions in the recited region of SEQ ID NO: 1 may result in a protein having LRP2 binding activity, as noted by the Examiner, this does not preclude patentability (see Example 11B of the Guidelines), since those of ordinary skill in the art would readily be able to determine where substitutions could be made in the RAP fragment based on the structural knowledge of the protein and can readily determine the substitutions that result in a protein having the required LRP2 binding activity. For example, one of ordinary skill in the art would first start with conservative substitutions of the natural amino acids.

As evidenced above, the polypeptides described herein are described in greater detail than those in Example 11B in the Written Description Guidelines, in that the full structure of residues 221-323 of RAP and methods to make variants of the polypeptide are disclosed, that RAP polypeptides are not the only known proteins in its class as in Example 11B of the Guidelines, and there is considerable description of the binding regions and secondary structure of the RAP protein available in the specification and in the art, i.e., considerable identifying characteristics. The specification teaches methods for determining if the RAP fragment binds to a particular receptor (see, e.g., Example 10, pages 96 – 97 and pages 103-104) and is transported across the blood brain barrier (BBB) (see Examples 3 and 11 of the specification), and also describes recombinant methods for making RAP fragments or variants (see page 80, line 26, to page 82, line 31).

As stated above, the standard for fulfilling the written description requirement is whether one of ordinary skill would understand that the inventor was in possession of the invention at the time of filing. Applicants have provided adequate structural and functional

identifying characteristics of the recited RAP fragments coupled with a disclosed correlation between structure and function of the fragments, such that one of ordinary skill would recognize Applicants were in possession of the invention. Thus, a person of the ordinary skill would understand that the inventors could were in possession of the claimed genus of chimeric RAP polypeptides consisting of a RAP polypeptide at least 80% identical to residues 221-323 of SEQ ID NO: 1, which binds LRP2, at the time of filing the application.

For the reasons above, the rejection of the claims under 35 U.S.C. §112, first paragraph, should be withdrawn.

III. The rejection of claims 17-19, 21 and 58-62 under 35 U.S.C. §103(a) should be withdrawn

The Examiner rejected the pending claims under 35 USC §103(a) asserting that it would have been obvious to combine the disclosures of Pardridge, Fillebeen, Neels and Saenko to arrive at the present invention. The Examiner asserts that because the art (*e.g.*, Neels, Fillebeen, Saenko) teaches that the LRP molecule binds to and endocytoses several of its ligands, and may transcytose the ligand lactoferrin, LRP necessarily transcytoses fragments of the ligand RAP across the blood brain barrier (BBB). Without providing further evidence or scientific reasoning explaining how the teachings of the art can be extrapolated to support these assertions, the Examiner maintained the position that the art renders obvious administration of fragments of RAP conjugated to a diagnostic or therapeutic agent in order to increase transport of the agents across the BBB.

Applicants respectfully disagree. For the reasons discussed previously and below, the factual assumptions on which the obviousness rejection is based are not supported by the evidence cited. Upon a challenge of such factual assumptions, the Examiner is obliged to provide supporting evidence. See Ex parte Natale, 11 U.S.P.Q.2d 1222, 1226-27 (Bd. Pat. App. & Interf. 1989). Moreover, there are multiple unexplained gaps in the scientific reasoning supporting the rejection. The Examiner has not explained why one of ordinary skill in the art would choose RAP for transcytosis of an agent across the BBB, when RAP is an *intracellular* ligand that has been characterized as an *antagonist* of LRP and that is *not specific for* membrane-bound LRP, since it binds strongly to *all* of the receptors in the LRP family, and binds soluble LRP circulating in blood (Quinn et al., J Biol. Chem. 272:23946-951, 1997) (Exhibit B). None

of the cited art shows or even suggests that RAP is transcytosed across the BBB. One cannot extrapolate data obtained using one ligand to predict the behavior of another unrelated antagonist ligand (*e.g.*, from lactoferrin to RAP), or from one activity (internalization and degradation within a cell) to another activity (transport across the BBB without internalization and degradation), or from one receptor to another receptor (*e.g.*, from LRP to LRP2).

The pending claims are directed methods of treating individuals comprising administration of a conjugate comprising a polypeptide consisting of a RAP portion having an amino acid sequence at least 80% identical to amino acids 221-323 of SEQ ID NO: 1, and which binds to megalin (LRP2).

Pardridge discloses that receptor mediated transport pathways may be useful to transport therapeutics (*e.g.*, BDNF) across the BBB using chimeric peptides that bind to a BBB receptor. Pardridge does not address LRP2 or RAP. In particular, Pardridge does not disclose or suggest that RAP is transcytosed across the BBB, does not teach that RAP might be transcytosed by LRP2, or that RAP may be used in a chimeric protein to mediate transport of a therapeutic agent. The Examiner acknowledges at page 5 that "Pardridge does not teach conjugates comprising RAP fragments, as recited in independent claims..."

Fillebeen demonstrates that lactoferrin (Lf) is transcytosed across the BBB but does not disclose or suggest that RAP, an entirely different and unrelated protein, is transcytosed across the BBB. Fillebeen suggests that LRP1 "might" be involved in this process (see Abstract) and later assumes that the receptor mediating 70% of Lf transcytosis is LRP since RAP blocks 70% of Lf transcytosis. Fillebeen's speculation, however, is inconsistent with other reports, e.g., Faucheux et al., Proc. Nat'l. Acad. Sci. (USA) 92:9603-9607 (1995) (submitted previously), that *lactoferrin receptor* (a different receptor than LRP) transports lactoferrin and iron across the BBB. Thus, Fillebeen's assumption regarding LRP and Lf transcytosis is premature based on the evidence in the art.

Fillebeen does not suggest that the observation with lactoferrin would be extrapolatable to RAP. Even if one assumes, *arguendo*, that LRP is the receptor responsible for transport of lactoferrin across the BBB, the Examiner is mistaken in concluding that one of ordinary skill in the art would predict that other LRP ligands would be transported across the BBB. Fillebeen states that LRP binds to and is responsible for internalization of many ligands,

including chylomicrons, Lf, alpha2-macroglobulin, *Pseudomonas* exotoxin, proteinases and proteinase-inhibitor complexes. The Examiner's factual assumption at page 6 of the Action that "[LRP] transports [any or all] molecules across the BBB" is not supported by the cited evidence. There would not be a reasonable expectation that any and all of these diverse LRP ligands would be transported across the BBB, and the cited art has not shown any differently.

The data with respect to lactoferrin is not extrapolatable to RAP because RAP is an *antagonist* of LRP and binds to LRP in a manner unlike any other LRP ligand. See, *e.g.*, the Neels abstract, which states that "RAP binding to LRP induces a conformational change in the receptor that is incompatible with ligand binding." See also Vash et al. (*Blood* 92:3277-85, 1998) (submitted previously) noting that RAP appears to cause a conformational change in the LRP protein preventing it from binding other ligands, thereby, rendering RAP the universal antagonist (see Vash, page 3277, 1st col.).

For these reasons, Fillebeen does not teach or suggest to one of ordinary skill in the art that RAP, or fragments or analogs of RAP, would be *transcytosed across the BBB*. In addition, Fillebeen neither discloses nor suggests that LRP transports RAP across the BBB, nor that LRP2 transports RAP across the BBB. Thus, Fillebeen does not disclose or suggest methods of delivering agents across the BBB involving a RAP fragment polypeptide at least 80% homologous to amino acids 221-323 of SEQ ID NO: 1 that retains LRP2 binding and is transported across the BBB. The Examiner acknowledges at page 5 of the Action that Fillebeen "does not explicitly teach administration of conjugates comprising RAP for increasing transport across the BBB and does not teach conjugates comprising RAP fragments. . ."

Neels discloses that LRP binds a diverse array of ligand types, including apolipoproteins, lipases, proteinases, proteinase-inhibitor complexes, and RAP. Neels provides no data on transport across the BBB. Neels neither discloses nor suggests that any or all of the diverse ligands of LRP, in particular RAP or fragments thereof, can be transcytosed across the BBB. Further, Neels does not disclose or suggest the specific RAP fragment polypeptides recited in the claims which retain binding to LRP2. The Examiner acknowledges at pages 5-6 that "Neels does not teach administration of conjugates comprising RAP for increasing transport across the BBB and does not teach conjugates comprising RAP fragments . . ."

Saenko teaches use of a RAP polypeptide to inhibit Factor VIII uptake by the LRP (LRP1) receptor, which is a different receptor from LRP2 recited in the pending claims. Saenko teaches that residues 203-319 of RAP bind LRP, but the Examiner admits that Saenko does not teach administration of conjugates comprising this fragment to subjects (page 6 of Action). Furthermore, Saenko does not disclose that RAP is endocytosed or transcytosed by the LRP1 receptor, or that RAP or fragments of RAP would be transported across the BBB, or that RAP binds to LRP2, and does not teach that the particular fragment of RAP disclosed in Saenko binds to LRP2.

To establish a *prima facie* case of obviousness, the Examiner must show that all the elements of the claim are taught or suggested in the prior art (MPEP 2143.03 and Federal Register Examination Guidelines for Determining Obviousness, Section III.A.1, Fed Reg., Vol 72, No. 195, 2007), and if prior art elements are described in the art, the combination of elements must yield predictable results to render a claimed invention obvious. Further, it should be demonstrated that the prior art reference(s) provide a teaching, suggestion or motivation to combine the references, and/or there is a reasonable expectation of success (MPEP 2142 and Federal Register Examination Guidelines for Determining Obviousness, Section III.G, Fed Reg., Vol 72, No. 195, 2007). The court in KSR v Teleflex (127 S.Ct. 1727 (2007)) further stated to support the mere conclusory statements are not sufficient to draw a conclusion of obviousness, but that there must be some articulated reasoning with some rational underpinning to support a legal conclusion of obviousness. See Fed Reg., Vol 72, No. 195, Pages 57529 and KSR v Teleflex, 127 S.Ct. 1727.

For reasons stated previously, Pardridge, Fillebeen, Neels and Saenko are improperly combined because they each deal with different receptors than that recited in the claims, and transport of ligands other than RAP as recited in the claims. These ligands and receptors are not shown in any of the cited references to be equivalent or interchangeable.

Even if combined, the references do not disclose or suggest that RAP would be transported across the BBB, or that domain 3 of RAP, without domains 1 and 2, would be transported across the BBB. The Examiner acknowledges that none of the references teach administration of conjugates comprising the RAP fragment recited in the claims to increase transport across the BBB, and does not appear to dispute that the cited art fails to disclose that

LRP2 (megalin) mediates transport across the BBB. Thus, the references fail to disclose (1) delivery of any portion of RAP across the blood brain barrier (BBB), as claimed, and (2) use of domain 3 of RAP as claimed, without domains 1 and 2, for such delivery.

The Supreme Court in KSR stated that: "A court must ask whether the improvement is more than the predictable use of prior-art elements according to their established functions." In this case, the use of RAP, and particularly domain 3 fragments thereof, for transport of agents across the BBB is neither an established function nor a predictable use of such fragment polypeptides. The Examiner acknowledges that there is no data in the cited art showing transport of RAP or any fragments of RAP across the BBB. Fillebeen is the only cited art that addresses transcytosis. One of ordinary skill in the art would not conclude from the data in Fillebeen (in which RAP inhibited lactoferrin transcytosis by an unknown receptor), that LRP1 was responsible for transporting lactoferrin in view of the known fact that RAP binds multiple receptors besides LRP1, and the fact that LRP is expressed on the wrong side of the BBB (See Marzolo et al., *Traffic* 4:273-88, 2003, submitted in the response of April 21, 2008). For reasons explained below, even if Fillebeen does teach that lactoferrin crosses the BBB, one of ordinary skill in the art would not reasonably predict that an LRP antagonist like RAP, which is primarily found intracellularly, would cross the BBB. Saenko is the only cited art that teaches that amino acids 203-319 of RAP bind LRP, but provides no basis for predicting that any fragment of RAP would be transported across the BBB.

a. RAP is primarily intracellular and was considered an antagonist to LRP ligands such as lactoferrin

RAP was considered a ligand of LRP in the sense that it bound to LRP, but was generally held in the art to be an antagonist to all ligands that bind LRP, and was more referred to as an antagonist of LRP than a ligand, *per se* (see *e.g.*, Vash et al. and Herz et al., submitted in the response of April 21, 2008). The Examiner's observation that RAP appears to bind to the same area of LRP receptor as some other LRP ligands does not detract from the statements in the art that RAP binds in a *different manner* that *antagonizes* and prevents binding of LRP to its other ligands. The Examiner has presented no evidence showing that RAP and lactoferrin are equivalent in their mode of binding and in their action upon the LRP receptor; indeed, it would

be impossible for RAP to mimic the ultimate biological activity of all of the various ligands of the various receptors in the LRP receptor family.

RAP has been shown to be expressed in the endoplasmic reticulum and act as a chaperone to the newly translated LRP and prevents LRP degradation. Significant levels of RAP are not detected extracellularly where typical ligands are located (Obermoeller et al., J Biol Chem 272:10761-68, 1997) (Exhibit C). Even assuming *arguendo* that LRP was known to transport lactoferrin across the LRP, a person of ordinary skill would not have expected RAP to be transcytosed by LRP as it was not seen as an activator of LRP function, it was not equivalent to lactoferrin, and it served no other function but to chaperone LRP intracellularly. Therefore, based on RAP's intracellular function in the cell, and its non-equivalence to lactoferrin, one of ordinary skill would not predict that RAP would be transcytosed and transported across the BBB.

Both Vash (page 3277, 1st col.) and Neels (Abstract) state that RAP binds LRP1 and causes a conformational change thereby preventing other ligands from binding LRP, and therefore it is a powerful antagonist. Neels further states that it is unclear how RAP antagonizes LRP ligand binding, since few ligands interfere with RAP/LRP binding (page 31306, col. 1), implying that RAP acts much differently than other LRP ligands. Additionally, Obermoeller et al. (*supra*) shows that the d3 region binds LRP differently than the d1 and d2 regions of RAP. Again, based on the clear difference in binding of RAP to the LRP receptor compared to other LRP ligands, and the structural differences between LRP and LRP2, one of ordinary skill would not have extrapolated from any suggestion that LRP transports lactoferrin across the BBB to reasonably predict that RAP (a non-equivalent antagonist ligand), and particularly RAP domain 3 fragment polypeptides as claimed, would be transported cross the BBB.

b. Other evidence conflicts with any suggestion that LRP transports ligands across the BBB

Fillebeen is the only cited art that addresses transcytosis. The Examiner is incorrect in discounting Applicants' evidence contradicting the assertion in Fillebeen that LRP transported lactoferrin across the BBB into the CNS. Applicants previously provided evidence that LRP1 is expressed on the wrong side of the cell membrane for transport. The Examiner asserts that the MDCK cells used in the Marzolo reference cited by applicants are NOT applicable to the BBB (see paragraph bridging pages 9-10 of the Action). On the contrary, Pan et al. (J Cell Sci. 117-

5071-78, 2003) (Exhibit D) teaches that "MDCK cells polarize and form tight junctions when cultured in Transwell inserts and have been used as an in vitro model of the BBB for drug screening (Irvine et al., 1999; Vilhart et al., 1999...", page 5077, col. 1)." Therefore, the teaching in Marzolo et al. (*supra*) that the LRP1 and LRP2 receptors are expressed on different sides of the polarized endothelial cell membranes is relevant to function and transport of proteins by the receptors and cannot be dismissed by the Examiner as irrelevant.. As such, since LRP1 is expressed basolaterally in polarized cells such as brain endothelium (*i.e.*, on the brain side of the membrane), one of ordinary skill in the art would question whether LRP is capable of transporting any ligand from the blood, across the BBB, into the brain. In contrast, LRP2 is apically expressed in polarized brain endothelium (*i.e.*, on the blood side of the membrane).

Applicants provide herewith further evidence conflicting with Fillebeen's assertion. The disclosure of Shibata et al. (J Clin Invest. 106:1489-99, 2000) (Exhibit E), supports the opposite conclusion by an *in vivo* demonstration that amyloid-beta (Aβ) is transported out of the CNS by LRP1 (see abstract and page 1495, col. 2), and LRP1 is therefore expressed on the basolateral side of the cell membrane. Shibata also notes that anti-LRP2 antibodies did not affect Aβ clearance (page 1494, col. 1) even though LRP2 has been shown to bind Aβ, confirming Applicant's position that not all proteins that bind LRP1 and LRP2 are transported equivalently. Thus, as stated previously, to effectively modulate blood to brain transport as required by the claims, receptor expression must be on the apical side of the membrane to bind ligand in the blood and transport it into the brain. Based on the basolateral expression pattern of LRP1 (See Marzolo and Shibata), one of ordinary skill in the art would not reasonably predict that LRP transports ligands from blood to brain across the BBB. Additionally, Quinn et al. (*supra*) have demonstrated that a soluble form of LRP exists in human plasma. This soluble form inhibits normal LRP ligand uptake and protein degradation. Thus, an additional form of LRP exists *in vivo* that is not able to transport ligand across the BBB.

As noted earlier, Applicants have also provided evidence that the assumption by Fillebeen that LRP is the primary transporter of Lf may be incorrect (see Faucheux et al., Proc. Nat'l. Acad. Sci. (USA) 92:9603-9607, 1995), which teaches lactoferrin receptor, a different receptor from LRP1, transports lactoferrin and iron across the BBB.

Where the teachings of two or more prior art references conflict, the examiner must weigh the power of each reference to suggest solutions to one of ordinary skill in the art, considering the degree to which one reference might accurately discredit another. In re Young, 927 F.2d 588 (Fed. Cir. 1991). See also MPEP 2143.01. Applicants have provided a plethora of evidence contradicting Fillebeen's assertion that LRP is responsible for transporting lactoferrin across the BBB into the brain. Applicants have provided citations from art-recognized, peer reviewed journals using *in vitro* and *in vivo* models of the BBB that demonstrate LRP is expressed on the wrong side of the BBB membrane to effect transcytosis of molecules into the brain, whereas the LRP2 protein is expressed on the correct side of the BBB thereby effectively mediating transport from the blood to the brain (see Shibata, Marzolo and Pan). Applicants have provided a peer-reviewed article stating that another receptor, lactoferrin receptor, is responsible for transport of lactoferrin. Thus, when *all of the evidence* is considered, the art neither teaches nor reasonably suggests that RAP, much less a RAP domain 3 fragment polypeptide as claimed, would be transported across the BBB via transcytosis. As such, one would not have been motivated to use conjugates comprising the RAP fragment to deliver therapeutic agents into the CNS as claimed.

Moreover, in view of the conflicting evidence, it is incumbent on the Examiner to provide evidence supporting the assumption that domain 3 RAP fragment polypeptides would be transcytosed across the BBB.

c. Endocytosis is not the same as transcytosis

The Examiner unreasonably extrapolates, based on the statement in Neels that LRP binds and internalizes a number of ligands, that LRP must necessarily transcytose all of its ligands. No evidence was provided to support this factual assumption.

The Examiner agrees that "the experiments reported by Neels are on point to binding and DO NOT mention internalization" and then makes the assumption, without factual evidence to support the theory that, "given that Neels teaches that the receptor was well-known to bind and internalize a very diverse set of ligands, an artisan of ordinary skill would, upon reading the reference, *clearly* understand that those ligands that bind are internalized," (page 5 of the Action, emphasis added). Applicants question the basis for the Examiner's "*clear*" assumption that one of ordinary skill would "clearly understand" that all ligands that bind LRP are internalized, and

the relationship of internalization to transcytosis as opposed to endocytosis of a ligand. Endocytosis (into a cell) is a different activity from transcytosis (transport across cell barrier), and the Examiner has failed to present any evidence showing that the two activities are equivalent.

Thus, the art neither teaches nor reasonably suggests that RAP, much less a RAP domain 3 fragment polypeptide as claimed, would be *transported across the BBB via transcytosis*. As such, one would not have been motivated to use conjugates comprising the RAP fragment to deliver therapeutic agents into the CNS as claimed.

d. Obviousness cannot be predicated on what is not known at the time an invention is made

The Examiner concludes that the receptor-binding property (LRP2) recited in the claims is inherently presumed to be provided for (page 8 of the Action), despite acknowledging that "the Examiner cannot determine whether residues 203-319 taught by Saenko will bind to LRP2 as claimed." The Examiner refers to domain 3 of RAP as "inherently" binding LRP2 simply because it binds LRP, despite evidence that the LRP2 binding property of domain 3 was not known prior to the filing date. For reasons stated previously, in light of the differences in the ligand binding domains of the LRP and LRP2 receptors, one of ordinary skill could not have predicted that RAP d3 binding to LRP2 necessarily followed from any suggestion that RAP d3 binds LRP. "Obviousness cannot be predicated on what is not known at the time an invention is made, even if the inherency of the certain feature is later established." (MPEP 2141.02 citing In re Rijckaert, 9 F.2d 1531, 28 USPQ2d 1955 (Fed. Cir. 1993).

Contrary to the Examiner's assertion, Applicants have provided evidence of non-obviousness necessary to rebut the assertion of inherency (see page 8 of the Action). The evidence presented above demonstrates that one of ordinary skill in the art would not be motivated by the cited art to make a chimeric RAP protein having the recited RAP polypeptide conjugated to a therapeutic agent for delivery of the therapeutic compound to the CNS.

For the reasons stated above, the Examiner has not established a *prima facie* case of obviousness with respect to the present claims because (1) not all elements are disclosed by the cited art, even when combined, and as such, the claimed invention was unpredictable until the

present disclosure, and (2) the cited art does not provide a reasonable expectation of success or motivation to carry out the claimed method. Therefore, the present invention is not obvious in light of the disclosures of Pardridge, Fillebeen, Neels and Saenko and the rejection under 35 U.S.C. §103(a) should be withdrawn.

IV. Conclusion

Applicants submit that the application is in condition for allowance and respectfully request notification of the same.

Dated: January 14, 2009

Respectfully submitted,

By /Katherine L. Neville/
Katherine L. Neville
Registration No.: 53,379
MARSHALL, GERSTEIN & BORUN LLP
233 S. Wacker Drive, Suite 6300
Sears Tower
Chicago, Illinois 60606-6357
(312) 474-6300
Attorneys for Applicant

EXAMPLE 11: PERCENT IDENTITY

11A: ART-RECOGNIZED STRUCTURE-FUNCTION CORRELATION NOT PRESENT

Specification:

The specification discloses a polynucleotide having the nucleic acid sequence of SEQ ID NO: 1, which encodes the polypeptide of SEQ ID NO: 2. The polypeptide of SEQ ID NO: 2 has the novel activity X, and does not share significant sequence identity with any known polypeptide or polypeptide family. The specification does not disclose any nucleic acid sequences that encode a polypeptide with novel activity X other than SEQ ID NO: 1.

Claims:

Claim 1. An isolated nucleic acid that encodes a polypeptide with at least 85% amino acid sequence identity to SEQ ID NO: 2.

Claim 2: An isolated nucleic acid that encodes a polypeptide with at least 85% amino acid sequence identity to SEQ ID NO: 2; wherein the polypeptide has activity X.

Analysis:

Claim 1

Claim 1 encompasses nucleic acids that encode the polypeptide of SEQ ID NO: 2, as well as those that encode any polypeptide having 85% structural identity to SEQ ID NO: 2. However, the specification discloses only a single species that encodes SEQ ID NO: 2; *i.e.*, SEQ ID NO: 1. There are no other drawings or structural formulas disclosed that encode either SEQ ID NO: 2 or a sequence with 85% identity to SEQ ID NO: 2.

The recitation of a polypeptide with at least 85% identity represents a partial structure, that is, at least 85% percent of the amino acids in the polypeptide will match those in SEQ ID NO: 2, and up to 15% of them may vary from those in SEQ ID NO: 2. However, there is no teaching regarding which 15% of the amino acids may vary from SEQ ID NO: 2. Consequently, there is also no information given about which nucleotides will vary from SEQ ID NO: 1 in the claimed genus of nucleic acids.

There is no functional limitation on the nucleic acids of claim 1 other than that they encode the polypeptide of SEQ ID NO: 2 or any polypeptide having 85% structural identity to SEQ ID NO: 2. The genetic code and its redundancies were known in the art before the application was filed.

The disclosure of SEQ ID NO: 2 combined with the pre-existing knowledge in the art regarding the genetic code and its redundancies would have put one in possession of the ge-

nus of nucleic acids that encode SEQ ID NO: 2. With the aid of a computer, one of skill in the art could have identified all of the nucleic acids that encode a polypeptide with at least 85% sequence identity with SEQ ID NO: 2. Thus, one of ordinary skill in the art would conclude that the applicant was in possession of the claimed genus at the time the application was filed.

Conclusion:

The specification satisfies the written description requirement of 35 U.S.C. 112, first paragraph, with respect to the scope of claim 1.

Claim 2

Claim 2 encompasses nucleic acids that encode the polypeptide of SEQ ID NO: 2, and nucleic acids that encode a polypeptide having 85% sequence identity to SEQ ID NO: 2 and have activity X. The specification discloses the reduction to practice of only a si gle species that encodes SEQ ID NO: 2 and has activity X; *i.e.*, SEQ ID NO: 1. There are no other drawings or structural formulas disclosed of a nucleic acid that encodes either SEQ ID NO: 2 or a polypeptide having 85% sequence identity to SEQ ID NO: 2 and activity X.

The claim includes a genus that can be analyzed at several levels sequentially for the purpose of focusing the issue.

First, the disclosure of SEQ ID NO: 2 combined with pre-existing knowledge in the art regarding the genetic code and its redundancies would have put one in possession of the genus of nucleic acids that encode SEQ ID NO: 2. With the aid of a computer, one of skill in the art could identify all of the nucleic acid sequences that encode a polypeptide with at least 85% sequence identity with SEQ ID NO: 2. However, there is no teaching regarding which 15% of the amino acids can vary from SEQ ID NO: 2 and still result in a protein that retains activity X. Further, there is no disclosed or art-recognized correlation between any structure other than SEQ ID NO: 2 and novel activity X.

An important consideration is that structure is not necessarily a reliable indicator of function. In this example, there is no disclosure relating similarity of structure to conservation of function. General knowledge in the art included the knowledge that some amino acid varia-

TECHNICAL NOTE

For information on amino acid substitution exchange groups and empirical similarities between amino acid residues, see a standard text such as Schulz et al., PRINCIPLES OF PROTEIN STRUCTURE, pp. 14-16, Springer-Verlag (New York 1979). There is a limit to how much substitution can be tolerated before the original tertiary structure is lost. Generally, tertiary structure conservation would be lost when the amino acid sequence varies by more than 50%. See, e.g., Cyrus Chothia and Arthur M. Lesk, "The relation between the divergence of sequence and structure in proteins," 5 THE EMBO JOURNAL 823-26 (1986).

tions are tolerated without losing a protein's tertiary structure. The results of amino acid substitutions have been studied so extensively that amino acids are grouped in so-called "exchange groups" of similar properties because substituting within the exchange group is expected to conserve the overall structure. For example, the expectation from replacing leucine with isoleucine would be that the protein would likely retain its tertiary structure. On the other hand, when non-exchange group members are substituted, e.g., proline for tryptophan, the expectation would be that the substitution would not likely conserve the protein's tertiary structure. Given what is known in the art about the likely outcome of substitutions on structure, those in the art would have likely expected the applicant to have been in possession of a genus of proteins having a tertiary structure similar to SEQ ID NO: 2 although the claim is not so limited.

However, conservation of structure is not necessarily a surrogate for conservation of function. In this case, there is no disclosed correlation between structure and function. The need for correlating information can vary. More specifically, those of skill in the art might require more or less correlating information depending on the kind of protein activity. If activity X is simply structural, e.g., a member of the collagen class, correlating information might not be a critical factor. However, if activity X is enzymatic, and there is no disclosure of the active site amino acid residues responsible for the catalytic activity, lack of that kind of correlating information may be a problem. Similarly, if activity X is as a ligand, and there is no disclosure of the domain(s) responsible for the ligand activity, the absence of information may be persuasive that those of skill in the art would not take the disclosure as generic.

Summarizing, there are no known or disclosed proteins having activity X other than SEQ ID NO: 2. As of the filing date, there was no known or disclosed correlation between a structure other than SEQ ID NO: 2 and activity X. While general knowledge in the art may have allowed one of skill in the art to identify other proteins expected to have the same or similar tertiary structure, in this example there is no general knowledge in the art about activity X to suggest that general similarity of structure confers the activity. Accordingly, one of skill in the art would not accept the disclosure of SEQ ID NO: 2 as representative of other proteins having activity X.

Conclusion:

The specification, taken with the pre-existing knowledge in the art of amino acid substitution and the genetic code, fails to satisfy the written description requirement of 35 U.S.C. 112, first paragraph, with respect to the scope of claim 2.

11B: ART-RECOGNIZED STRUCTURE-FUNCTION CORRELATION PRESENT

Specification:

The specification discloses a polynucleotide having the nucleic acid sequence of SEQ ID NO: 1, which encodes the polypeptide of SEQ ID NO: 2. The polypeptide of SEQ ID NO: 2

has a novel activity Y, and does not share significant sequence identity with any known polypeptide or polypeptide family. The specification does not disclose any nucleic acid sequences that encode a polypeptide with novel activity Y other than SEQ ID NO: 1. However, the specification discloses data from deletion studies that identify two domains as critical to activity Y, *i.e.*, a binding domain and a catalytic domain. The specification proposes that conservative mutations in these domains (e.g., one basic amino acid substituted for another basic amino acid) will still result in a protein having activity Y, whereas most non-conservative mutations in these domains will not result in a polypeptide having the recited activity. The specification also proposes that most mutations, conservative or non-conservative, outside the two domains will not affect activity Y to any great extent.

Claims:

Claim 1. An isolated nucleic acid that encodes a polypeptide with at least 85% amino acid sequence identity to SEQ ID NO: 2.

Claim 2. An isolated nucleic acid that encodes a polypeptide with at least 85% amino acid sequence identity to SEQ ID NO: 2; wherein the polypeptide has activity Y.

Analysis:

Claim 1

(This analysis proceeds the same as the analysis for claim 1 in Example 11A (Art-Recognized Structure-Function Correlation Not Present)

Claim 1 encompasses a vast genus of nucleic acids that encode the polypeptide of SEQ ID NO: 2, as well as those that encode any polypeptide having 85% structural identity to SEQ ID NO: 2.

The specification, however, discloses the reduction to practice of only a single species that encodes SEQ ID NO: 2, *i.e.*, SEQ ID NO: 1. There are no other drawings or structural formulas disclosed that encode either SEQ ID NO: 2, or a sequence with 85% identity to SEQ ID NO: 2.

Although the recitation of a polypeptide with at least 85% identity represents a partial structure -- in that 85% percent of the polypeptide is known, while 15% of the structure may vary -- there is no teaching regarding which 15% of the amino acids will vary from SEQ ID NO: 2. Consequently, there is also no information about which nucleotides will vary from SEQ ID NO: 1 in the claimed genus of nucleic acids.

There are no functional characteristics disclosed for the nucleic acids of claim 1 other than they encode the polypeptide of SEQ ID NO: 2 or any polypeptide having 85% structural identity to SEQ ID NO: 2. Further, the specification fails to disclose a method of making nucleic acids encoding polypeptides having 85% identity to SEQ ID NO: 2.

Nonetheless, the disclosure of SEQ ID NO: 2 combined with the knowledge in the art regarding the genetic code would put one in possession of the genus of nucleic acids that encode SEQ ID NO: 2. Further, with the aid of a computer, one could list all of the nucleic acid sequences that encode a polypeptide with at least 85% sequence identity with SEQ ID NO: 2. Additionally, the level of skill and knowledge in the art is such that one of ordinary skill would be able to use conventional sequencing and nucleic acid synthesis techniques to routinely generate and identify nucleic acids that encode the polypeptide of SEQ ID NO: 2, as well as those that encode any polypeptide having 85% structural identity to SEQ ID NO: 2. Thus, one of ordinary skill in the art conclude that the applicant would have been in possession of the claimed genus at the time of filing.

Conclusion:

The specification satisfies the written description requirement of 35 U.S.C. 112, first paragraph, with respect to the scope of claim 1.

Claim 2

Claim 2 encompasses a genus of nucleic acids that encode the polypeptide of SEQ ID NO: 2 and those that encode any polypeptide having 85% structural identity to SEQ ID NO: 2, wherein the polypeptide additionally has activity Y.

The specification, however, discloses the reduction to practice of only a single species that encodes SEQ ID NO: 2 and has activity Y, *i.e.*, SEQ ID NO: 1. There are no other drawings or structural formulas disclosed of a nucleic acid that encodes either (i) SEQ ID NO: 2 or (ii) a polypeptide with 85% sequence identity to SEQ ID NO: 2 wherein the polypeptide also has activity Y.

The disclosure of SEQ ID NO: 2 combined with the knowledge in the art regarding the genetic code would have put one in possession of the genus of nucleic acids that encode SEQ ID NO: 2. Further, with the aid of a computer, one could list all of the nucleic acid sequences that encode a polypeptide with at least 85% sequence identity to SEQ ID NO: 2. However, the specification fails to teach which of the nucleic acid sequences that encode a polypeptide with at least 85% sequence identity to SEQ ID NO: 2 encode a polypeptide having the required activity Y.

PRACTICE NOTE

This example deals only with the written description analysis of the claimed nucleic acids. Enablement issues that may be raised by the recited facts are not addressed here, but should be considered during examination. A separate rejection for nonenablement should be made when appropriate.

Nonetheless, the specification identifies two domains responsible for activity Y, *i.e.*, a binding domain and catalytic domain. The specification also predicts that conservative mutations in these domains will result in a protein having activity Y. Although all conservative amino acid substitutions in these domains will not nec-

THE JOURNAL OF BIOLOGICAL CHEMISTRY
Vol. 272, No. 38, Issue of September 19, pp. 23946–23951, 1997
Printed in U.S.A.

Soluble Low Density Lipoprotein Receptor-related Protein (LRP) Circulates in Human Plasma*

(Received for publication, March 17, 1997, and in revised form, June 9, 1997)

Kathryn A. Quinn‡, Philip G. Grimsley‡, Yang-Ping Dai‡, Michael Tapner§, Colin N. Chesterman‡, and Dwain A. Owensby‡¶‖

From the ‡Center for Thrombosis and Vascular Research, University of New South Wales, Sydney 2052, Australia, the §Storr Liver Unit, Department of Medicine, University of Sydney at Westmead Hospital, Westmead 2145, Australia, and the ¶Illawarra Regional Hospital, Wollongong, New South Wales 2500, Australia

Our studies have identified a soluble molecule in normal human plasma and serum with the characteristics of the α-chain of the low density lipoprotein receptor-related protein (LRP). LRP is a large multifunctional receptor mediating the clearance of diverse ligands, including selected lipoproteins, various protease inhibitor complexes, and thrombospondin. A soluble molecule (sLRP) has been isolated from plasma using an affinity matrix coupled with methylamine-activated α_2-macroglobulin, the ligand uniquely recognized by LRP, and eluted with EDTA. This eluate contains a protein that co-migrates on SDS-polyacrylamide gel electrophoresis with authentic human placental LRP α-chain, is recognized by anti-LRP α-chain monoclonal antibodies, and binds the 39-kDa receptor-associated protein (RAP) and tissue plasminogen activator-inhibitor complexes. A similar RAP-binding molecule was detected in medium conditioned for 24 h by primary cultures of rat hepatocytes, suggesting that the liver may be the *in vivo* source of sLRP. In contrast, immunoprecipitation experiments failed to detect the production of sLRP by cultured HepG2 hepatoma and primary human fibroblast cells. Addition of a soluble form of LRP to cultured HepG2 cells resulted in a significant inhibition of capacity of these cells to degrade tPA, a process that has been demonstrated to be mediated by cell surface LRP. Preliminary data indicate that the concentration of sLRP is altered in the plasma of patients with liver disease. Increased levels of sLRP may antagonize the clearance of ligands by cell bound LRP perturbing diverse processes including lipid metabolism, cell migration and extracellular proteinase activity.

The low density lipoprotein receptor-related protein (LRP)[1] has been previously identified as a membrane-bound endocytic receptor (1, 2). Studies have demonstrated that LRP mediates the internalization of multiple, structurally unrelated ligands, including selected lipoproteins, proteinase-inhibitor complexes, plasminogen activators, and thrombospondin (reviewed in Refs. 3 and 4). The binding of all ligands to LRP is inhibited by the receptor-associated protein (RAP), a protein that was co-purified with LRP (2, 5). The range of ligands recognized by LRP suggests that it plays a role in diverse processes including lipid metabolism, cell growth, migration, and tissue invasion. LRP expression is widespread; however, it is most highly expressed in the liver, brain, and placenta. The remarkable degree of cross-species identity conserved in the LRP amino acid sequence (3) and the embryonic lethal phenotype obtained after targeted disruption of the LRP gene in the mouse (6) underscore the biological importance of this molecule.

Here we report the identification of a soluble form of LRP circulating in human plasma. The characterization of this molecule, which maintains the ligand binding characteristics of cell surface LRP, introduces a new dimension to the biology of LRP. Accumulation of soluble LRP in plasma may antagonize the clearance of ligands by cell-bound LRP, perturbing lipid metabolism and cellular processes involving extracellular proteinase activity.

MATERIALS AND METHODS

Proteins and Reagents—All chemicals were of analytical grade and purchased from BDH (Kilsyth, Australia). Bovine serum albumin (BSA), benzamidine, phenylmethylsulfonyl fluoride, bacitracin, leupeptin, 2,2′-azino-bis(3-ethylbenzthiazoline-6-sulfonic acid (ABTS) and HEPES were purchased from Sigma. Electrophoresis reagents were purchased from Bio-Rad. Proteins were iodinated with carrier free $Na^{125}I$ (Australian Radioisotopes, Lucas Heights, Australia) and iodogen reagent (Pierce), according to the manufacturer's instructions. Protein concentrations were determined using the BCA protein assay (Pierce). Recombinant RAP was synthesized as a glutathione *S*-transferase fusion protein in *Escherichia coli* and purified as described previously (5). The RAP-GST/pGex plasmid was a generous gift from Joachim Herz, University of Texas Southwestern Medical Center, Dallas, TX. α_2-Macroglobulin (α_2M) was purified from human plasma by Zn^{2+}-chelate chromatography and gel filtration, as described previously (7). It was activated by the addition of 0.2 M methylamine, 30 min, room temperature, dialyzed into 20 mM Mes, pH 6.0, and stored at 4 °C. Purified recombinant human tissue plasminogen activator (tPA) was donated by Karl Thomae GmbH (Biberach, Germany). Recombinant plasminogen activator inhibitor-1 (PAI-1) was expressed in *E. coli* transformed with a plasmid (pMBL11/PAI-1) containing full-length PAI-1 cDNA (Ref. 8, a generous gift of A. Zonneveld, University of Amsterdam) and purified as described previously (9), with additional purification by size exclusion chromatography on Bio-Gel P-60 (Bio-Rad). The anti-LRP α-chain monoclonal antibody (mAb 8G1) and affinity-purified rabbit anti-LRP (R777) were kind gifts of Dr. Dudley Strickland, American Red Cross, Rockville MD (2). A commercial anti-LRP α-chain mAb (number 3402) was also purchased (American Diagnostica, Greenwich, CT). A hybridoma secreting an anti-LRP β-chain COOH-terminal peptide mAb (11H4; ATCC CRL-1936) was obtained

* This work was supported by a grant from the National Health and Medical Research Council of Australia. The costs of publication of this article were defrayed in part by the payment of page charges. This article must therefore be hereby marked "*advertisement*" in accordance with 18 U.S.C. Section 1734 solely to indicate this fact.

‖ To whom correspondence should be addressed: Center for Thrombosis and Vascular Research, School of Pathology, Wallace Wurth Bldg., University of New South Wales, Kensington 2052, Australia. Fax: 61-2-9385-1389.

[1] The abbreviations used are: LRP, low density lipoprotein receptor related protein; sLRP, soluble LRP-like molecule; BSA, bovine serum albumin; mAb, monoclonal antibody; RAP, receptor-associated protein; PAGE, polyacrylamide gel electrophoresis; PAI-1, plasminogen activator inhibitor-1; tPA, tissue plasminogen activator; ABTS, 2,2′-azino-bis(3-ethylbenzthiazoline-6-sulfonic acid; α_2M, α_2-macroglobulin; Mes, 4-morpholineethanesulfonic acid; EMEM, Earle's modified Eagle's medium; HFF, human foreskin fibroblasts; FBS, fetal bovine serum; NIDDM, non-insulin-dependent diabetes mellitus.

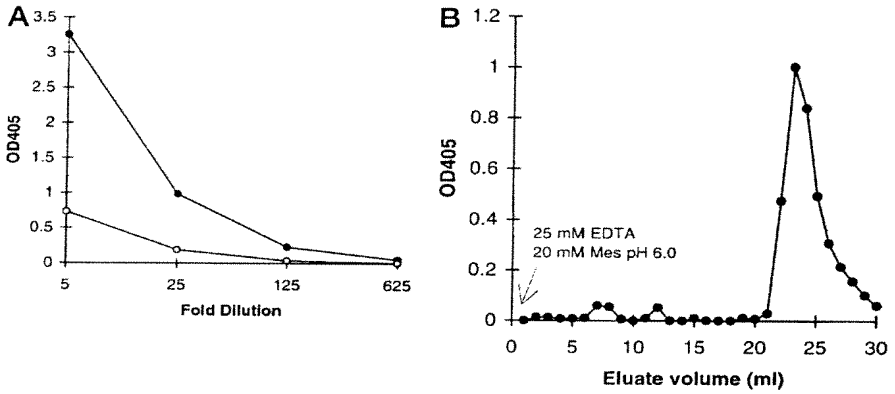

FIG. 1. **Affinity isolation of sLRP from plasma.** An affinity column of activated α_2M-Sepharose (280 mg of activated α_2M coupled to 25 ml of gel) was used to affinity-purify LRP from 200 ml of human plasma. *A*, human plasma contains immunoreactivity detected in an LRP immunoassay (●), which was removed by incubation with the activated α_2M-Sepharose (○). *B*, the immunoreactivity was recovered by eluting (1-ml fractions collected) the affinity matrix with 25 mM EDTA, 20 mM Mes, pH 6.0. Fractions eluting between 21 and 25 ml were pooled and analyzed.

from the American Type Culture Collection (Rockville, MD). Antibodies were purified from culture supernatant using protein G-Sepharose (Pharmacia Biotech Inc., Uppsala, Sweden), according to the manufacturer's instructions. All cell culture reagents were purchased from ICN (Costa Mesa, CA) and culture-ware was from Costar (Cambridge, MA).

LRP Immunoassay—Microtiter plates (Maxisorp, Nunc, Denmark) were coated with 1 μg/well rRAP (100 μl) diluted in carbonate buffer, pH 9.6 (2 h, 37 °C). After blocking in assay buffer (HBSC (20 mM HEPES, 0.15 M NaCl, 2 mM Ca^{2+}, pH 7.4) containing 0.1% Tween 80, 1% BSA), 30 min, 37 °C, a 100-μl sample (diluted in assay buffer) was added to the well and incubated 2 h at room temperature. After washing, the plates were incubated with 100 μl/well anti-LRP mAb (8G1, 5 μg/ml) in assay buffer, 1 h at room temperature. After washing, 100 μl of 1/1000 dilution rabbit anti-mouse Ig-horseradish peroxidase conjugate (Dako, Carpenteria, CA) was added (30 min, room temperature), and bound antibody was quantitated with 200 μl/well chromogenic substrate (1 mg/ml ABTS, 0.003%, v/v, H_2O_2 diluted in citrate buffer, pH 4.5). Color development was stopped after 20 min by addition of 50 μl/well 3% oxalic acid, and the optical density at 405 nm (A_{405}) was determined.

Affinity Isolation of LRP—An affinity matrix was prepared by coupling 280 mg of methylamine-activated α_2M to 25 ml of CNBr-Sepharose (Pharmacia Biotech Inc.), according to the manufacturer's instructions. Fresh frozen human plasma (200 ml) containing a mixture of protease inhibitors (1 mM phenylmethylsulfonyl fluoride, 2 mM benzamidine, 2 mM bacitracin, 1 μM leupeptin) was thawed at 37 °C. The plasma was adjusted to pH 7.4 by addition of 1/10 volume 0.1 M HEPES, pH 7.4, 10 IU/ml heparin, 5 mM Ca^{2+}, clarified by centrifugation (4 °C, 20 000*g*, 30 min), and filtered through a 0.4-μm nitrocellulose filter (Millipore-Waters, Milford, MA). The plasma was mixed with blank Sepharose gel for 1 h at 4 °C. The precleared plasma supernatant was then mixed with methylamine activated α_2M-Sepharose for 6 h at 4 °C. The affinity matrix was washed on a scintered glass funnel with 250 ml of HBSC, packed into a column and eluted with 25 mM EDTA, 20 mM Mes, pH 6.0. Protease inhibitors (as above) were added to each fraction (1 ml). LRP was also isolated from detergent-solubilized human placental membranes, prepared as described previously (10), using the activated α_2M-Sepharose affinity matrix. The fractions were screened by specific LRP immunoassay and pooled positive fractions were stored at −20 °C. The material eluted from the activated α_2M affinity matrix was fractionated by electrophoresis on 5–15% gradient SDS-polyacrylamide gels (SDS-PAGE) and analyzed by silver staining (11).

Western and Ligand Blots—Prior to Western and ligand blot analysis samples were electrophoresed on 6% SDS-PAGE minigels for 2 h at 150 V. The gels were electroblotted onto polyvinylidene difluoride membrane (NEN Life Science Products) and incubated, according to the manufacturer's instructions, with 5 μg/ml mAb and 1/2000 dilution rabbit anti-mouse immunoglobulin-horseradish peroxidase conjugate (Dako). Bound antibody was visualized with chemiluminescence reagent (Renaissance, NEN Life Science Products) and exposed to film (Hyperfilm-MP, Amersham Corp.). For ligand blotting, blots were blocked in 5% milk, HBSC, 0.1% Tween 20 and incubated (4 h at room temperature) in either 4 nM ^{125}I-ligand (RAP or tPA), washed, and exposed to film (24 h, −80 °C, intensifying screen). Blots were incubated in ^{125}I-tPA in the presence of 100 nM PAI-1, resulting in the complete conversion of ^{125}I-tPA to an SDS-stable tPA·PAI-1 complex (data not shown). The specificity of binding was indicated by the absence of ^{125}I-ligand binding in the presence of 1 μM unlabeled RAP or tPA.

Cell Culture—All cell lines were cultured under standard conditions at 37 °C, 5% CO_2 in a humidified incubator. Hepatocytes were isolated from 230–270 g of anesthetized male Wistar rats by *in situ* two-stage collagenase perfusion of the liver, as described elsewhere (12). The liver was excised and dispersed in modified Waymouth medium containing sodium bicarbonate (24 mM), penicillin (100 units/ml), HEPES (18 mM), and insulin (25 milliunits/ml). Viability was determined by trypan blue exclusion, and only preparations with greater than 80% viable hepatocytes were used. Cells (3.0×10^6 in a final volume of 3 ml of Williams' medium E, supplemented as above) were overlaid onto 60-mm culture plates (Medos Company, Sydney, Australia) coated with 400 μl of matrigel prepared as described previously (13). The culture medium was replaced after a 3-h attachment period and at 24-h intervals thereafter. HepG2 cells (ATCC HB8065, provided by M. Gallicchio, Monash University, Melbourne, Australia) were maintained in Earle's modified Eagle's medium (EMEM) supplemented with 10% fetal bovine serum (FBS). Human foreskin fibroblasts (HFF) were kindly provided by Dr. Gabrielle Delbridge (Center for Thrombosis and Vascular Research, University of New South Wales) and maintained in Dulbecco's modified Eagle's medium supplemented with 10% FBS. For experiments, cell monolayers were trypsinized, with HepG2 cells plated at 2×10^4 cells/ml and HFF plated at 5×10^3 cells/ml. The cells were fed on day 3 and used for experiments on day 4 of culture when they were approximately 80% confluent.

Analysis of Primary Rat Hepatocyte Cultures—On day 7 of culture, cells and medium were harvested from rat hepatocyte cultures. Protease inhibitors were added to conditioned medium after it was centrifuged 4000 × *g*, 10 min. The cells, on ice, were lysed in 2 ml of 0.25% Triton X-100, HBSC + protease inhibitors (as above) and clarified by centrifugation 4000 × *g* for 10 min at 4 °C. The conditioned medium (8 ml) and the whole cell lysate (4 ml) were diluted 1/5 in 20 mM Mes, pH 6.0, and mixed with 1 ml of DEAE-Sephacel (Pharmacia Biotech Inc.) equilibrated in 20 mM Mes, pH 6.0. After washing with 20 mM Mes, pH 6.0, the gel was eluted with 0.5-ml aliquots of 20 mM Mes, pH 6.0, 0.5 M NaCl. The eluted fractions (25 μl/lane) were electrophoresed on 6% SDS-PAGE gels, electroblotted onto polyvinylidene difluoride membrane, and incubated with ^{125}I-RAP, as described above.

Immunoprecipitation—HepG2 cells and HFF were plated in 60-mm Petri dishes in 10 ml of culture medium. When the cells were 80% confluent, the monolayers were washed twice with phosphate-buffered saline and incubated in 4 ml of cysteine/methionine-free EMEM, 10% FBS for 20 min at 37 °C. The cultures were then pulsed by incubation, 1 h, in the presence of 66 μCi/ml [^{35}S]methionine/cysteine (Tran^{35}S-label, ICN Biomedical). Long term labeling was conducted overnight in the presence of 20% cysteine/methionine complete EMEM. The chase period (0, 30, 60, 180, or 240 min) was initiated by the addition of 4 ml of EMEM, 10% FBS containing 0.2 mM unlabeled cysteine/methionine. Medium was collected and centrifuged 1200 × *g* for 5 min. Cell monolayers were washed twice with phosphate-buffered saline and lysed in the dish by the addition of 4 ml of 1% Triton, HBSC + protease inhibitors (as above) and clarified by centrifugation 4000 × *g* for 10 min at 4 °C. Samples were mixed with 25 μl of protein G-Sepharose (1:1 slurry, 30 min, 4 °C) and then incubated (4 °C, 2 h) in the presence or absence of 5 μg of anti-LRP α-chain mAb. After incubation with 25 μl of protein G-Sepharose (1:1 slurry, 30 min, 4 °C), the Sepharose was washed five times in 20 mM HEPES, 0.5 M NaCl, 0.1% Triton X-100, pH 7.4, suspended in 50 μl of SDS-PAGE sample buffer and electrophoresed on a 5–15% gradient SDS-PAGE gel. Gels were fixed in 10% acetic

acid, 50% methanol, soaked in Amplify (Amersham Life Science, Inc., Little Chalfont, United Kingdom), and dried before exposing to film for 3 days.

Degradation of ^{125}I-tPA by HepG2 Cells—HepG2 cells plated in 24-well culture dishes were washed three times in EMEM, 0.2% BSA and incubated in 2 ml of medium containing 3 nM ^{125}I-tPA in the presence or absence of the following ligands: 1) 1 μM unlabeled tPA, 2) 2 μg/ml (3.3 nM) purified placental LRP, and 3) 10 μg/ml (16.7 nM) purified placental LRP. After incubation for appropriate times, binding medium was removed and mixed with an equal volume of 20% trichloroacetic acid containing 4% phosphotungstic acid, incubated on ice for 10 min, centrifuged 10,000 $\times$ *g* for 5 min, and a 1-ml aliquot of supernatant was counted in a γ-counter to determine counts/min of ^{125}I-tPA degraded from triplicate cultures at each time point.

Determination of sLRP Concentration in Human Plasma—The LRP immunoassay was used to determine the concentration of sLRP in human plasma. A standard curve was prepared by diluting affinity-purified placental LRP in the concentration range 0.125–2.5 μg/ml. sLRP concentrations were calculated from the standard curve using a four parameter curve fit. A preliminary study was conducted to determine the effect of blood additives and storage conditions on the estimation of LRP concentration by the LRP immunoassay. To determine the range of LRP in normal human plasma, citrated plasma was obtained from 50 healthy blood donors giving informed consent. In addition, citrated plasma samples (n = 45) were collected by the Clinical Chemistry Department, Prince of Wales Hospital, Randwick, New South Wales, Australia. These plasma samples were obtained from patients with clinical manifestation of liver disease, which was confirmed by routine liver function test assessing plasma and urinary bilirubin, plasma alkaline phosphatase, plasma transaminases, plasma γ-glutamyltransferase. A third set of plasma samples from patients (n = 49) with non-insulin-dependent diabetes mellitus (NIDDM) were kindly provided by Drs T. Mori and D. Dunstan, Department of Hematology, Royal Perth Hospital, Western Australia.

RESULTS

Human Plasma Contains a Soluble Molecule with the Characteristics of LRP (sLRP)—An affinity matrix consisting of activated α_2M-Sepharose is able to deplete plasma of an LRP-like molecule detected using a specific LRP immunoassay (Fig. 1*A*). Consistent with Ca^{2+}-dependent ligand binding, the immunoreactivity was recovered by washing the column with 25 mM EDTA, pH 6.0 (Fig. 1*B*). Analysis of the EDTA eluate of human plasma adsorbed to α_2M-Sepharose by SDS-PAGE (reducing) revealed the presence of a single chain molecule which co-migrates with the α-chain of LRP (M_r 500,000) isolated from human placental membranes (Fig. 2*A*). The high molecular weight protein appears to be structurally and functionally related to human LRP α-chain, as it is recognized by an anti-LRP mAb (8G1) on Western blot and binds ^{125}I-RAP in a ligand blot (Fig. 2*A*). In contrast, a mAb specific for the COOH terminus of LRP β-chain (M_r 85,000) failed to specifically recognize any species in the enriched plasma fraction either by specific immunoassay (data not shown) or Western blot (Fig. 2*B*). A second, distinct anti-LRP mAb detected sLRP in the enriched plasma fraction, providing further evidence that the affinity eluate of human plasma contains a molecule closely related to LRP (Fig. 2*C*). A molecule of identical electrophoretic mobility was also recognized by an affinity-purified rabbit anti-human LRP polyclonal antibody (R777, a generous gift of Dr. Dudley Strickland, American Red Cross; data not shown).

sLRP Is Secreted by Primary Cultures of Rat Hepatocytes—Ligand blot analysis of culture medium conditioned by primary cultures of rat hepatocytes revealed the presence of a ^{125}I-RAP-binding protein that co-migrated on SDS-PAGE with human placental LRP and a cell-associated molecule in cellular lysates of cell rat hepatocytes (Fig. 3*A*). Prior to analysis the conditioned medium was concentrated 16-fold by ion exchange chromatography on DEAE-Sephacel. Immunoprecipitation of metabolically labeled human HepG2 and HFF cells with an anti-LRP α-chain antibody (8G1) failed to detect the accumulation of a soluble form of LRP in the supernatant medium after a 4-h chase (Fig. 3*B*). Cell-associated LRP was readily detected at each chase time point, *i.e.* from the end of the 1-h pulse onwards. Long term labeling experiments (up to 24 h) also failed to detect soluble forms of LRP in medium conditioned by these cells (data not shown).

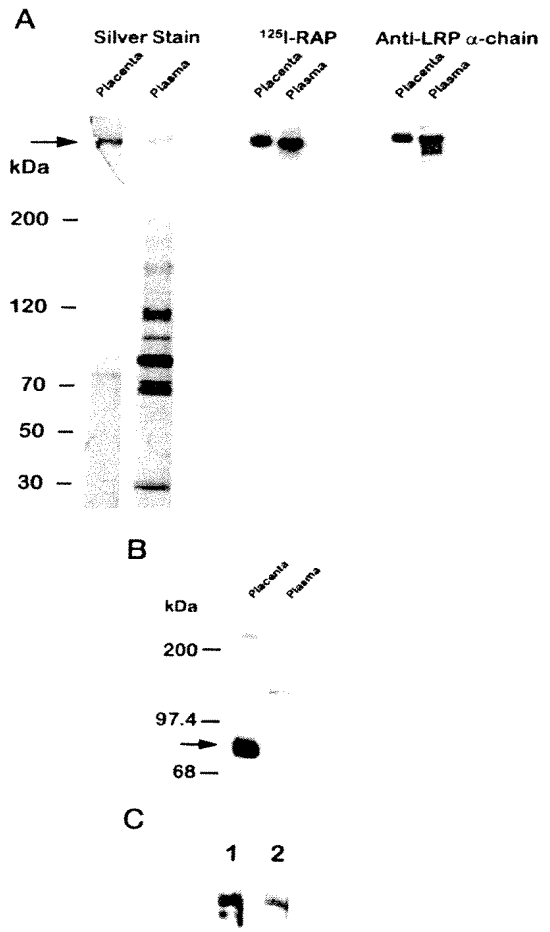

FIG. 2. **Characterization of affinity-isolated sLRP.** *A*, analysis of the plasma eluate (*lane 2*) by SDS-PAGE and silver stain revealed the presence of a band of M_r 500,000, which co-migrated with the α-chain of placental LRP (*lane 1, arrow*), was recognized by an anti-LRP α-chain mAb, 8G1, and bound ^{125}I-RAP on a ligand blot. *B*, LRP β-chain migrates on SDS-PAGE with M_r 85,000. The placental LRP preparation contains two molecules specifically recognized by the anti-LRP β-chain antibody: the strong band at M_r 85,000 represents the mature LRP β-chain (*arrow*), while the size of the weaker high molecular weight band (M_r >500,000) is consistent with incompletely processed LRP prohormone, which has not been cleaved into the two LRP subunits. The plasma affinity eluate did not contain a molecule that specifically reacted with the anti-LRP β-chain antibody. The band present at M_r 120,000 in *lane 2* was a nonspecific contaminant in this preparation, which was recognized directly by the secondary (rabbit anti-mouse Ig-horseradish peroxidase) antibody. *C*, further confirmation that the plasma affinity eluate contains a molecule closely related to LRP is provided by the recognition of a band, which co-migrated with placental LRP α-chain (not shown), by both the 8G1 mAb (*lane 1*) and a second, distinct anti-LRP α-chain mAb (*lane 2*) on Western blot.

A Soluble form of LRP Is Able to Perturb the Degradation of tPA by HepG2 Cells—The uptake and degradation of tPA has been demonstrated to be mediated by LRP and can be inhibited by the LRP antagonist RAP (14). Ligand blot analysis demonstrates that both the purified placental LRP and the plasma-

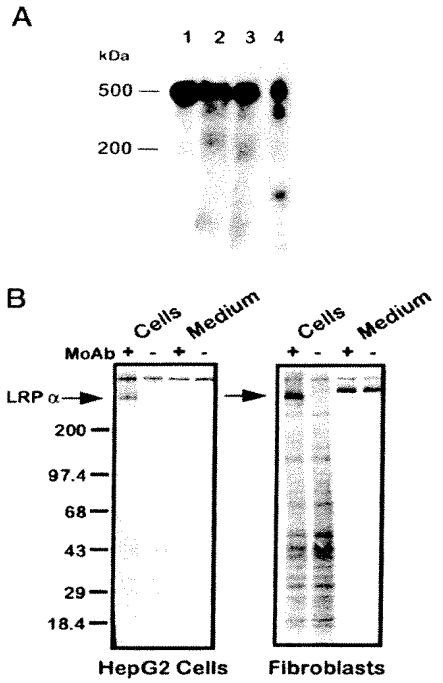

FIG. 3. **sLRP is released by cultured primary rat hepatocytes.** *A*, rat hepatocytes were cultured for 7 days in serum-free medium on matrigel to maintain a differentiated phenotype characteristic of adult liver. Samples, prepared as described under " Materials and Methods," were electrophoresed on 6% SDS-PAGE gels for ligand blot analysis. Blots were incubated with ^{125}I-RAP to detect LRP in human placental LRP (40 ng; *lane 1*), hepatocyte cell lysate (*lane 2*), hepatocyte cell lysate eluted from DEAE-Sephacel (*lane 3*), and rat hepatocyte conditioned medium concentrated 16-fold on DEAE-Sephacel (*lane 4*). *B*, monolayer cultures of human HepG2 and foreskin fibroblast cells were biosynthetically labeled by incubation at 37 °C in [^{35}S]Cys/Met containing medium. At selected chase time points, medium and cells were collected and immunoprecipitated with an anti-LRP mAb, as described under "Materials and Methods." Immunoprecipitates were electrophoresed on 5–15% gradient SDS-PAGE gels and processed for autoradiography. Autoradiographs from the 4-h chase time point are shown above. + indicates immunoprecipitate obtained with anti-LRP mAb, and − indicates negative control in which no antibody was present. The position of specifically immunorprecipitated LRP α-chain is marked by the *arrow*.

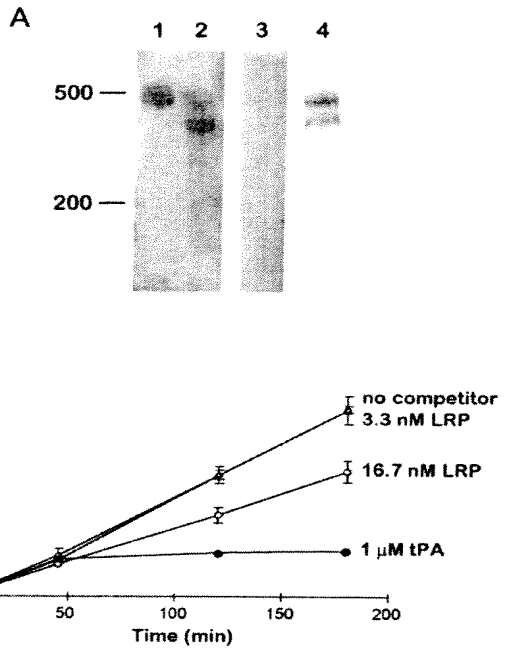

FIG. 4. **A soluble form of LRP inhibits the degradation of ^{125}I-tPA by HepG2 cells.** *A*, ligand blot analysis confirms that placental LRP is able to bind ^{125}I-tPA·PAI-1 complexes in a ligand blot (*lane 1*). Similarly, the circulating molecule enriched from human plasma by α_2M-Sepharose affinity chromatography binds ^{125}I-tPA·PAI-1 complexes in a ligand blot (*lane 2*). The specificity of binding is indicated by the absence of binding in the presence of excess unlabeled tPA (*lane 3*). The faster migrating, second band binding ^{125}I-tP·PAI-1 in *lane 2* was also recognized by the anti-LRP mAb 8G1 (*lane 4*) and frequently appears after storage of the affinity eluate. *B*, HepG2 monolayers were incubated at 37 °C with 4 nM ^{125}I-tPA diluted in Dulbecco's modified Eagle's medium, 1% BSA in the presence or absence of competitors as indicated. Endocytosis and degradation of the ligand were indicated by the appearance of trichloroacetic acid-soluble counts/min in the culture supernatant. Each symbol represents the average of triplicate determinations ± S.D.

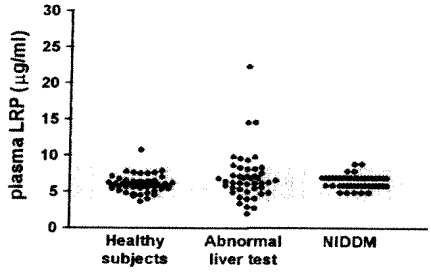

FIG. 5. **The plasma concentration of sLRP is altered in patients with liver disease.** The normal concentration range of sLRP in the plasma of healthy subjects (n = 50), estimated using the LRP immunoassay, is shown alongside that detected in patients (n = 45) displaying abnormal liver function and patients with NIDDM (n = 49). The normal concentration range of plasma sLRP concentration is indicated by the *hatched area* on the graph; this area corresponds to the mean concentration in the healthy subjects (6.1 μg/ml) ± 2 S.D. (±2.4).

derived sLRP bind ^{125}I-tPA·PAI-1 complexes (Fig. 4*A*). Fig. 4*B* demonstrates the inhibition of ^{125}I-tPA degradation by HepG2 cells when assays were conducted in the presence of 10 μg/ml (16.7 nM) purified placental LRP.

Plasma sLRP Levels Are Increased in Patients with Liver Disease—sLRP levels were measured in healthy subjects to define the normal concentration range. The plasma sLRP concentration estimated using the LRP immunoassay did not vary significantly when blood from healthy donors was collected into a dry tube (serum, 6.9 μg/ml), EDTA (6.5 μg/ml), or citrate (6.8 μg/ml), when samples were assayed at 10–20-fold dilution in Ca^{2+}-containing assay buffer. Addition of 10 IU/ml heparin to the assay buffer to prevent postdilution clotting also did not interfere with the estimation of sLRP concentration. The range of sLRP concentration detected in the plasma of healthy subjects (n = 50; mean 6.1 ± 1.2 μg/ml; range 3.7–10.8 μg/ml), patients with abnormal liver function (n = 45; mean 7.1 ± 3.44 μg/ml, range = 2.0–22.4 μg/ml), and patients with NIDDM (n = 49; mean 6.5 ± 0.9 μg/ml, range = 5.0–9.0 μg/ml) is shown in Fig. 5. The plasma concentration of sLRP was significantly altered (varied by >2 S.D. from the mean normal concentration, *i.e.* outside the range 3.7–8.5 μg/ml) in 24% plasma samples from patients with abnormal liver function. In the NIDDM disease control group, only two plasma samples (4%) contained a significantly altered sLRP concentration (both above 8.5 μg/ml). The altered plasma sLRP concentrations associated with

abnormal liver function test did not correlate with disease etiology nor with the level of any plasma proteins assayed, including bilirubin, alkaline phosphatase, transaminases, γ-glutamyltransferase or 5′-nucleotidase.

DISCUSSION

LRP belongs to the low density lipoprotein receptor family, the members of which share many structural and functional characteristics (3). The α-chain of the heterodimeric LRP contains multiple, Ca^{2+}-dependent ligand binding domains and is noncovalently bound on the cell surface to the membrane-spanning β-chain (15). The characteristics of the soluble molecule circulating in human plasma suggest it is a molecule closely related to the α-chain of LRP: it displays Ca^{2+}-dependent binding to two established LRP ligands RAP and activated α_2M, a ligand uniquely recognized by LRP; it is a single chain molecule which co-migrates on SDS-PAGE with authentic human placental LRP α-chain; and it is recognized by two distinct anti-LRP α-chain monoclonal antibodies. We were unable to detect the intracellular COOH terminus of the LRP β-chain in the affinity-isolated sLRP. However, it is possible that a truncated β-chain may be associated with the soluble α-chain. Precise determination of the exact structure of plasma sLRP and its relative affinity for the various LRP ligands will only be possible with a highly purified preparation of sLRP. These studies are currently under way. The presence of a circulating LRP-like molecule is not confined to human plasma, and a similar molecule has been detected in plasma and serum from a variety of mammals and the chicken.[2]

LRP is most highly expressed in the liver, and analysis of culture medium conditioned by primary cultures of rat hepatocytes revealed the presence of an sLRP-like ^{125}I-RAP-binding protein. Our experiments could not detect the release of a soluble form of LRP from the human hepatoma cell line HepG2, nor from cultured normal human fibroblasts, suggesting that the release of sLRP is not a constitutive property of all cultured cells. The absence of sLRP in medium conditioned by the hepatoma cell line suggests that the production of sLRP may be associated with the more differentiated phenotype of the primary hepatocytes cultured on matrigel (16). Further studies are required to investigate the factors regulating the production of sLRP.

The detection of sLRP in hepatocyte-conditioned medium provides a model system for the further characterization of sLRP and the elucidation of the mechanism generating the soluble form. A wide variety of receptors and other plasma membrane proteins have been identified as having soluble counterparts in serum (17). There are examples in the literature of soluble receptors liberated by proteolytic cleavage of receptor exodomains (18, 19) and those that derive from differential splicing of a common mRNA transcript or transcription of closely related, but distinct, genes (20). In the case of LRP, another potential mechanism for the generation of sLRP could be the disruption of the noncovalent bond that anchors the α-chain to the membrane-spanning β-chain (15). A soluble form of gp330, another member of the low density lipoprotein receptor family, has been detected in the supernatant of a yolk sac carcinoma cell line (21). Interestingly, in this cell line gp330 was present on the cell surface and in supernatant as a complex with RAP. No further characterization of the cellular and molecular events regulating gp330/RAP release has been reported.

Soluble receptors, generally, have reduced ligand affinity constants compared with their membrane-bound counterparts, and the circulating receptor concentration may be insufficient to effectively compete ligand binding to the cell-bound molecule (22). Our preliminary experiment indicates that the addition of soluble purified placental LRP at a physiologically relevant concentration (10 μg/ml) was able to inhibit the degradation of tPA by cultured HepG2 cells, a process that has been demonstrated previously to be mediated by cell surface LRP (14). This indicates that the sLRP may act as a competitive inhibitor of ligand uptake by cell surface-bound LRP. The inhibition of tPA uptake by soluble LRP may have negligible consequences to the level of extracellular proteolysis, because the enzyme is rapidly inactivated before endocytosis by complex formation with plasminogen activator inhibitor-I (PAI-1), present in large excess in the extracellular matrix of HepG2 cells (23, 24). However, LRP mediates the uptake of many biologically active molecules, including the potent angiogenesis inhibitor, thrombospondin (25), apoE-enriched lipoproteins (26), lipoprotein-lipase (27), and is able to bind directly active tPA (28) and urokinase PA (29). Increased levels of soluble LRP may extend the half-life of these active ligands and influence diverse biological processes, including lipid metabolism, cell growth, and migration and extracellular proteinase activity.

The identification of a soluble molecule with the characteristics of LRP introduces a new dimension into the biology of this unique molecule. Further studies are required to understand the biochemical mechanisms involved in the generation of sLRP and establish its physiological role. The concentration of plasma sLRP appears to alter in some patients with impaired liver function. A more extensive study is required to substantiate this preliminary data and elucidate the functional implications of the moderate changes. As LRP has been implicated to be overexpressed in a range of other pathological processes, including atherosclerosis (30) and Alzheimer's disease (31), the functional or prognostic implications of plasma sLRP concentration requires investigation.

Acknowledgment—We thank Dr. Philip Hogg for critical reading of the manuscript.

REFERENCES

1. Herz, J., Hamann, U., Rogne, S., Myklebost, O., Gausepohl, H., and Stanley, K. K. (1988) *EMBO J.* **7,** 4119–4127
2. Strickland, D. K., Ashcom, J. D., Williams, S., Burgess, W. H., Migliorini, M., and Argraves, W. S. (1990) *J. Biol. Chem.* **265,** 17401–17404
3. Krieger, M., and Herz, J. (1994) *Annu. Rev. Biochem.* **63,** 601–637
4. Strickland, D. K., Kounnas, M. Z., and Argraves, W. S. (1995) *FASEB J.* **9,** 890–898
5. Herz, J., Goldstein, J. L., Strickland, D. K., Ho, Y. K., and Brown, M. S. (1991) *J. Biol. Chem.* **266,** 21232–21238
6. Herz, J., Clouthier, D. E., and Hammer, R. E. (1992) *Cell* **71,** 411–421
7. Kurecki, T., Kress, L. F., and Laskowski Sr, M. (1979) *Anal. Biochem.* **99,** 415–420
8. Ehrlich, H. J., Gebbink, R. K., Keijer, J., Linders, M., Preissner, K. T., and Pannekoek, H. (1990) *J. Biol. Chem.* **265,** 13029–13035
9. Sancho, E., Tonge, D., Hockney, R., and Booth, N. (1994) *Eur. J. Biochem.* **224,** 125–134
10. Ashcom, J. D., Tiller, S. E., Dickerson, K., Cravens, J. L., Argraves, W. S., and Strickland, D. K. (1990) *J. Cell Biol.* **110,** 1041–1048
11. Morrissey, J. H. (1981) *Anal. Biochem.* **117,** 307–310
12. Goodwin, B., Liddle, C., Murray, M., Tapner, M., Rooney, T., and Farrell, G. (1996) *Biochem. Pharmacol.* **52,** 219–227
13. Kleinman, H., McGarvey, M., Hassell, J., Star, V., Cannon, F., Laurie, G., and Martin, G. (1986) *Biochemistry* **25,** 312–318
14. Bu, G., Williams, S., Strickland, D. K., and Schwartz, A. L. (1992) *Proc. Natl. Acad. Sci. U. S. A.* **89,** 7427–7431
15. Herz, J., Kowal, R. C., Goldstein, J. L., and Brown, M. S. (1990) *EMBO J.* **9,** 1769–1776
16. Scheutz, E. G., Li, D., Omiecinski, C. J., Muller-Eberhard, U., Kleinman, H. K., Elswick, B., and Guzelian, P. S. (1988) *J. Cell. Physiol.* **134,** 309–323
17. Ehlers, M. R. W., and Riordan, J. F. (1991) *Biochemistry* **30,** 10065–10071
18. Lantz, M., Gulberg, U., Nilsson, E., and Olsson, I. (1990) *J. Clin. Invest.* **86,** 1396–1402
19. Rutledge, E. A., Green, F. A., and Enns, C. A. (1994) *J. Biol. Chem.* **269,** 31864–31868
20. Horiuchi, S., Koyanagi, Y., Zhou, Y., Miyamoto, H., Tanaka, Y., Waki, M., Matsumoto, A., Yamamoto, M., and Yamamoto, N. (1994) *Eur. J. Immunol.* **24,** 1945–1948
21. Orlando, R. A., and Farquhar, M. G. (1993) *Proc. Natl. Acad. Sci. U. S. A.* **90,** 4082–4086

[2] P. G. Grimsley, K. A. Quinn, and D. A. Owensby, manuscript in preparation.

22. Rose-John, S., and Heinrich, P. C. (1994) *Biochem. J.* **300,** 281–290
23. Owensby, D. A., Sobel, B. E., and Schwartz, A. L. (1988) *J. Biol. Chem.* **263,** 10587–10594
24. Owensby, D. A., Morton, P. A., and Schwartz, A. L. (1989) *J. Biol. Chem.* **264,** 18180–18187
25. Mikhailenko, I., Kounnas, M. Z., and Strickland, D. K. (1995) *J. Biol. Chem.* **270,** 9543–9549
26. Kowal, R. C., Herz, J., Goldstein, J. L., Esser, V., and Brown, M. S. (1989) *Proc. Natl. Acad. Sci. U. S. A.* **86,** 5810–5814
27. Chappell, D. A., Fry, G. L., Waknitz, M. A., Muhonen, L. E., Pladet, M. W., Iverius, P.-H., and Strickland, D. K. (1993) *J. Biol. Chem.* **268,** 14168–14175
28. Bu, G., Morton, P. A., and Schwartz, A. L. (1992) *J. Biol. Chem.* **267,** 15595–15602
29. Kounnas, M. Z., Henkin, J., Argraves, W. S., and Strickland, D. K. (1993) *J. Biol. Chem.* **268,** 21862–21867
30. Lupu, F., Heim, D., Bachmann, F., and Kruithof, E. K. O. (1994) *Arterioscler. Thromb. Vasc. Biol.* **14,** 1438–1444
31. Rebeck, G. W., Reiter, J. S., Strickland, D. K., and Hyman, B. T. (1993) *Neuron* **11,** 575–580

THE JOURNAL OF BIOLOGICAL CHEMISTRY

Vol. 272, No. 16, Issue of April 18, pp. 10761–10768, 1997
Printed in U.S.A.

Differential Functions of Triplicated Repeats Suggest Two Independent Roles for the Receptor-associated Protein as a Molecular Chaperone*

(Received for publication, December 10, 1996, and in revised form, January 27, 1997)

Lynn M. Obermoeller, Ilka Warshawsky, Mark R. Wardell‡, and Guojun Bu§

From the Edward Mallinkrodt Department of Pediatrics and the ‡Department of Biochemistry and Molecular Biophysics, Washington University School of Medicine, St. Louis, Missouri 63110

The 39-kDa receptor-associated protein (RAP) is a molecular chaperone for the low density lipoprotein receptor-related protein (LRP), a large endocytic receptor that binds multiple ligands. The primary function of RAP has been defined as promotion of the correct folding of LRP, and prevention of premature interaction of ligands with LRP within the early secretory pathway. Previous examination of the RAP sequence revealed an internal triplication. However, the functional implication of the triplicated repeats was unknown. In the current study using various RAP and LRP domain constructs, we found that the carboxyl-terminal repeat of RAP possesses high affinities to each of the three ligand-binding domains on LRP, whereas the amino-terminal and central repeats of RAP exhibit only low affinity to the second and the fourth ligand-binding domains of LRP, respectively. Using truncated soluble minireceptors of LRP, we identified five independent RAP-binding sites, two on each of the second and fourth, and one on the third ligand-binding domain of LRP. By coexpressing soluble LRP minireceptors and RAP repeat constructs, we found that only the carboxyl-terminal repeat of RAP was able to promote the folding and subsequent secretion of the soluble LRP minireceptors. However, when the ability of each RAP repeat to inhibit ligand interactions with LRP was examined, differential effects were observed for individual LRP ligands. Most striking, both the amino-terminal and central repeats, but not the carboxyl-terminal repeat, of RAP inhibited the interaction of α_2-macroglobulin with LRP. These differential functions of the RAP repeats suggest that the roles of RAP in the folding of LRP and in the prevention of premature interaction of ligand with the receptor are independent.

The 39-kDa receptor-associated protein (RAP)[1] is an unique receptor antagonist. The target receptors for RAP are cysteine-rich endocytic receptors that belong to the low density lipoprotein (LDL) receptor family (1). The four representative receptors in this family are the LDL receptor (2), the LDL receptor-related protein (LRP, Ref. 3), glycoprotein gp330/megalin (4), and the VLDL receptor (5). Among these receptors, LRP and gp330/megalin are large multifunctional receptors with multiple ligand-binding domains, which bind several structurally and functionally distinct ligands (for reviews, see Refs. 1 and 6). While RAP exhibits high affinities for LRP, gp330/megalin, and the VLDL receptor, it binds only weakly to the LDL receptor (7). Upon binding to these receptors, RAP inhibits the binding and/or endocytosis of all the ligands by the receptors. This unique feature of RAP has allowed its extensive use in biological studies of these endocytic receptors. Recent evidence has suggested that, under normal physiological conditions, RAP is an endoplasmic reticulum (ER) resident protein and functions within the early secretory pathway (8–10). Using LRP as the target protein, it was found that RAP retained within the ER functions as a regulator of LRP activity by transiently interacting with LRP and maintaining LRP in an inactive ligand-binding state. As RAP dissociates from LRP in response to the lower pH within the Golgi, LRP becomes active as it transits to the cell surface (9). The role of RAP in the maturation and trafficking of LRP is further supported by gene-knockout studies (11), which demonstrate that cells lacking RAP exhibit a 75% reduction of functional LRP.

LRP is the largest endocytic receptor identified to date (~600 kDa). It is synthesized as a single polypeptide chain and cleaved in the *trans*-Golgi into two subunits (12, 13). The 515-kDa extracellular subunit contains 31 copies of complement-type ligand-binding domains arranged in four clusters with 2, 8, 10, and 11 repeats, respectively (1, 3). Also present in this subunit are 22 copies of cysteine-rich epidermal growth factor (EGF) precursor-type repeats which flank the ligand-binding domains. The complement-type repeats in LRP are similar to those in the LDL receptor in which the 40-residue-long cysteine-rich repeats exhibit a highly conserved spacing pattern of six cysteine residues that form three intramolecular disulfide bonds (14). The disulfide bonds are believed to be important for the stability of the ligand-binding sites on the receptor. The complexity of LRP's structure, largely due to the extensive intradomain disulfide bonds, presents a challenging task for proper folding during its biosynthesis. This process may well be assisted by molecular chaperone(s) within the ER. Indeed, using anchor-free, soluble mini-receptors that represent each of the four putative ligand-binding domains of LRP (SLRPs), our most recent studies (15) showed that coexpression of RAP is both necessary and sufficient for the correct folding and subsequent secretion of the SLRPs. Without the coexpression of RAP, SLRPs are misfolded due to the formation of intermolec-

* This work was supported by American Cancer Society Research Project Grant RPG-97-010-01-CB (to G. B.) and Alzheimer Association Faculty Scholar Award FSA95-051 (to G. B.). The costs of publication of this article were defrayed in part by the payment of page charges. This article must therefore be hereby marked "*advertisement*" in accordance with 18 U.S.C. Section 1734 solely to indicate this fact.

§ To whom all correspondence should be addressed: Dept. of Pediatrics, Washington University School of Medicine, One Children's Place St. Louis, MO 63110. Tel.: 314-454-2726; Fax: 314-454-2685; E-mail: bu@kids.wustl.edu.

[1] The abbreviations used are: RAP, receptor-associated protein; LDL, low density lipoprotein; VLDL, very low density lipoprotein; LRP, LDL receptor-related protein; SLRP, soluble LRP; ER, endoplasmic reticulum; PCR, polymerase chain reaction; GST, glutathione *S*-transferase; t-PA, tissue-type plasminogen activator; α_2M*, protease- or methylamine-activated α_2-macroglobulin; EGF, epidermal growth factor; HA, hemagglutinin.

ular disulfide bonds and are retained within the ER with little secretion. It is not known at present whether the role of RAP in the receptor's folding is independent from its function in preventing premature ligand interaction with the receptor.

The HNEL tetrapeptide at the carboxyl terminus of RAP has been shown to mediate its ER localization and retention (9). In addition to this ER-retention signal, examination of the RAP sequence also identified an internal triplication (9). In the present study, using various molecular and cellular approaches, we have analyzed the function of each of the three repeats of RAP. We found that while the carboxyl-terminal repeat of RAP functions similarly to the full-length RAP in terms of interacting with the receptor and in assisting the receptor to fold, inhibition of at least one LRP ligand, α_2-macroglobulin, can only be achieved with the amino-terminal or the central repeats of RAP. These differential functions of the RAP repeats suggest that the functions of RAP in receptor folding and inhibition of ligand interactions are independent.

MATERIALS AND METHODS

Construction of cDNAs for SLRPs—Construction of cDNAs for SLRP1, SLRP2, SLRP3, and SLRP4 using polymerase chain reaction (PCR) have been described previously (15). The same strategies were used for generating additional soluble minireceptors of LRP with an HA tag inserted after the signal cleavage site. All oligonucleotides were synthesized in the Washington University School of Medicine Protein Chemistry Laboratory. The regions represented in the new SLRPs are illustrated in Fig. 4, and contain the following amino acid sequences (3): SLRP2N, 787–994; SLRP2C, 995–1244; SLRP2N-EGF, 826–994; SLRP2C-EGF, 995–1164; SLRP3N, 2462–2712; SLRP3C, 2713–3004; SLRP4N, 3274–3553; and SLRP4C, 3554–3843.

Construction of cDNAs for RAP Repeats—Construction of RAP repeats for cell-transfection was carried out via two sequential steps of subcloning. In the first step, the 5′ fragment of RAP (signal peptide + amino acids 1–17) was generated by PCR using pcDNA-RAP (9) as the template and the following two primers: forward primer (5′-GATCAAGCTTGGATGATGGCGCCGCGGAGGGTCA-3′) and reverse primer (5′-GATCGGATCCCATCATCATCATCATAGCGTAGTCCGGGACGTCGTACGGGTATCCGGACTCGCGTTTCGGGGACGG-3′). The reverse primer contained a sequence encoding an HA epitope and five methionine residues. The HA epitope sequence, YPYDVPDVA, is derived from influenza hemagglutinin and can be recognized by a monoclonal anti-HA antibody, 12CA5 (16). The resulting PCR product was subcloned into pcDNA3 vector, and the resulting plasmid, termed pcDNA-RAP5′, was used as the base vector for generating various constructs of RAP. In the second step, the carboxyl-terminal portions of RAP (amino acids 18–323, 18–110, 91–210, 191–323, or 18–250) were generated by PCR and subcloned into pcDNA-RAP5′. The resulting plasmids were used for cell transfection.

The methods for constructing GST/RAP constructs have been described previously (9).

Cell Culture and Transfection—Human glioblastoma U87 cells were cultured in Earle's minimum essential medium supplemented with 10% fetal calf serum, 2 mM L-glutamine, 100 units/ml penicillin, 100 μg/ml streptomycin, 1 mM sodium pyruvate, and maintained at 37 °C in humidified air containing 5% CO_2 (8). For transient transfection, U87 cells were transfected with various plasmids at 40–60% confluence using a calcium phosphate precipitation method (17). For each well of six-well dishes (3.5 cm in diameter), 10 μg of DNA were used in a total volume of 4 ml of medium. Sixteen hours after the start of transfection, cells were washed with medium and cultured continuously for an additional 24 h before use in experiments. The efficiency of transient transfection in these studies was consistently about 20–30% as assessed by immunofluorescent staining of expressed proteins.

Metabolic and Pulse-Chase Labeling—Metabolic labeling with [^{35}S]methionine or [^{35}S]cysteine was performed essentially as described before (9). For pulse-chase experiments, cells were pulse-labeled for 1 h and chased with serum-containing medium for 3 h.

Antibodies, Immunoprecipitation, and SDS-Polyacrylamide Gel Electrophoresis—Polyclonal anti-RAP and anti-LRP antibodies have been described before (9). Monoclonal anti-HA antibody was obtained from BabCo (12CA5). Immunoprecipitations were carried out essentially as described before (18), except the washing buffer for monoclonal anti-HA antibody contained 0.1% SDS instead of 1% SDS. Preliminary experiments were performed to ensure that the primary antibody used in each immunoprecipitation was in excess. Protein A-agarose beads were used to precipitate protein-IgG complexes. The immunoprecipitated material was released from the beads by boiling each sample for 5 min in Laemmli sample buffer (62.5 mM Tris-HCl, pH 6.8, 2% (w/v) SDS, 10% (v/v) glycerol) (19). If the immunoprecipitated material was analyzed under reducing conditions, 5% (v/v) β-mercaptoethanol was included in the Laemmli sample buffer. The percentage of SDS-polyacrylamide gels is indicated in each figure legend. Rainbow molecular weight markers (Bio-Rad) were used as the molecular weight standards.

Interaction of GST/RAP Constructs with SLRPs—GST or GST/RAP constructs were electrophoresed on SDS gels and transferred to nitrocellulose membrane. After blocking with tissue culture medium, membranes were incubated with conditioned media harvested from SLRP and RAP cDNAs-cotransfected cells. The bound SLRPs were then detected with anti-HA antibody and enhanced chemiluminescence (ECL, Amersham).

Ligand Blotting, Binding, and Degradation Analysis—For ligand blotting analysis, purified human LRP was electrophoresed on SDS gel and transferred to nitrocellulose membrane. Strips of membrane were then incubated with GST or GST/RAP constructs, and bound proteins were detected using anti-GST antibody. For binding and degradation analysis, GST/RAP fusion proteins were subjected to thrombin cleavage and cleaved GST was removed with glutathione agarose beads (20). The resulting recombinant proteins of RAP constructs (RAP-(1–323), RAP-(1–110), RAP-(91–210), and RAP-(191–323)) were used for competition assays. Each of analyzed RAP and its constructs was iodinated using the IODOGEN method (21). Binding of ^{125}I-RAP to U87 cells in the absence or the presence of cold competitor has been described previously (8). All the LRP ligands tested have been described before (23–26). Each of these ligands was iodinated and used for cellular degradation analysis by measuring cell-mediated trichloroacetic acid-soluble radioactivity released into the overlying medium, in the absence or the presence of excess unlabeled RAP constructs. Each assay was carried out in triplicate, and the standard deviations were used for error bars.

RESULTS

Sequence Analysis for RAP—In our previous studies (9), we noted a possible internal triplication in the primary structure of RAP. However, the boundaries and the relationship among the three repeats were not clear. In the present studies, we have used several DNA computer analysis programs to examine the RAP sequence. Shown in Fig. 1 is the sequence analysis using the GCG package (Program Manual for the Wisconsin Package, version 8, Genetics Computer Group). The programs Compare and Dotplot examine the sequence homology by identifying both identical and similar residues along the sequence. When RAP was compared with itself using a window of 30 residues and a stringency of 15 residues, we found significant homology between regions within 1–100 and 201–300, as well as between regions 101–200 and 201–300 (Fig. 1*A*). Only scattered homology was found between regions of 1–100 and 101–200. Thus, we assigned the RAP sequence into three repeats approximately equal in sizes (repeat 1 = 1–100; repeat 2 = 101–200; repeat 3 = 201–323). Using these boundaries, we compared the sequence homology among the three repeats. The lower homology between repeat 1 and repeat 2 prompted us to compare each of the two repeats separately, using the Gap program of the GCG package. We found that both repeat 1 and repeat 2 have high homology with repeat 3 (46.4% and 45.5% similarity, respectively), whereas repeat 1 and repeat 2 have relatively low homology (38.9% similarity). Thus, we speculate that if the three repeats of RAP were derived from the same ancestral sequence, repeat 1 and repeat 2 may have been derived from repeat 3 separately during evolution. Two regions between repeat 1 and 3 were further identified for high homology, which are represented by the two elongated homology lines in Fig. 1*A*. Only one (albeit longer) region was found between repeat 2 and repeat 3 that shares high homology. These homologous regions are graphically illustrated in Fig. 1*B*.

Differential Interactions of RAP Repeats with LRP—To analyze whether each of the three triplicated repeats interact similarly with LRP, we performed ligand blotting analysis us-

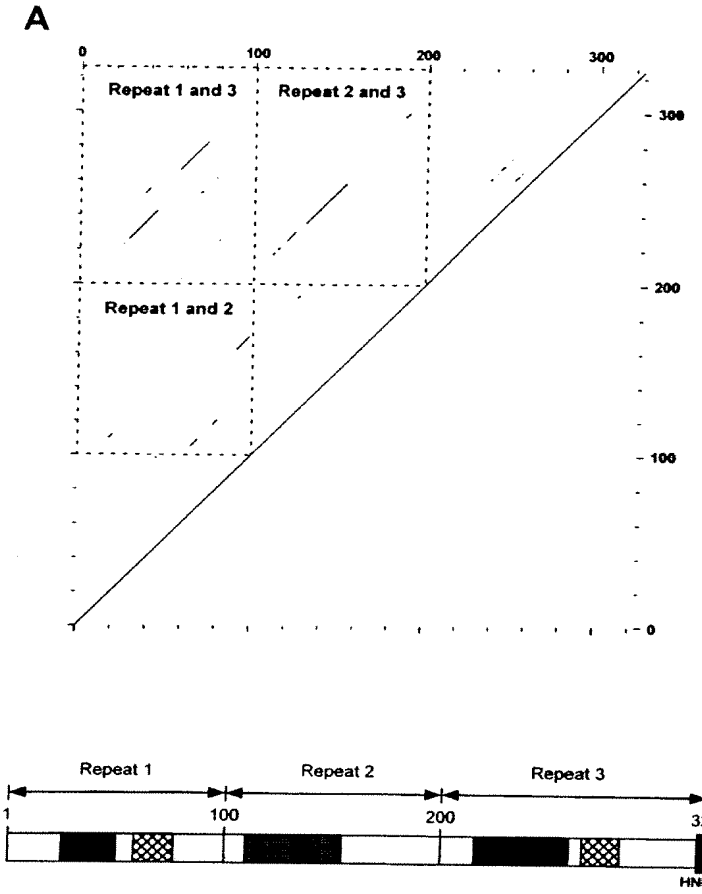

FIG. 1. **Internal triplication of RAP.** Protein sequence analysis of human RAP was performed using GCG package. *A*, linear sequence comparison of RAP (323 residues) to itself using the Compare and Dotplot programs of GCG with a window of 30 residues and a stringency of 15 residues. Region of 1–100 is defined as repeat 1, 101–200 is defined as repeat 2, and 201–323 is defined as repeat 3. *Dots* are generated when a homology is found, and *lines* are regions where continuous homology (*dots*) are found. *B*, graphical illustration of internal triplicated repeats of RAP. The *black* and *cross-hatched boxes* are high homologous regions between repeat 1 and repeat 3. The *stippled boxes* represent high homologous regions between repeat 2 and repeat 3. The ER-retention signal HNEL at the carboxyl terminus is also labeled.

ing GST/RAP constructs representing each of the three repeats (9). In addition to the full-length RAP (GST/RAP-(1–323)), three GST/RAP repeat constructs were made, which slightly overlapped at the assigned boundaries (*i.e.* GST/RAP-(1–110), GST/RAP-(91–210), and GST/RAP-(191–323), see Fig. 2*A*). When these GST fusion proteins were tested for interaction with LRP via ligand blotting (Fig. 2*B*), we found that repeat 3 possessed similar affinity for LRP as full-length RAP. Although they have much lower affinities, repeat 1 and repeat 2 of RAP also appear to be capable of interacting with LRP. Due to low specific radioactivity following iodination of repeats 1 and 2, we were unable to conclusively compare the affinities of RAP repeats with LRP on the cell surface directly. However, to examine the relationships of these interactions at the cell surface, we performed competition analysis for the binding of full-length RAP to U87 cells (8, 9) by each of the RAP repeat constructs. To eliminate potential steric hindrance effects of GST on ligand inhibition, we removed the GST portion from each of the fusion constructs, and thereafter repurified the resulting RAP fragments. Shown in Fig. 2*C* are the binding of either ^{125}I-RAP-(1–323) or ^{125}I-RAP-(191–323) to U87 cells in the absence or the presence of excess unlabeled competitors (100-fold excess). As seen in the figure, in addition to the full-length RAP, only repeat 3, but not repeats 1 and 2, demonstrated inhibition of the binding of ^{125}I-RAP-(1–323). For binding of ^{125}I-RAP-(191–323), both unlabeled full-length RAP and repeat 3 maximally inhibited, while repeat 1 and repeat 2 inhibited binding slightly. These results suggest that, among the three repeats of RAP, the third repeat possesses the highest affinity for LRP, consistent with the results obtained from the ligand blotting analysis.

Differential Interactions of RAP Repeats with Ligand-binding Domains of LRP—In our previous studies, we have shown that RAP binds to the second, third, and fourth ligand-binding domains of LRP (15). To analyze to which of the ligand-binding domains each of the RAP repeat binds, we performed experiments in which potential interactions between a given RAP repeat and a given ligand-binding domain of LRP were examined. Ligand-binding domains of LRP were represented by SLRPs, which upon coexpression with RAP, are secreted into the media (15) (also see illustrations in Fig. 4 for schematic representations of SLRPs). GST/RAP constructs, separated via SDS-polyacrylamide gel electrophoresis, were transferred onto nitrocellulose and incubated with conditioned media containing SLRP2 (Fig. 3*A*), SLRP3 (Fig. 3*B*), or SLRP4 (Fig. 3*C*). The SLRPs that interacted with GST/RAP constructs were then detected using anti-HA antibody (15). As seen in the figures, no interaction of the negative control, GST, with any SLRP was detected. Both full-length RAP (GST/RAP-(1–323)) and repeat 3 of RAP (GST/RAP-(191–323)) interacted with each of the three SLRPs, suggesting that repeat 3 of RAP contains the binding determinants for interacting with each of the three ligand-binding domains on LRP. Weak interaction of repeat 1 of RAP was detected only with SLRP2, whereas weak interaction of repeat 2 of RAP was seen with only SLRP4. These weaker interactions were enhanced when the amounts of GST/RAP fusion protein were increased by 10-folds (as is the case presented in Fig. 3). These results suggest differential interac-

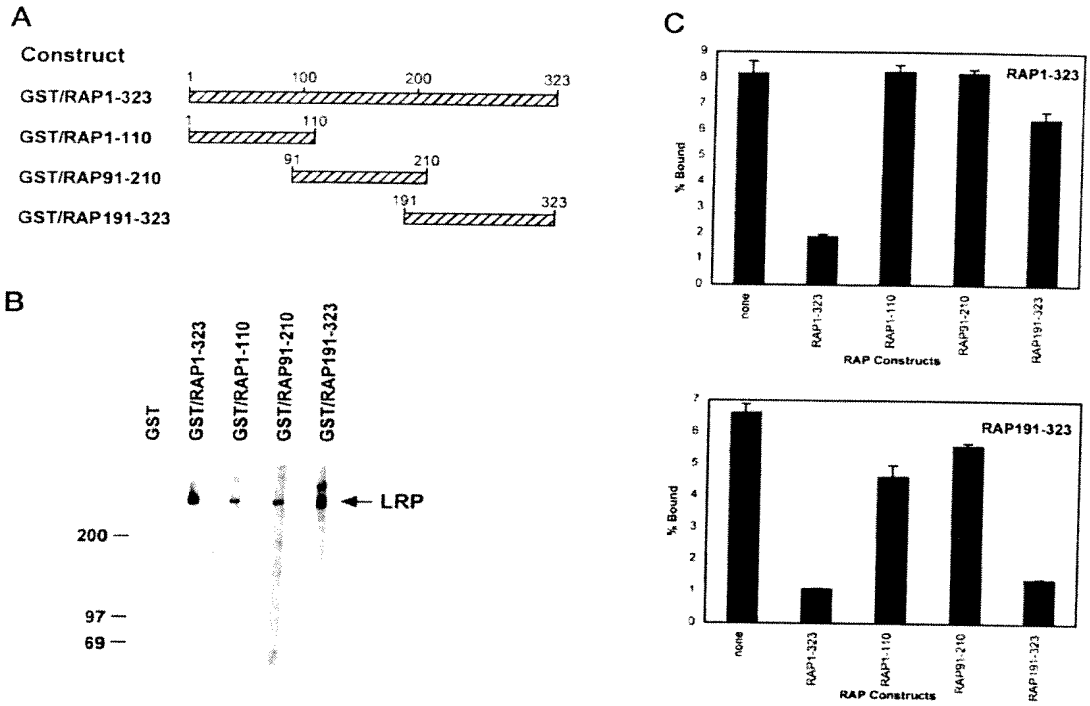

FIG. 2. **Interaction of triplicated repeats with LRP.** *A*, schematic representation of GST/RAP constructs. *Numbers* represent amino acid residue positions. *B*, ligand blotting of GST/RAP constructs to LRP. Purified human LRP was electrophoresed on 5% SDS gel and transferred to nitrocellulose membrane. Strips of membrane were then incubated with GST or GST/RAP constructs, and bound proteins were detected using anti-GST antibody and enhanced chemiluminescence (ECL, Amersham) detection method. *C*, competition of ^{125}I-RAP-(1–323) or ^{125}I-RAP-(191–323) binding to U87 cells by RAP repeat constructs. Binding of ^{125}I-RAP-(1–323) or ^{125}I-RAP-(191–323) (4 nM) to U87 cells was performed in the absence or presence of unlabeled competitors (400 nM) as labeled in the figure. The GST portion had been cleaved off from each of the proteins used in these experiments.

FIG. 3. **Interaction of SLRPs with repeat constructs of RAP.** GST (10 μg), GST/RAP-(1–323) (1 μg), GST/RAP-(1–110) (10 μg), GST/RAP-(91–210) (10 μg), GST/RAP-(191–323) (1 μg), GST/RAP-(1–319) (1 μg), or GST/RAP-(1–250) (10 μg) were electrophoresed on 10% SDS gels and transferred to nitrocellulose membrane. After blocking, membranes were incubated with conditioned media harvested from SLRP2 (*A*), SLRP3 (*B*), or SLRP4 (*C*) cDNA-transfected U87 cells. Each transfection was carried out with the cotransfection of cDNA for RAP. The bound SLRPs were then detected with anti-HA antibody and ECL detection method.

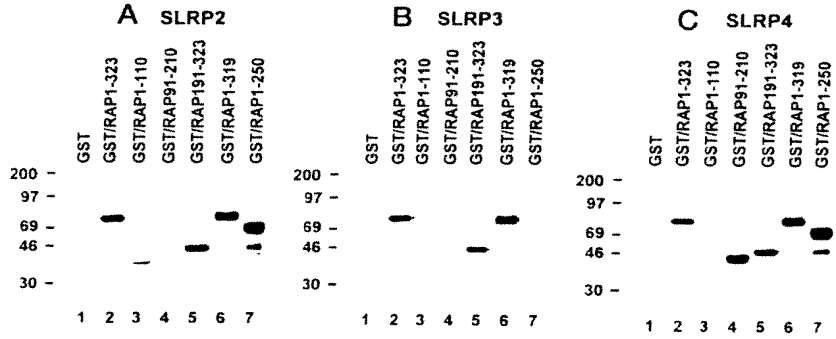

tions of RAP repeats with ligand-binding domains on LRP. Two additional RAP repeat constructs were tested in these experiments, one with the ER-retention signal HNEL deleted (GST/RAP-(1–319)), and one containing repeats 1 and 2, and part of repeat 3 of RAP (GST/RAP-(1–250)). As shown in Fig. 3, GST/RAP-(1–319) interacted similarly to full-length RAP with LRP, indicating that the HNEL signal is not important for RAP interaction with LRP. The fact that GST/RAP-(1–250) does not interact with SLRP3 is consistent with the notion that neither repeat 1, nor repeat 2 of RAP interacts with the third ligand-binding domain of LRP, and suggests residue 250–323 are important for interacting with SLRP3.

Our previous cell surface saturation binding analyses have suggested that each LRP molecule contains 5–7 binding sites for RAP (22). Thus, to further define the binding sites of RAP on the subdomains of LRP, we prepared constructs representing approximately each half of the three ligand-binding domains, with or without the flanking EGF precursor type repeats (see "Materials and Methods"). These regions are graphically illustrated in Fig. 4. Using these SLRPs and the coexpression of RAP, we have analyzed the interaction with each of the repeats within RAP, as well as the full-length RAP. The results are summarized in Table I. As seen in the table, the amino-terminal (SLRP2N) and carboxyl-terminal (SLRP2C) halves of the second ligand-binding domain of LRP (SLRP2) interacted equally well with both full-length RAP and the repeat 3 of RAP, suggesting that at least two independent RAP-binding sites exist within the second ligand-binding domain of LRP. Removal of the EGF precursor repeats from either the amino-terminal half (SLRP2N-EGF) or the carboxyl-terminal half (SLRP2C-EGF) had no effect on their interactions with RAP, suggesting that the EGF precursor repeats are not re-

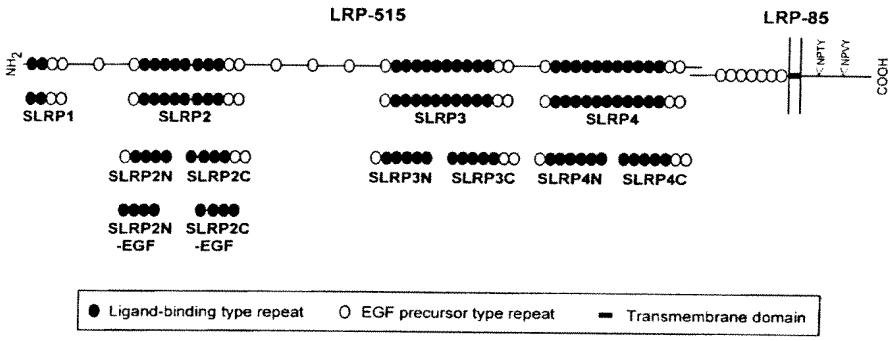

FIG. 4. **Soluble domain and subdomain constructs of LRP.** Figure is a schematic representation of domain and subdomain constructs of SLRPs used in our studies.

TABLE I
Interaction of SLRPs with GST/RAP constructs

GST or GST/RAP constructs were electrophoresed on SDS gels and transferred to nitrocellulose membrane. Membranes were then incubated with conditioned media harvested from SLRP and RAP cDNA-cotransfected U87 cells. The bound SLRPs were then detected with anti-HA antibody and enhanced chemiluminescence (ECL, Amersham) detection method. −, no detectable interaction; +, ++, +++, and ++++ represent various degree of interactions from minimum to maximum.

	GST	GST/RAP	GST/RAP-(1–110)	GST/RAP-(91–210)	GST/RAP-(191–323)	GST/RAP-(1–319)	GST/RAP-(1–250)
SLRP1	−	−	−	−	−	−	−
SLRP2	−	++++	++	−	++++	++++	+++
SLRP2N	−	++++	++	−	++++	++++	+++
SLRP2N-EGF	−	++++	++	−	++++	++++	+++
SLRP2C	−	++++	−	−	++++	++++	+++
SLRP2C-EGF	−	++++	−	−	++++	++++	+++
SLRP3	−	++++	−	−	++++	++++	−
SLRP3N	−	−	−	−	−	−	−
SLRP3C	−	+	−	−	+	+	−
SLRP4	−	++++	−	+++	++++	++++	+++
SLRP4N	−	++++	−	+++	++++	++++	+++
SLRP4C	−	++	−	−	++	++	−

quired for RAP's interactions with LRP. When the third ligand-binding domain of LRP was divided in half, only the carboxyl-terminal half (SLRP3C) exhibited interaction, albeit weak, with RAP, consistent with the notion that this repeat contains only one RAP-binding site likely localized near the middle of this repeat. Although the carboxyl-terminal half (SLRP4C) exhibited somewhat weaker interaction, both the amino-terminal (SLRP4N) and carboxyl-terminal (SLRP4C) halves of the fourth ligand-binding domain of LRP reacted with RAP, suggesting that this ligand-binding domain of LRP likely contains two RAP-binding sites. Taken together, we have thus identified at least five independent RAP-binding sites on LRP. The exact number of RAP-binding sites on LRP and their precise localization will require further investigation.

Also shown in Table I are results of interactions between different SLRPs and the three RAP repeat constructs. It appears that the binding sites for repeats 1 and 2 of RAP are both localized on the amino-terminal halves of the second and fourth repeats of LRP, respectively.

Role of RAP Repeats in the Folding and the Secretion of SLRPs—To examine the ability of RAP repeats to promote the folding process of LRP, we constructed cDNAs corresponding to the full-length RAP and each of its three repeats of RAP. An HA epitope and five methionine residues were included in the constructs to monitor the expression of these proteins after cell transfection. When these cDNAs were transfected into U87 cells (8), we found abundant expression for each of them following metabolic labeling with [^{35}S]methionine and immunoprecipitation with anti-HA antibody (Fig. 5*A*). The expression levels of RAP and its individual repeats after transfection were approximately 50-fold higher when compared with the endogenous RAP (data not shown, see Ref. 15). In our previous studies, we developed a system by which the folding of LRP can be evaluated using SLRPs (15). Correct folding and the subsequent secretion of each of the three ligand-binding domains of LRP (SLRP2, SLRP3, and SLRP4) require the coexpression of RAP. Shown in Fig. 5*B* is an experiment in which SLRP2 is expressed in U87 cells without or with coexpression of full-length RAP (RAP-(1–323)). The secretion level of SLRP2 was monitored by analyzing radiolabeled SLRP2 in the media and cell lysates after pulse labeling with [^{35}S]cysteine for 1 h and chase for 3 h. As seen in the figure, without coexpression of RAP-(1–323), little secretion (~8% of total radioactivity) of SLRP2 was seen, whereas when RAP-(1–323) was coexpressed, about 50% of total ^{35}S-SLRP2 was secreted. Using the same assay, we analyzed the ability of each RAP repeat construct in the secretion of SLRPs. Shown in Fig. 5*C* are results from a representative experiment of the four performed. The percent of SLRP secretion after pulse-chase labeling was plotted against individual constructs. As seen in the figure, repeat 3 of RAP (RAP-(191–323)) functioned at least as well (SLRP4) if not better (SLRP2 and SLRP3) than the full-length RAP in its ability to assist the folding and secretion of each of the three SLRPs. Both repeat 1 and 2 of RAP had little effect on the secretion of SLRPs, possibly due to their lower affinity for the SLRPs. Also examined in these experiments was RAP-(1–250), which functioned similarly to the full-length RAP in the secretion of SLRP2 and SLRP4, but not SLRP3, consistent with its ability to bind LRP (see Fig. 3).

Role of RAP Repeat Constructs in the Inhibition of Ligand Interactions with LRP—RAP has been used extensively in the study of LRP ligands due to its ability to antagonize ligand interactions with the receptor (1). To examine the ability of each of the RAP repeats to inhibit LRP ligands, we analyzed the interaction of several ligands with LRP in the absence or the presence of either the full-length RAP or each of the repeat constructs of RAP. To exclude any possible steric hindrance by GST, we proteolytically removed it from each of the fusion

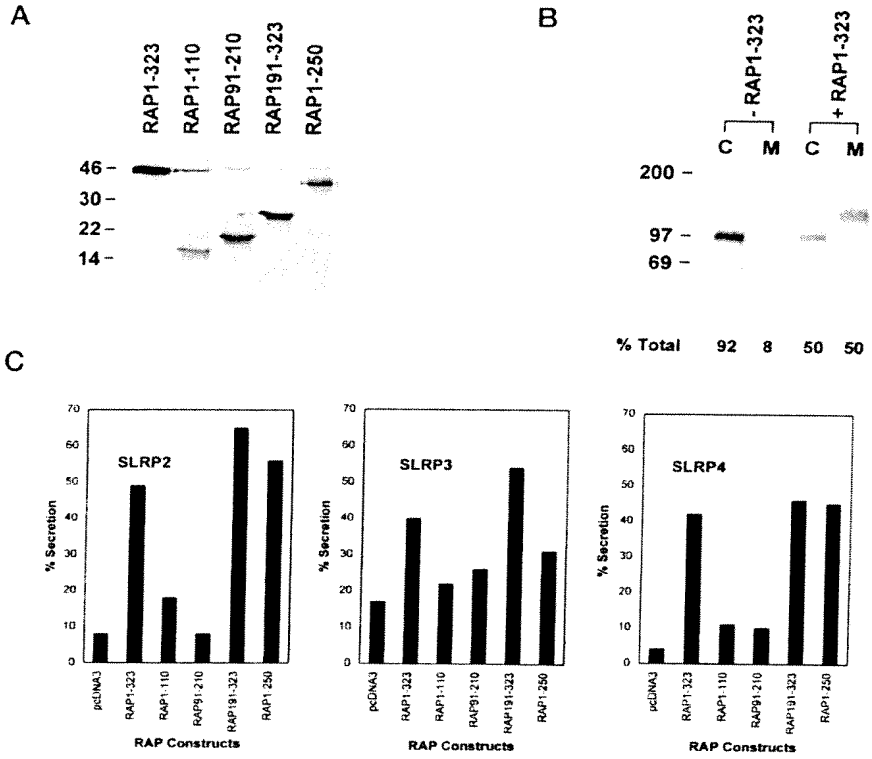

FIG. 5. **Effects of RAP repeat constructs on the folding and secretion of SLRPs.** *A*, expression of RAP repeat constructs via cell transfection. U87 cells were transfected with cDNAs for each of the RAP constructs as labeled. Transfected cells were then metabolically labeled with [^{35}S]methionine for 4 h and immunoprecipitated with anti-HA antibody. The immunoprecipitated proteins were analyzed on 15% SDS-polyacrylamide gel and exposed to film overnight. *B*, secretion of SLRP2 without or with the cotransfection of cDNA for RAP-(1–323). U87 cells were transfected with cDNA for SLRP2 with the cotransfection of either vector alone (*−RAP1–323*), or cDNA for RAP-(1–323) (*+RAP1–323*). Transfected cells were then metabolically pulse-labeled with [^{35}S]cysteine for 1 h, and chased in complete media for 3 h. The SLRP2 was then immunoprecipitated with anti-HA antibody and examined via 7.5% SDS gel. The band intensities were quantitated by the Storm phosphorimaging analysis (Molecular dynamics) and the percentage of ^{35}S-SLRP2 radioactivity associated with cell lysates (*C*) or media (*M*) are given below each lane. *C*, secretion of SLRPs in the absence or presence of coexpression with RAP repeat constructs. U87 cells were transiently cotransfected with cDNAs for one of the SLRPs and one of the RAP repeats constructs as indicated (pcDNA for negative controls). After transfection, cells were metabolically pulse-chase labeled as described in *B*. The percentage of SLRPs secreted into the overlying media was analyzed as in *B*, and plotted for each RAP repeat construct.

proteins and repurified the RAP constructs. Since the primary binding sites on the cell surface of some LRP ligands are not on LRP (*e.g.* tissue factor pathway inhibitor, or TFPI; see Ref. 23), but subsequent internalization and degradation is, we performed ligand degradation assays using U87 cells. Each of the ligands examined was radioiodinated and incubated with U87 cells for 4 h in the absence or the presence of RAP constructs. Shown in Fig. 6 are summaries for four LRP ligands: t-PA (24), α_2M* (25), antithrombin III-thrombin complex (26), and TFPI (23). As seen in the figure, full-length RAP inhibited the degradation of each of the ligands with LRP. Repeat 3 of RAP inhibited the degradation of ^{125}I-t-PA, ^{125}I-antithrombin III-thrombin complex, and ^{125}I-TFPI, but not ^{125}I-α_2M*. Interestingly, while both repeat 1 and repeat 2 of RAP were generally inefficient in inhibiting other ligands, these repeats were very effective in inhibiting the interaction of α_2M* with LRP. Thus, LRP ligands were differentially inhibited by RAP repeat constructs, consistent with the hypothesis that LRP ligands bind to different sites on the receptor.

DISCUSSION

Despite being widely used as an antagonist to LRP on the cell surface, RAP has recently been defined as a specialized ER chaperone and functions during LRP's folding and subsequent trafficking along the early compartments of the secretory pathway (9, 10, 15). Previously it had been noted that RAP contained a triplicated repeat within its sequence (9). However, the functional aspects of these repeats have not been defined. In the current report, we have re-examined the sequence of RAP using several sequence analysis programs. Although no clear boundaries can be defined among the three repeats, we found that the homologous regions are retained within each boundary if RAP is divided into three approximately equally sized regions (*i.e.* repeat 1, amino acids 1–100; repeat 2, amino acids 101–200; and repeat 3, amino acids 201–323).

Several studies have suggested that there are multiple RAP-binding sites on each LRP molecule. However, the exact number of RAP-binding sites on LRP is unknown. Using cell surface binding analyses, we have previously shown that there were approximately 5–7 times more RAP-binding sites on hepatocytes when compared with t-PA binding sites (*i.e.* functional LRP molecules, see ref. 22). However, other reported binding studies of RAP to purified LRP concluded that two RAP-binding sites are present on each LRP molecule (27). Using the soluble LRP minireceptors, we have recently reported that each of the three putative ligand-binding domains of LRP is capable of interacting with RAP (15). In the current report, we have further analyzed the RAP-binding sites on LRP using domain and subdomain constructs of LRP. We found that there were at

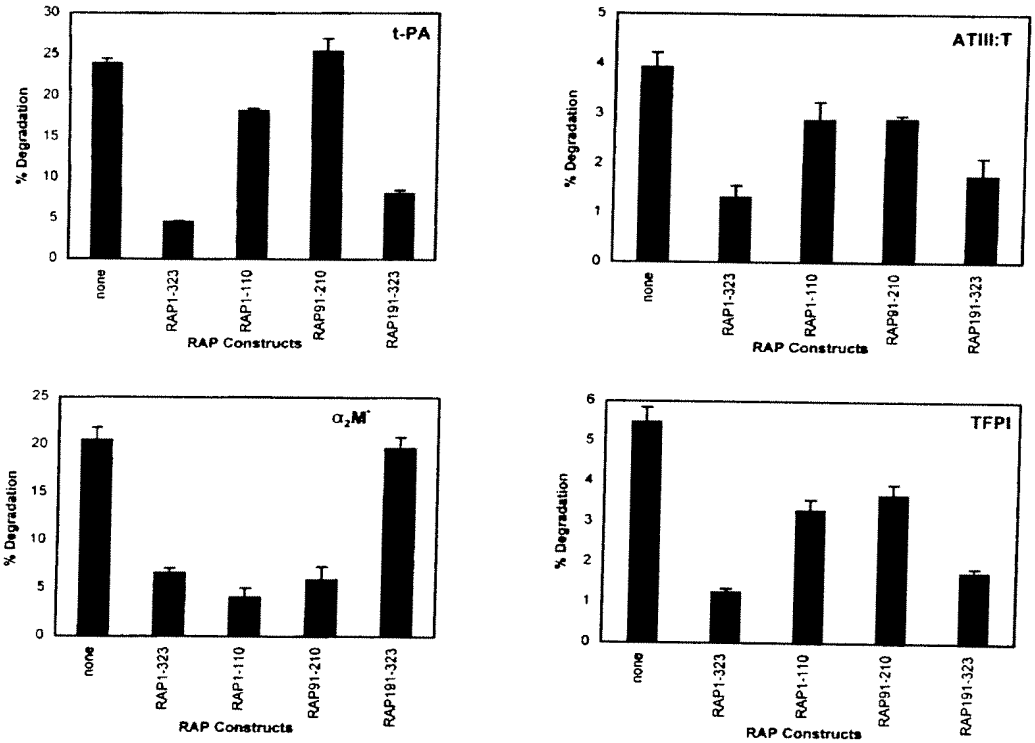

FIG. 6. **Inhibition of ligand degradation by RAP repeat constructs.** Ligand uptake and degradation was performed for ^{125}I-t-PA, ^{125}I-α_2M*, ^{125}I-antithrombin III-thrombin complex, and ^{125}I-TFPI (4 nM for each ^{125}I-ligand) in the absence or presence of each of the RAP repeat constructs (400 nM). Cell-mediated degradation of each ligand was determined by analyzing trichloroacetic acid-soluble radioactivity in the overlying buffer and subtracting trichloroacetic acid-soluble radioactivity from dishes without cells. The percentage of degradation refers to the percentage relative to the total radioactivity of added ligands.

least two RAP-binding sites on the second and fourth, and one on the third ligand-binding domains of LRP, yielding a total of at least five RAP-binding sites on the receptor. It should be pointed out that, given the fact that each half of the second and fourth ligand-binding domains of LRP is capable of binding RAP, these repeats may contain more than two RAP binding sites. The exact number of RAP-binding sites, as well as the regions where RAP binds, will require further investigation.

The physiological function of RAP has become more clear during the past 2 years. The fact that RAP is localized primarily within the ER with little or no secretion suggests an intracellular role for this protein. It appears that RAP associates with LRP during or immediately after the biosynthesis of the receptor (9). Association of RAP with LRP would ensure that LRP remains in an inactive ligand-binding state during its trafficking along the early secretory pathway. This appears to be important for receptor trafficking as LRP ligands are secreted proteins and often expressed in the same cells as the receptor. By associating with the receptor, RAP prevents premature interaction of ligands with the receptor (9, 10). This function of RAP resembles that of the invariant chain in preventing premature binding of peptides with the MHC class II molecules during their trafficking along the secretory pathway (28). Interestingly, using the soluble minireceptor system, our recent studies also suggest that RAP is required for the folding process of LRP by preventing the formation of intermolecular disulfide bonds (15). It is not clear at present whether the function of RAP in the folding of the receptor and in preventing premature ligand interaction with the receptor are related. For example, if a ligand interacts with LRP before the receptor completes its folding, the folding process might be impaired. In this case, preventing ligand interaction with the receptor ensures the proper folding of LRP. On the other hand, it is possible that RAP is independently involved in the folding, but remains associated with the receptor after the folding. Thereafter, premature ligand interaction with the receptor may be prevented. The precise role of RAP as a chaperone for LRP, as well as the mechanisms involved, await further definition.

The differential functions of the RAP repeats may also explain their roles and appearance during evolution. Since repeat 3 of RAP is capable of assisting the folding of each of the ligand-binding domains of LRP and of inhibiting most of the ligand interactions with the receptor, it is likely that this repeat is essential for RAP's function and may be the ancestral region for the whole molecule; consistent with the indications from sequence alignment. However, the fact that interaction of some of the LRP ligands (*e.g.* α_2-macroglobulin, shown in this study) is not inhibited by repeat 3 of RAP suggests the need for the first two repeats, which do inhibit these ligand interactions with the receptor. It is interesting to note that LRP is present in an organism as primitive as the nematode *Caenorhabditis elegans* (29). Examination of the *C. elegans* gene bank also identifies a 290-amino acid protein sequence (gene accession no. Z75527) that shares high sequence homology with human RAP, particularly in the portion where repeat 2 and repeat 3 of human RAP share most homology. However, no ER-retention signal is present at the carboxyl terminus of this sequence. Whether this protein is the nematode equivalent of RAP requires functional studies. It will be interesting in future studies to examine the appearance of LRP ligands during evolution. For example, α_2-macroglobulin has been described in the horseshoe crab (30). If most LRP ligands are absent in the nematode,

the primary function of RAP may be to aid in receptor folding. The role of RAP in inhibiting ligand interaction with the receptor may have evolved only after LRP expression became high in tissues (*e.g.* liver and brain) of higher organisms and with the appearance of the diverse array of LRP ligands.

Acknowledgments—We thank Dr. Joachim Herz for providing cDNA for human LRP, Dr. Mark Heiny for assistance in the analysis of RAP sequences, and Dr. Alan Schwartz for general support.

REFERENCES

1. Krieger, M., and Herz, J. (1994) *Annu. Rev. Biochem.* **63,** 601–637
2. Yamamoto, T., Davis, G. C., Brown, M. S., Schneider, W. J., Casey, M. L., Goldstein, J. L., and Russell, D. W. (1984) *Cell* **39,** 27–38
3. Herz, J., Hamann, U., Rogne, S., Myklebost, O., Gausepohl, H., and Stanley, K. K. (1988) *EMBO J.* **7,** 4119–4127
4. Saito, A., Pietromonaco, S., Loo, A. K., and Farquhar, M. G. (1994) *Proc. Natl. Acad. Sci. U. S. A.* **91,** 9725–9729
5. Takakashi, S., Kawarabayasi, Y., Nakai, T., Sakai, J., and Yamamoto, T. (1992) *Proc. Natl. Acad. Sci. U. S. A.* **89,** 9252–9256
6. Kounnas, M. Z., Stefansson, S., Loukinova, E., Argraves, K. M., Strickland, D. K., and Argraves, W. S. (1994) *Ann. N. Y. Acad. Sci.* **737,** 114–123
7. Medh, J. D., Fry, G. L., Bowen, S. L., Pladet, M. W., Strickland, D. K., and Chappell, D. A. (1995) *J. Biol. Chem.* **270,** 536–540
8. Bu, G., Maksymovitch, E. A., Geuze, H., and Schwartz, A. L. (1994) *J. Biol. Chem.* **269,** 29874–29882
9. Bu, G., Geuze, H. J., Strous, G. J., and Schwartz, A. L. (1995) *EMBO J.* **14,** 2269–2280
10. Willnow, T. E., Rohlmann, A., Horton, J., Otani, H., Braun, J. R., Hammer, R. E., and Herz, J. (1996) *EMBO J.* **15,** 2632–2639
11. Willnow, T. E., Armstrong, S. A., Hammer, R. E., and Herz, J. (1995) *Proc. Natl. Acad. Sci. U. S. A.* **92,** 4537–4541
12. Herz, J., Kowal, R. C., Goldstein, J. L., and Brown, M. S. (1990) *EMBO J.* **9,** 1769–1776
13. Willnow, T. E., Moehring, J. M., Inocencio, N. M., Moehring, T. J., and Herz, J. (1996) *Biochem. J.* **313,** 71–76
14. Daly, N. L., Scanlon, M. J., Djordjevic, J. T., Kroon, P., and Smith, R. (1995) *Proc. Natl. Acad. Sci. U. S. A.* **92,** 6334–6338
15. Bu, G. J., and Rennke, S. (1996) *J. Biol. Chem.* **271,** 22218–22224
16. Handley-Gearhart, P. M., Stephen, A. G., Trausch-Azar, J. S., Ciechanover, A., and Schwartz, A. L. (1994) *J. Biol. Chem.* **269,** 33171–33178
17. Chen, C., and Okayama, H. (1987) *Mol. Cell. Biol.* **7,** 2745–2752
18. Bu, G., Maksymovitch, E. A., and Schwartz, A. L. (1993) *J. Biol. Chem.* **268,** 13002–13009
19. Laemmli, U. K. (1970) *Nature* **227,** 680–685
20. Warshawsky, I., Bu, G., and Schwartz, A. L. (1993) *J. Biol. Chem.* **268,** 22046–22054
21. Bu, G., Morton, P. A., and Schwartz, A. L. (1992) *J. Biol. Chem.* **267,** 15595–15602
22. Iadonato, S. P., Bu, G., Maksymovitch, E. A., and Schwartz, A. L. (1993) *Biochem. J.* **296,** 867–875
23. Warshawsky, I., Broze, G. J., Jr., and Schwartz, A. L. (1994) *Proc. Natl. Acad. Sci. U. S. A.* **91,** 6664–6668
24. Bu, G., Williams, S., Strickland, D. K., and Schwartz, A. L. (1992) *Proc. Natl. Acad. Sci. U. S. A.* **89,** 7427–7431
25. Strickland, D. K., Ashcom, J. D., Williams, S., Burgess, W. H., Migliorini, M., and Argraves, W. S. (1990) *J. Biol. Chem.* **265,** 17401–17404
26. Kounnas, M. Z., Church, F. C., Argraves, W. S., and Strickand, D. K. (1996) *J. Biol. Chem.* **271,** 6523–6529
27. Williams, S. E., Ashcom, J. D., Argraves, W. S., and Strickland, D. K. (1992) *J. Biol. Chem.* **267,** 9035–9040
28. Sant, A. J., and Miller, J. (1994) *Curr. Opin. Immunol.* **6,** 57–63
29. Yochem, J., and Greenwald, I. (1993) *Proc. Natl. Acad. Sci. U. S. A.* **90,** 4572–4576
30. Armstrong, P. B., Mangel, W. F., Wall, J. S., Hainfield, J. F., Van Holde, K. E., Ikai, A., and Quigley, J. P. (1991) *J. Biol. Chem.* **266,** 2526–2530

Efficient transfer of receptor-associated protein (RAP) across the blood-brain barrier

Weihong Pan[1,*], Abba J. Kastin[1], Todd C. Zankel[2], Peter van Kerkhof[3], Tetsuya Terasaki[4] and Guojun Bu[3]

[1]Pennington Biomedical Research Center, Louisiana State University System, 6400 Perkins Road, Baton Rouge, LA 70808, USA
[2]BioMarin Pharmaceutical Incorporated, 371 Bel Marin Keys Boulevard, Suite 210, Novato, CA 94949, USA
[3]Department of Pediatrics, and Department of Cell Biology and Physiology, Washington University School of Medicine, 660 South Euclid Avenue, St Louis, MO 63110, USA
[4]Department of Molecular Biopharmacy and Genetics, Tohoku University, 1-1 katahira 2-chome, Aoba-ku, Sendai, 980-8577, Japan
*Author for correspondence (e-mail: weihong.pan@pbrc.edu)

Accepted 24 June 2004
Journal of Cell Science 117, 5071-5078 Published by The Company of Biologists 2004
doi:10.1242/jcs.01381

Summary

We have sought to identify a high-capacity transport system that mediates transcytosis of proteins from the blood to the brain. The 39 kDa receptor-associated protein (RAP) functions as a specialized endoplasmic reticulum chaperone assisting in the folding and trafficking of members of the low-density lipoprotein (LDL) receptor family. RAP efficiently binds to these receptors and antagonizes binding of other ligands. Previous studies have shown that two large members of the LDL receptor family, LDL receptor-related protein 1 (LRP1) and LDL receptor-related protein 2 (LRP2 or megalin), possess the ability to mediate transcytosis of ligands across the brain capillary endothelium. Here, we tested whether blood-borne RAP crosses the blood-brain barrier (BBB) by LRP1- or megalin-mediated transport by studying the pharmacokinetics of [^{125}I]-RAP transport into the brain in intact mice and across cell monolayers in vitro. Our results show that [^{125}I]-RAP is relatively stable in blood for 30 minutes and has a mean influx constant of 0.62±0.08 μl/g-minute from blood to brain. In situ brain perfusion in blood-free buffer shows that transport of [^{125}I]-RAP across the BBB is a saturable process. Capillary depletion of brain homogenates indicates that 70% of [^{125}I]-RAP is localized in the parenchyma rather than in the vasculature of the brain. Results of transport in stably transfected MDCK cells are consistent with the hypothesis that megalin mediates most of the apical-to-basolateral transport across polarized epithelial cells. The inhibition of [^{125}I]-RAP influx by excess RAP and the involvement of megalin indicate the presence of a saturable transport system at the BBB. The higher permeability of RAP compared with that of melanotransferrin and transferrin show that the LRP receptor is a high capacity transport system. These studies suggest that RAP may provide a novel means of protein-based drug delivery to the brain.

Key words: Receptor-associated protein, Blood-brain barrier, Drug delivery, Megalin, LRP, Receptor-mediated transport

Introduction

Receptor-associated protein (RAP) is found mainly in the endoplasmic reticulum. RAP plays a key role in the proper folding and trafficking of members of the low-density lipoprotein (LDL) receptor family within the secretory pathway, including LDL receptor-related protein 1 (LRP1) and LDL receptor-related protein 2 (LRP2, megalin) (Bu et al., 1995). RAP has an apparent molecular mass of 39 kDa in humans and 44 kDa in rats, and binds with low affinity to heparin sulfate (Orlando and Farquhar, 1994; Melman et al., 2001). When administered intravenously, recombinant RAP significantly prolongs the plasma half-life of tissue-type plasminogen activator (tPA), which uses LRP1 as a clearance receptor (Warshawsky et al., 1993). This result indicates that binding of circulating RAP to members of the LDL receptor family can significantly inhibit the clearance of other ligands from the blood.

Megalin is expressed primarily in a subset of epithelial cell layers including those lining the renal proximal tubule, thyroid colloid, epididymis, alveolae, brain vasculature, and the ciliary body of the eye (Orlando and Farquhar, 1993; Zheng et al., 1994). Of particular interest are the cerebral microvessel endothelial cells (specialized squamous epithelial cells) composing the blood-brain barrier (BBB). In at least three cases, megalin has been shown to transcytose ligands in the apical-to-basolateral direction across some of these epithelial cell layers. Marinò and colleagues have shown efficient megalin-dependent transcytosis of thyroglobulin across the thyroid epithelium (Marinò et al., 2003) and megalin-dependent transcytosis of retinol binding protein across the renal proximal tubule epithelium (Marinò et al., 2001). Transport of apoJ across the brain capillary endothelium in situ also was shown to involve megalin-dependent transcytosis (Zlokovic et al., 1996; Shayo et al., 1997). Another study has shown that the complex between RAP and megalin remains stable as far as the late endosome (Czekay et al., 1997), an indication of pH stability that often signifies transcytotic competence.

Exogenously applied RAP can be endocytosed efficiently by all members of the LDL receptor family (Bu et al., 1994; Savonen et al., 1999; Li et al., 2000; Li et al., 2001b). RAP has also been shown to be functional in both N- and C-terminal

fusions with other proteins (personal communication, BioMarin Pharmaceutical). Thus, RAP has potential as a vehicle to bring other proteins into cells by receptor-mediated endocytosis. If RAP undergoes megalin-dependent transcytosis across the brain capillary endothelium as do thyroglobulin and retinol binding protein across other epithelial cells (Marinò et al., 2003; Marinò et al., 2001), and if the RAP fusion proteins maintain domain conformation and the ability to be transported across the BBB, RAP could serve as a vehicle for receptor-mediated transcytotic delivery of other proteins into the brain in vivo.

The BBB dynamically regulates the availability of proteins from blood to brain and spinal cord. In general, peptides and proteins in the periphery are excluded from substantial entry into the central nervous system. The ability to treat neurological disorders with powerful protein and peptide drugs is largely hindered by this effect. Therefore, vehicle-mediated delivery targeting brain endothelial antigens as transporters has been widely explored as a means of protein-based drug delivery. The transferrin receptor is highly expressed in brain microvessel endothelial cells, and transferrin may be transcytosed by this receptor or recycled back to the apical surface of the endothelial cells (Morris et al., 1992; Ueda et al., 1993; Moos and Morgan, 2001). Moreover, high concentrations of transferrin in the blood block efficient transcytosis of exogenously administered transferrin in vivo. The murine OX26 monoclonal antibody to the rat transferrin receptor has been used as a vehicle for the delivery of attached ligands to the brain (Skarlatos et al., 1995; Broadwell et al., 1996). The related ligand, human melanotransferrin, which shares 37% sequence homology with transferrin, has been shown to have a high rate of brain uptake and a high permeability constant in cultured bovine brain capillary endothelial cells (Demeule et al., 2002). In this report, we describe studies to determine whether RAP crosses the BBB and how the rate at which this occurs compares with that of transferrin and melanotransferrin.

There are two main implications for the study of RAP transport across the BBB. First, the transport system could be enhanced to facilitate the transport of ligands such as RAP and its homologous proteins. An alternative approach is the use of a transport system with a ligand as a carrier protein. Therefore, it may be possible to attach the target drug to RAP to provide efficient transport into the brain.

Materials and Methods

RAP, transferrin and melanotransferrin were provided by BioMarin Pharmaceutical (Novato, CA) and radioactively labeled with [^{125}I] by the Iodogen or chloramine-T methods. Albumin was radioactively labeled with [^{99m}Tc] sodium pertechnetate as previously described (Kastin et al., 2001), or with [^{131}I] by the chloramine-T method. The estimated specific activity for the labeled proteins ranged from 60-120 Ci/g. The purity of the labeled proteins was verified by HPLC and acid precipitation.

BBB permeability studies

Male CD1 mice, weighing 25-35 g (Charles River Laboratories), were anesthetized immediately before the study. For multiple time regression analysis (Kastin et al., 2001), the mouse received a bolus mixture of [^{125}I]-RAP and [^{131}I]-albumin (0.5-1 μCi/mouse in 100 μl of lactated Ringer's with 1% albumin, except when otherwise specified) through the left jugular vein. At designated times (1-30 minutes after injection), blood was collected from a cut in the right common carotid artery and the mouse was decapitated immediately. Brain and peripheral tissue samples were obtained, weighed, and assayed for radioactivity. Radioactivity in 50 μl of serum was also measured for calculation of the volume of distribution.

To correct for the decay of serum radioactivity over time, 'exposure time' was calculated as the integral of serum radioactivity from time zero to time t divided by the radioactivity at time t. The unidirectional influx constant, Ki, expressed in μl/g-minute, and the apparent volume of distribution, Vi, in μl/g, were determined from the linear portion of the following equation:

$$Am/Cpt = Ki\,[\int_0^t \mathrm{Cp}(\tau)\,d\tau] / Cpt + Vi\,,$$

where Am is the amount of radioactivity in a tissue sample per unit mass (cpm/g), Cpt is the amount of radioactivity in 1 μl serum at time t (cpm/μl), and exposure time is measured by the term $[\int_0^t \mathrm{Cp}(\tau)\,d\tau]/Cpt$ (Blasberg et al., 1983; Patlak et al., 1983).

The Ki values were compared by analysis of variance (ANOVA) to determine whether there were differences within groups. This was followed by a Newman-Keuls post-hoc test to determine which values within a group differed. The standard deviation of the mean for the slope was taken as the standard error of the mean and, because two means (the slope and the intercept) were calculated from the data, n–1 was used as the n value in the ANOVA and range tests. Statistically significant differences among groups were determined with the aid of the GraphPad Prism statistical program (Banks et al., 2003).

For in situ brain perfusion, the descending aorta was clamped and bilateral jugular veins were severed. After a minute of perfusion with oxygenated, modified Zlokovic's buffer (Zlokovic et al., 1990; Pan et al., 1998), the mouse received [^{125}I]-RAP and [^{99m}Tc]-albumin (0.5-1 μCi/ml each) at a perfusion rate of 2 ml /minute for designated times between 1 and 10 minutes. Mice were then perfused with buffer alone for another minute before decapitation. In some experiments, [^{125}I]-transferrin and [^{125}I]-melanotransferrin were studied under conditions identical to [^{125}I]-RAP.

Degradation assays

Acid precipitation was performed with the stock solution, perfusion buffer, serum and tissue homogenates. Brain and peripheral tissue were homogenized in 1 ml phosphate-buffered saline containing a protease inhibitor cocktail. The supernatant was precipitated with an equal volume of 30% trichloroacetic acid. Control samples to assess ex vivo degradation of radioactively labeled compounds during processing were prepared simultaneously by direct addition of [^{125}I]-RAP to the test tubes.

In vitro transport assays

Stably transfected MDCK cells and their control were originally obtained from Maria Paz Marzolo (Catholic University, Chile). The LRP1 mini-receptor constructs contain the fourth ligand-binding domain of human LRP1, followed by the transmembrane domain and either the complete cytosolic tail of LRP1 (mLRP/LRPTmT=LRPt) or the complete cytoplasmic tail of megalin (mLRP/LRPTmMegT= MEGt). The LRPt is distributed basolaterally as shown by indirect immunofluorescence with an anti-HA antibody, and MEGt localizes to the apical surface of the transfected MDCK cells (Marzolo et al., 2003). These cells were plated on the surface of polyacetate membrane inserts of the Transwell system (Costar, Cambridge, MA) with a uniform pore size of 0.4 μm. Cells were seeded at a density of 2×10^5 cells/ml and cultured in DMEM supplemented with 10% FBS. Medium was exchanged every three days. The cells were kept in a 5% CO_2 incubator at 37°C. Transcytosis studies were performed in triplicate for either apical-to-basolateral or basolateral-to-apical transport, with or without inclusion of 2 μg/ml of excess unlabeled RAP.

Twenty minutes before the transport assay, the Transwell insert and its supporting endothelial cell monolayer were equilibrated in the transport buffer (Hank's balanced salt solution with 25 mM HEPES and 0.1% albumin) at 37°C. Transport was initiated by addition of [^{125}I]-RAP (1 μCi/ml) and [^{99m}Tc]-albumin (2 μCi/ml) to the donor (upper or lower) chamber at time zero. The plate was kept at 37°C with gentle mixing at about 130 rpm during the entire procedure. At 5, 10, 15, 20, 30, 40, 50 and 60 minutes, a 10 μl aliquot of sample was collected from the acceptor (lower or upper) chamber of each well. At 60 minutes, solutions in both chambers were transferred to separate test tubes at 4°C. The radioactivity of [^{125}I]-RAP and [^{99m}Tc]-albumin was measured simultaneously in a γ-counter with a dual-channel program. The amount of intact [^{125}I]-RAP and [^{99m}Tc]-albumin after transport was measured by acid precipitation. HPLC analysis was performed on selected samples, with a linear gradient of 10-90% acetonitrile in 0.1% trifluoroacetic acid over 40 minutes with 1 ml fractions collected.

To determine the flux transfer constant, a linear regression analysis was performed for the acceptor/donor ratio of radioactivity (mean±s.e.m.) and time of transport by use of the GraphPad Prism program. The slope of the regression line represents the permeability-surface area product (*PS*, in cm^3/second). The permeability coefficient *P* was obtained by dividing the *PS* product by the filter surface area (1 cm^2 in the 12-well insert) and expressed in cm/second. The permeability coefficients among groups were compared.

All in vitro experiments were performed in triplicate. Group designs of the experiments are described in detail in the Results section. For experiments with repeated acquisition of data, statistical analysis was performed by use of SPSS with one-way ANOVA followed by Tukey's post-hoc test. For comparison of linear regression lines, analysis of covariance was performed with the aid of GraphPad Prism software.

Results

Fate of [^{125}I]-RAP after intravenous bolus delivery to mice

Chromatography was performed on both serum and brain homogenates from mice 30 minutes after intravenous injection of [^{125}I]-RAP and compared with that of the stock solution and of processing controls in which [^{125}I]-RAP was directly added to the test tubes containing whole blood and brain. In the processing controls, 75% of radioactivity in blood and 57% of radioactivity in brain represented intact [^{125}I]-RAP. After correction for the ex vivo degradation in the processing controls, 100% of radioactivity in blood and 63% of radioactivity in the brain was accounted for by intact [^{125}I]-RAP.

To determine the influx transfer constant of [^{125}I]-RAP after an iv bolus injection, four groups of mice were studied simultaneously. The amount of [^{125}I]-RAP differed in the groups: 0.3, 0.6, 1.2, and 2.4 μCi/mouse, respectively. In each group, blood, brain, liver, kidney and muscle samples from eight mice were obtained at 1, 2, 5, 7, 10, 15, 20 and 30 minutes after injection (each mouse represented one time point). Disappearance of serum radioactivity fitted a one-phase exponential decay model and was not significantly different among the four groups. The mean serum half-life of RAP was 1.5±0.1 minutes (Fig. 1). In the kidney and liver, uptake of [^{125}I]-RAP had a rapid distribution phase peaking at about 12 and 17 minutes, respectively, followed by a slower distribution phase. In the gluteus major muscle, the linear transfer constant was similar among groups with a mean of 3.1±0.2 μl/g-minute. In the brain, the linear influx transfer constant was not significantly different among groups and had a mean of 0.6±0.1 μl/g-minute (Fig. 2). The amount of [^{125}I]-RAP in the brain at 30 minutes was 1%/g brain of the total [^{125}I]-RAP delivered intravenously at 0.3 μCi/mouse. This, however, was reduced to 0.5% in groups receiving 0.6, 1.2, and 2.4 μCi/mouse of [^{125}I]-RAP without additional unlabeled RAP, suggesting possible saturability of the blood-brain transfer. In all groups, the vascular marker [^{99m}Tc]-albumin did not have significant entry. The results indicate that despite the first-pass effect and metabolism in the liver and kidneys, intact RAP had linear influx to a third peripheral organ (muscle) and also across the BBB to the brain.

Interactions of RAP with peripheral blood before reaching the BBB

Excess non-radioactively labeled RAP, when injected intravenously with [^{125}I]-RAP, did not significantly decrease the influx transfer constant of [^{125}I]-RAP but rather enhanced it. However, 25 minutes after intravenous injection, the percentage of brain uptake of the injected dose of [^{125}I]-RAP

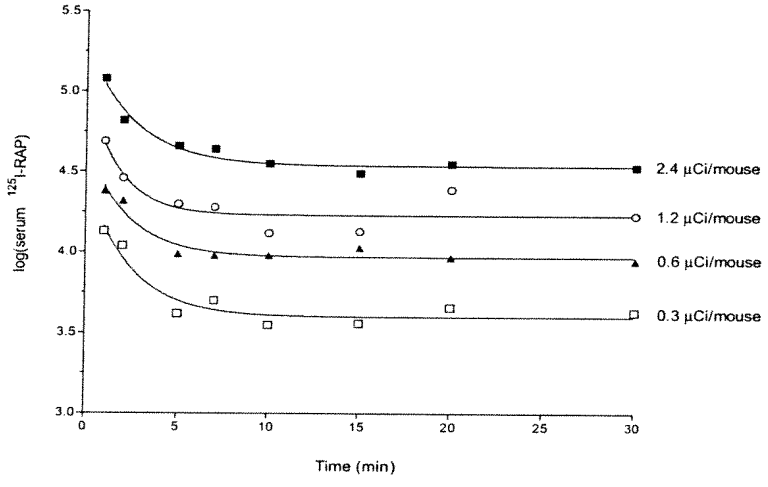

Fig. 1. Serum disappearance pattern of receptor-associated protein (RAP). The four groups represent different doses of [^{125}I]-RAP delivered intravenously in a bolus at time zero. In each group, different mice were studied at various time points, and the serum decay pattern was used to calculate exposure time, the theoretical steady-state time for the integral of serum radioactivity.

was decreased from 0.9%/g brain to 0.4% and 0.2% in mice receiving 5 μg/mouse and 200 μg/mouse of excess unlabeled RAP, respectively. This again suggested the possible presence of a saturable transport system at the BBB. The lack of a significant decrease of the influx transfer constant in the groups receiving excess RAP may be explained by peripheral binding, although preliminary studies with capillary electrophoresis did not show high-affinity binding of RAP with serum proteins. Nonetheless, RAP does have potential binding to blood cells and undergoes clearance by the liver and kidney (Warshawsky et al., 1993). Regardless, the degradation and kinetic transfer studies indicate that most [^{125}I]-RAP in the circulation is available to interact with the BBB before being degraded in the periphery.

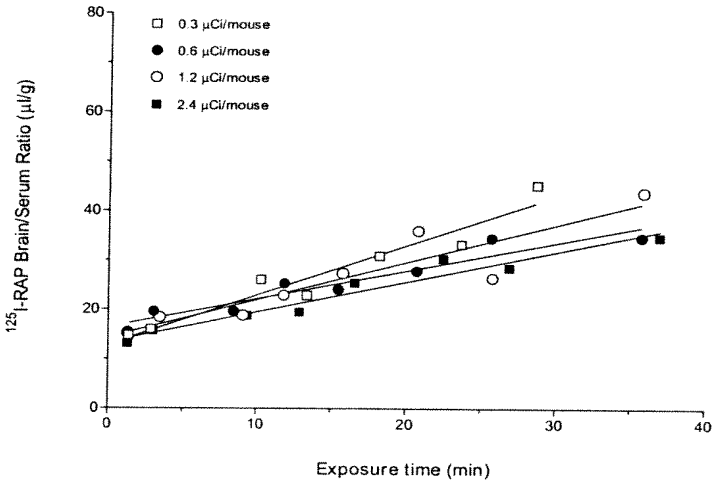

Fig. 2. The blood-to-brain transfer of [^{125}I]-RAP had a linear regression correlation with study time for each of the four groups as in Fig. 1, in which different amounts of radioactivity were administered to the mice.

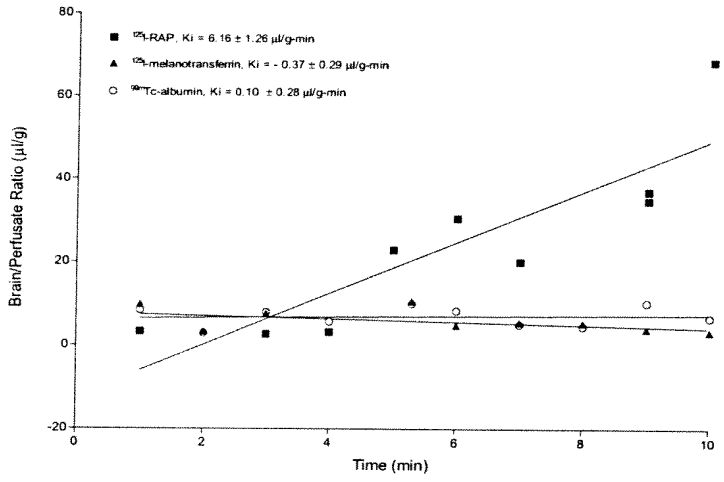

Fig. 3. In situ brain perfusion of [^{125}I]-RAP , [^{125}I]-melanotransferrin and [^{99m}Tc]-albumin. [^{125}I]-RAP had a higher influx transfer constant into the mouse brain when compared with that of [^{125}I]-melanotransferrin and the paracellular permeability marker [^{99m}Tc]-albumin.

Influx of [^{125}I]-RAP after in situ brain perfusion

To determine the direct interactions of RAP with the BBB, we used a blood-free perfusion system. The influx transfer constant of [^{125}I]-RAP, determined from mice studied during 1-10 minutes of in situ brain perfusion was 6.2±1.3 μl/g-minute. By contrast, there was no significant influx of [^{125}I]-melanotransferrin or [^{99m}Tc]-albumin in the same study (Fig. 3).

The influx of [^{125}I]-RAP into the right hyoglossus muscle was measured simultaneously during in situ brain perfusion as a positive control. The value was 10.8±1.8 μl/g-minute. By contrast, the influx rate of ^{99m}Tc-albumin to the same muscle was 2.7±1.5 μl/g-minute, whereas [^{125}I]-melanotransferrin had no significant influx (Fig. 4).

In addition to the comparison of RAP with melanotransferrin, transferrin was also studied in separate experiments. During a perfusion period of 1-5 minutes, [^{125}I]-RAP entered both cortical and subcortical areas significantly faster than [^{125}I]-transferrin (Fig. 5).

The compartmental distribution of [^{125}I]-RAP after in situ brain perfusion was determined by capillary depletion studies. After 5 minutes of in situ perfusion, the amount of radioactivity in the brain parenchyma was significantly higher than in the vasculature. As shown in Fig. 6, more than 70% of [^{125}I]-RAP that had reached the brain compartment was present in the parenchyma. Moreover, addition of 5 μg/mouse of excess unlabeled RAP decreased the uptake of [^{125}I]-RAP in parenchyma significantly [$F(1,9)=5.7$, $P<0.05$] without affecting that in the capillary fraction. This indicates the presence of a saturable transport system for RAP at the BBB. The uptake of [^{99m}Tc]-albumin was significantly lower in brain parenchyma than that of [^{125}I]-RAP and was not decreased in the presence of excess non-radioactively labeled RAP. Collectively, these results indicate that the uptake of [^{125}I]-RAP into brain parenchyma was a saturable process.

Degradation of [^{125}I]-RAP after intravenous injection and in situ brain perfusion

Acid precipitation of the supernatant of the brain homogenate, corrected for ex vivo degradation, showed that intact [^{125}I]-RAP accounted for 72%, 73%, and 61% of the radioactivity in the brain at 2, 10 and 30 minutes after intravenous injection, respectively. This is consistent with HPLC results. Similarly, intact [^{125}I]-RAP accounted for 89% and 88% of total radioactivity at 1 and 10 minutes after in situ brain perfusion, respectively. Because of the lack of substantial degradation of [^{125}I]-RAP in either blood or perfusion buffer during the multiple-time regression study, the influx transfer constants measured probably reflect entry of [^{125}I]-RAP rather than free iodine or RAP degradation products.

Involvement of megalin in the transcytosis of [^{125}I]-RAP

To identify the receptor system responsible for delivering RAP across the BBB, apical-to-basolateral and basolateral-to-apical transport of [^{125}I]-RAP was studied in three types of MDCK cells: (a) non-transfected MDCK cells; (b) MDCK cells stably transfected with an LRP domain IV mini-receptor (LRPt); and (c) MDCK cells stably transfected with a chimeric mini-receptor consisting of LRP1 extracellular domain IV and the megalin tail (MEGt). Our previous studies have shown that LRPt mimics the endogenous LRP and distributes basolaterally. MEGt, however, resembles endogenous megalin and localizes to the apical membrane (Marzolo et al., 2003). The transepithelial electrical resistance (TEER) of the confluent monolayer, an indicator of the tightness of the barrier, was 757±35 Ω cm^2 (mean±s.e.m.) for native MDCK, 364±22 Ω cm^2 for LRPt transfected MDCK, and 370±29 Ω cm^2 for MEGt transfected MDCK.

The transcytosis assays were initiated by simultaneous addition of [^{125}I]-RAP and the paracellular permeability marker [^{99m}Tc]-albumin at time zero. At the end of the study (60 minutes), intact [^{125}I]-RAP accounted for 99% of the acid precipitable radioactivity in the donor chamber and 91% of that in the acceptor chamber. This indicates that the majority of radioactivity measured represented intact [^{125}I]-RAP. Extension of the study period to 120 minutes did not change the percentage of intact [^{125}I]-RAP or the flux rate. For apical-to-basolateral flux in non-transfected MDCK cells, the permeability coefficient of [^{125}I]-RAP after transport for 60 minutes was 5.1±0.8×10^{-6} cm/second. This is probably explained by low-level expression of native megalin by MDCK. By contrast, in MDCK cells transfected with MEGt, the permeability coefficient of [^{125}I]-RAP was increased to 18.1±1.2×10^{-6} cm/second, significantly higher than the control [$F(1,11)=77.9$, $P<0.001$]. No significant flux was observed in MDCK cells transfected with LRPt, consistent with the basolateral localization pattern of this receptor (Fig. 7). In all groups, [^{99m}Tc]-albumin had no significant flux.

Addition of excess non-radioactively labeled RAP at 2 μg/ml significantly decreased the permeability coefficient of [^{125}I]-RAP in MEGt-transfected cells (6.3±0.4×10^{-6} cm/second) [$F(1,12)=86.1$, $P<0.0001$]. Whereas the non-transfected cells had no significant flux after addition of excess RAP, the difference between the groups with and without excess RAP was also statistically significant [$F(1,11)=24$, $P<0.0005$]. Thus, the results support the presence of a saturable transport system for RAP at the apical surface and the essential role of megalin in the transport process.

For basolateral-to-apical flux, the transport of [^{125}I]-RAP in all three groups was not significantly higher than that of [^{99m}Tc]-albumin, the marker of paracellular permeability. For MDCK cells stably transfected with MEGt, the apical-to-basolateral permeability coefficient of [^{125}I]-RAP was 460 times higher than the basolateral-to-apical permeability coefficient (Fig. 8). Taken together, these results support megalin-mediated transcytosis of RAP.

LRPt-transfected cells had lower flux transfer constants in both apical-to-basolateral and basolateral-to-apical directions than the non-transfected MDCK cells. It is possible that whereas LRP1 is universally expressed in the native cells, overexpression of LRPt interferes with RAP endocytosis. Therefore, our finding of megalin-mediated transcytosis does not exclude the possibility of co-existing LRP1-mediated transport in either direction.

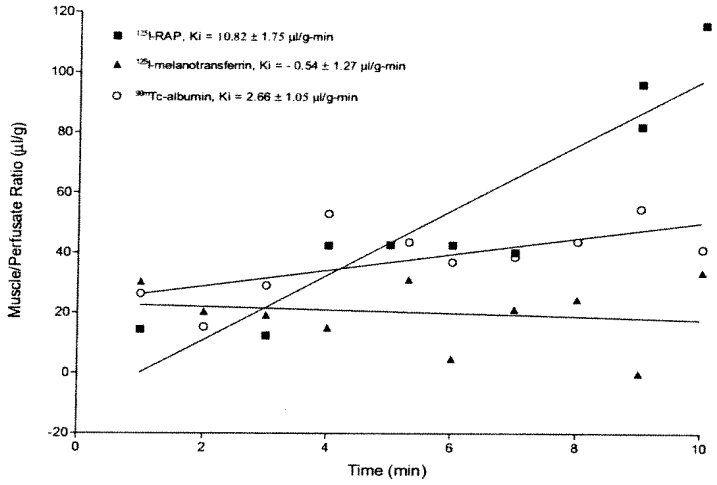

Fig. 4. Hyoglossus muscle was used as a positive control to determine the influx transfer constant of [^{125}I]-RAP during in situ brain perfusion. The value was higher for [^{125}I]-RAP when compared with that of [^{125}I]-melanotransferrin and the paracellular permeability marker [^{99m}Tc]-albumin.

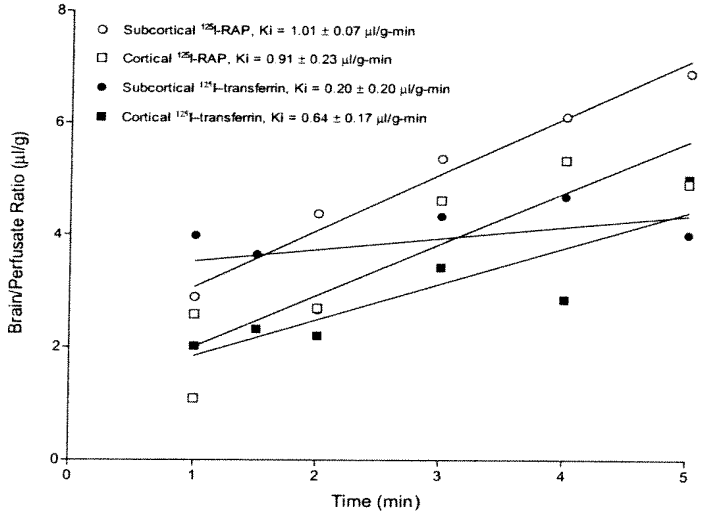

Fig. 5. In situ brain perfusion of [^{125}I]-RAP and [^{125}I]-transferrin. [^{125}I] ratio in brain and perfusate were measured over 5 minutes. RAP had greater permeability across the blood-brain barrier into both cortical and subcortical areas than transferrin.

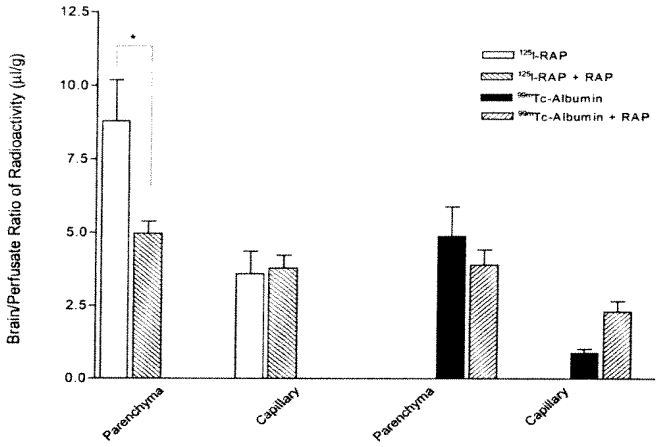

Fig. 6. The uptake of [^{125}I]-RAP by brain parenchyma was greater than that in the capillaries and that of [^{99m}Tc]-albumin, and was inhibited by excess RAP. This indicates the presence of a saturable transport system. *Significant difference (P<0.05) in reactivity ratio between parenchymal [^{125}I]-RAP and inhibited [^{125}I]-RAP groups.

Discussion

The identification of a substantial brain influx constant for RAP and the identification of a saturable RAP transport system at the BBB are potentially significant for the treatment of a variety of neurological disorders. Not only may attachment of therapeutic proteins to RAP facilitate their entry into the brain, but also delivery of RAP to the brain might be beneficial by itself. RAP has been shown to rescue neurodegeneration when infused into the lateral ventricle of the brain along with apoE3 (Veinbergs et al., 2001) and plays an important role in blocking the tPA-induced disruption of the BBB (Yepes et al., 2003). RAP has a higher influx transfer constant into the brain than most of the cytokines and neurotrophins that we have studied, and its high percent uptake per gram of brain tissue indicates the presence of an efficient transport system (Pan et al., 1997; Pan et al., 1998; Pan et al., 2000; Pan and Kastin, 2003).

In order to assess the feasibility of RAP delivery from the periphery to the brain, we first determined its fate after intravenous injection. The relative stability of [^{125}I]-RAP within the study period indicates that the brain/blood ratios of radioactivity reflect intact RAP in tissue samples, and that there is a sufficient window of time for RAP to interact with the BBB.

At 30 minutes after intravenous bolus delivery, about 0.1% of [^{125}I]-RAP was able to enter a gram of brain. Moreover, this uptake was decreased to half its value when excess RAP was added to the injection. This suggests the presence of a saturable transport system at the BBB. To further test the possibility of saturable transport, we co-administered excess non-radioactively RAP with [^{125}I]-RAP in a blood-free perfusion system. In situ brain perfusion, although less physiological than intravenous injection, avoids confounding factors like peripheral binding of RAP to heparin sulfate proteoglycans (Berryman and Bensadoun, 1995; Melman et al., 2001), LRP1, and megalin, especially in the liver and kidney (Warshawsky et al., 1993). Although we did not detect a decrease of the [^{125}I]-RAP influx transfer constant by excess unlabeled RAP in the intravenous studies, the self-inhibition characteristic of a specific saturable transport system was evident during in situ perfusion. This is similar to the finding with insulin-like growth factor 1 (IGF-1) (Pan and Kastin, 2000), where a saturable transport system occurs during in situ brain perfusion despite the observation that excess unlabeled IGF-1 paradoxically increases the influx of [^{125}I]-IGF-1 after intravenous administration. Furthermore, entry of [^{125}I]-RAP into brain parenchyma was confirmed by capillary depletion analyses, indicating that RAP, unlike transforming growth factor β, which also has a high apparent influx transfer constant (Pan et al., 1999), does not merely associate with the cerebral vasculature but crosses the BBB completely.

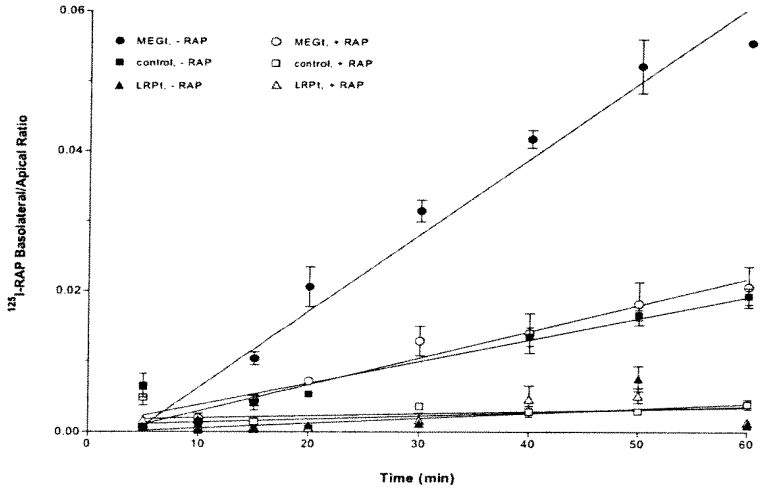

Fig. 7. Basolateral-to-apical [^{125}I]-RAP ratio over time in megalin (MEGt) and LDL receptor-related protein (LRPt) transfected MDCK cells and control MDCK cells. Although non-transfected MDCK cells had a basal, saturable apical-to-basolateral flux of [^{125}I]-RAP, overexpression of the chimeric receptor containing the cytoplasmic tail of megalin significantly enhanced this flux, which remained saturable.

Transferrin receptors are highly expressed on endothelial cells, and molecules targeted at the transferrin receptor (such as OX-26 antibody) have been designed as delivery vehicles to bring peptide and protein ligands into the brain. Therefore, we used transferrin and its related ligand melanotransferrin as positive controls for blood-to-brain transfer (Skarlatos et al., 1995; Demeule et al., 2002). In both in vivo and in vitro situations, BBB permeability appeared higher for RAP than for either transferrin or melanotransferrin. This indicates that RAP is a promising vehicle for efficient delivery across the BBB.

One of the RAP receptors, LRP1, is abundantly expressed in brain microvessels in young mice (Shibata et al., 2000). Although megalin has a more restricted distribution

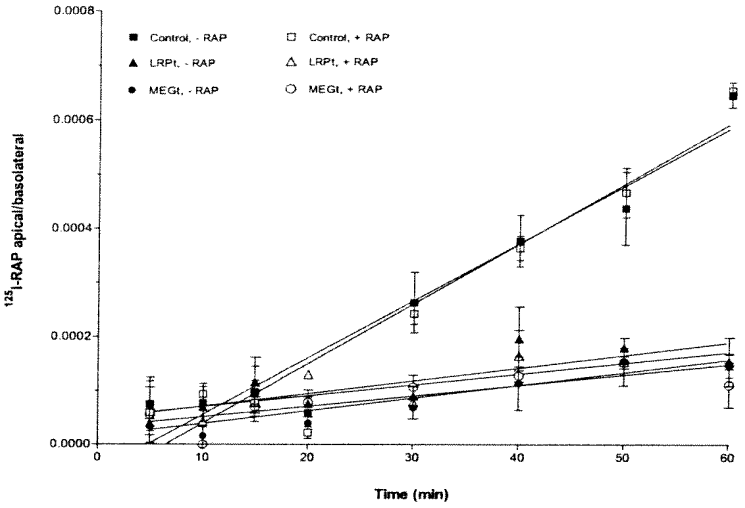

Fig. 8. Apical-to-basolateral [^{125}I]-RAP ratio over time in megalin (MEGt) and LDL receptor-related protein (LRPt) transfected MDCK cells and control MDCK cells. Basolateral-to-apical efflux of ^{125}I-RAP was significantly lower than the influx and further reduced by stable transfection of LRPt or MEGt.

(Kounnas et al., 1994; Zheng et al., 1994), it is expressed in brain microvessels and the choroid plexus (Chun et al., 1999). Megalin plays an important role in forebrain development (Wilnow et al., 1996) and is probably the receptor that mediates the transport of apoJ/amyloid β protein across the BBB and blood-cerebrospinal fluid barrier (Zlokovic et al., 1996). The important role of LRP1 in the efflux transport of amyloid β protein (Shibata et al., 2000) supports its basolateral localization and therefore LRP1 is probably not essential for blood-to-brain transport of RAP, whereas megalin is apically expressed and might be directly responsible for RAP transport at the BBB.

To test this possibility, we studied the kinetics of transcytosis in MEGt transfected MDCK cells. MDCK cells polarize and form tight junctions when cultured in Transwell inserts and have been used as an in vitro model of the BBB for drug screening (Irvine et al., 1999; Vilhardt et al., 1999; Zhang et al., 2002). As members of the RAP-binding LDL receptor family are large transmembrane proteins (Li et al., 2001a), functional analysis has been accomplished by domain reconstruction and studies of mini-receptors. In the transfected MDCK cells used for this study, the LRP mini-receptor (LRPt) is sorted basolaterally because of the NPTY motif in its cytoplasmic domain (Marzolo et al., 2003). Our previous studies have shown that the megalin cytoplasmic tail (MEGt) directs apical sorting. Thus, the polarized localization of the two mini-receptors in MDCK cells in vitro is identical to that occurring in vivo. Our results here show that megalin is mainly responsible for the apical-to-basolateral transport of RAP.

Basolateral-to-apical flux in vitro represents brain-to-blood efflux out of the brain in vivo. The basolateral-to-apical flux of [^{125}I]-RAP, even in the presence of LRPt, was significantly lower than that in control non-transfected cells. This indicates that neither overexpressed megalin nor LRPt mini-receptors is involved in basolateral-to-apical transport. It is possible that the transfected MDCK cells had reduced expression of endogenous LRP1 that was responsible for significant efflux of RAP in the control cells.

Published results with intracellular trafficking of RAP show its dissociation from megalin (Czekay et al., 1997) or LRP1 (Bu et al., 1995) at low pH accompanied by receptor recycling. However, the RAP/megalin complex is more stable than other LRP complexes. It remains together as far as the late endosome whereas the lipoprotein lipase/megalin complex only lasts as far as the early endosome. Thus, a significant amount of RAP may escape intracellular degradation and undergo complete transcytosis in polarized epithelial/endothelial cells. The lack of significant degradation in the donor chambers in all our study groups indicates that the radioactivity measured represents actual transfer of RAP across the cell barrier rather than endocytosis and degradation. This is supported by the high TEER and the minimal transfer of the paracellular permeation marker albumin. Therefore, RAP has saturable, receptor-mediated apical-to-basolateral transport in MEGt-transfected MDCK cells.

In summary, RAP crosses the BBB by an efficient, saturable transport system probably mediated by megalin. In this process, RAP enters the brain parenchyma intact. Identification of a specific transport system for RAP at the BBB indicates the potential for RAP-mediated delivery of therapeutic peptides and proteins from blood to brain.

Supported by NIH (NS46528, NS45751 and DK54880) and BioMarin Pharmaceutical, Inc. We thank Maria Paz Marzolo (Catholic University, Chile) for providing the MDCK cells stably transfected with LRP mini-receptor and megalin chimera.

References

Banks, W. A., Robinson, S. M., Verma, S. and Morley, J. E. (2003). Efflux of human and mouse amyloid β proteins 1-40 and 1-42 from brain: impairment in a mouse model of Alzheimer's disease. *Neurosci.* **121**, 487-492.

Berryman, D. E. and Bensadoun, A. (1995). Heparan sulfate proteoglycans are primarily responsible for the maintenance of enzyme activity, binding, and degradation of lipoprotein lipase in Chinese hamster ovary cells. *J. Biol. Chem.* **270**, 24524-24531.

Blasberg, R. G., Fenstermacher, J. D. and Patlak, C. S. (1983). Transport of α-aminoisobutyric acid across brain capillary and cellular membranes. *J. Cereb. Blood Flow Metab.* **3**, 8-32.

Broadwell, R. D., Baker-Cairns, B. J., Friden, P. M., Oliver, C. and Villegas, J. C. (1996). Transcytosis of protein through the mammalian cerebral epithelium and endothelium. III. Receptor-mediated transcytosis through the blood-brain barrier of blood-borne transferrin and antibody against the transferrin receptor. *Exp. Neurol.* **142**, 47-65.

Bu, G., Maksymovitch, E. A., Geuze, H. and Schwartz, A. L. (1994). Subcellular localization and endocytic function of low density lipoprotein receptor-related protein in human glioblastoma cells. *J. Biol. Chem.* **269**, 29874-29882.

Bu, G., Geuze, H. J., Strous, G. J. and Schwartz, A. L. (1995). 39 kDa receptor-associated protein is an ER-resident protein and molecular chaperon for LDL receptor-related protein. *EMBO J.* **14**, 2269-2280.

Chun, J. J., Wang, L., Pasinetti, G. M., Finch, C. E. and Zlokovic, B. V. (1999). Glycoprotein 330 /megalin (LRP-2) has low prevalence as mRNA and protein in brain microvessel and choroid plexus. *Exp. Neurol.* **157**, 194-201.

Czekay, R. P., Orlando, R. A., Woodward, L., Lundstrom, M. and Farquhar, M. G. (1997). Endocytic trafficking of megalin/RAP complexes: dissociation of the complexes in late endosomes. *Mol. Biol. Cell* **8**, 517-532.

Demeule, M., Poirier, J., Jodoin, J., Bertrand, Y., Desrosiers, R. R., Dagenais, C., Nguyen, T., Lanthier, J., Gabathuler, R., Kennard, M. et al. (2002). High transcytosis of melanotransferrin (p97) across the blood-brain barrier. *J. Neurochem.* **83**, 924-933.

Irvine, J. D., Takahashi, L., Lockhart, K., Cheong, J., Tolan, J. W., Selick, H. E. and Grove, J. R. (1999). MDCK (Madin-Darby canine kidney) cells: a tool for membrane permeability screening. *J. Pharm. Sci.* **88**, 28-33.

Kastin, A. J., Akerstrom, V. and Pan, W. (2001). Validity of multiple-time regression analysis in measurement of tritiated and iodinated leptin crossing the blood-brain barrier: meaningful controls. *Peptides* **22**, 2127-2136.

Kounnas, M. Z., Haudenschild, C. C., Strickland, D. K. and Argraves, W. S. (1994). Immunological localization of glycoprotein 330, low density lipoprotein receptor related protein and 39 kDa receptor associated protein in embryonic mouse tissues. *In Vivo* **8**, 343-351.

Li, Y., Marzolo, M. P., van Kerkhof, P., Strous, G. J. and Bu, G. (2000). The YXXL motif, but not the two NPXY motifs, serves as the dominant endocytosis signal for low density lipoprotein receptor-related protein. *J. Biol. Chem.* **275**, 17187-17194.

Li, Y., Cam, J. and Bu, G. (2001a). Low-density lipoprotein receptor family. Endocytosis and signal transduction. *Mol. Neurobiol.* **23**, 53-67.

Li, Y., Lu, W., Marzolo, M. P. and Bu, G. (2001b). Differential functions of members of the low density lipoprotein receptor family suggested by their distinct endocytosis rates. *J. Biol. Chem.* **276**, 18000-18006.

Marinò, M., Chiovato, L., Lisi, S., Pinchera, A. and McCluskey, R. T. (2001). Binding of the low density lipoprotein receptor-associated protein (RAP) to thyroglobulin (Tg): putative role of RAP in the Tg secretory pathway. *Mol. Endocrinol.* **15**, 1829-1837.

Marinò, M., Zheng, G. and McCluskey, R. T. (2003). Megalin (gp330) is an endocytic receptor for thyroglobulin on cultured Fisher rat thyroid cells. *J. Biol. Chem.* **274**, 12898-12904.

Marzolo, M. P., Yuseff, M. I., Retamal, C., Donoso, M., Ezquer, F., Farfán, P., Li, Y. and Bu, G. (2003). Differential distribution of low-density lipoprotein-receptor-related protein (LRP) and megalin in polarized epithelial cells is determined by their cytoplasmic domains. *Traffic* **4**, 273-288.

Melman, L., Cao, Z.-F., Rennke, S., Marzolo, M. P., Wardell, M. R. and Bu, G. (2001). High affinity binding of receptor-associated protein to heparin and low density lipoprotein receptor-related protein requires similar basic amino acid sequence motifs. *J. Biol. Chem.* **276**, 29338-29346.

Moos, T. and Morgan, E. H. (2001). Restricted transport of anti-transferrin receptor antibody (OX26) through the blood-brain barrier in the rat. *J. Neurochem.* **79**, 119-129.

Morris, C. M., Keith, A. B., Edwardson, J. A. and Pullen, R. G. (1992). Uptake and distribution of iron and transferrin in the adult rat brain. *J. Neurochem.* **59**, 300-306.

Orlando, R. A. and Farquhar, M. G. (1993). Identification of a cell line that expresses a cell surface and a soluble form of the gp330 /receptor-associated protein (RAP) Heymann nephritis antigenic complex. *Proc. Natl. Acad. Sci. USA* **90**, 4082-4086.

Orlando, R. A. and Farquhar, M. G. (1994). Functional domains of the receptor-associated protein (RAP). *Proc. Natl. Acad. Sci. USA* **91**, 3161-3165.

Pan, W. and Kastin, A. J. (2000). Interactions of IGF-1 with the blood-brain barrier in vivo and in situ. *Neuroendocrinol.* **72**, 171-178.

Pan, W. and Kastin, A. J. (2003). Transport of cytokines and neurotrophins across the BBB and their regulation after spinal cord injury, In *Blood-Spinal Cord and Brain Barriers in Health and Disease* (ed. H. Shanker and J. Westman), pp. 395-407. San Diego, CA: Academic Press.

Pan, W., Banks, W. A. and Kastin, A. J. (1997). Permeability of the blood-brain and blood-spinal cord barriers to interferons. *J. Neuroimmunol.* **76**, 105-111.

Pan, W., Banks, W. A. and Kastin, A. J. (1998). Permeability of the blood-brain barrier to neurotrophins. *Brain Res.* **788**, 87-94.

Pan, W., Vallance, K. and Kastin, A. J. (1999). TGFα and the blood-brain barrier: accumulation in cerebral vasculature. *Exp. Neurol.* **160**, 454-459.

Pan, W., Kastin, A. J. and Brennan, J. M. (2000). Saturable entry of leukemia inhibitory factor from blood to the central nervous system. *J. Neuroimmunol.* **106**, 172-180.

Patlak, C. S., Blasberg, R. G. and Fenstermacher, J. D. (1983). Graphical evaluation of blood-to-brain transfer constants from multiple-time uptake data. *J. Cereb. Blood Flow Metab.* **3**, 1-7.

Savonen, R., Obermoeller, L. M., Trausch-Azar, J. S., Schwartz, A. L. and Bu, G. (1999). The carboxyl-terminal domain of receptor-associated protein facilitates proper folding and trafficking of the very low density lipoprotein receptor by interaction with the three amino-terminal ligand-binding repeats of the receptor. *J. Biol. Chem.* **274**, 25877-25882.

Shayo, M., McLay, R. N., Kastin, A. J. and Banks, W. A. (1997). The putative blood-brain barrier transporter for the β-amyloid binding protein apolipoprotein J is saturated at physiological concentrations. *Life Sci.* **60**, PL115-PL118.

Shibata, M., Yamada, S., Kumar, S. R., Calero, M., Bading, J., Frangione, B., Holtzman, D. M., Miller, C. A., Strickland, D. K., Ghiso, J. et al. (2000). Clearance of Alzheimer's amyloid-β_{1-40} peptide from brain by LDL receptor-related protein-1 at the blood-brain barrier. *J. Clin. Invest.* **106**, 1489-1499.

Skarlatos, S., Yoshikawa, T. and Pardridge, W. M. (1995). Transport of [^{125}I]transferrin through the rat blood-brain barrier. *Brain Res.* **683**, 164-171.

Ueda, F., Raja, K. B., Simpson, R. J., Trowbridge, I. S. and Bradbury, M. W. (1993). Rate of 59Fe uptake into brain and cerebrospinal fluid and the influence thereon of antibodies against the transferrin receptor. *J. Neurochem.* **60**, 106-113.

Veinbergs, I., van Uden, E., Mallory, M., Alford, M., McGiffert, C., DeTeresa, R., Orlando, R. and Masliah, E. (2001). Role of apolipoprotein E receptors in regulating the differential *in vivo* neurotrophic effects of apolipoprotein E. *Exp. Neurol.* **170**, 15-26.

Vilhardt, F., Nielsen, M., Sandvig, K. and van Beurs, B. (1999). Urokinase-type plasminogen activator receptor is internalized by different mechanisms in polarized and nonpolarized Madin-Darby canine kidney epithelial cells. *Mol. Biol. Cell* **10**, 179-195.

Warshawsky, I., Bu, G. and Schwartz, A. L. (1993). 39-kD protein inhibits tissue-type plasminogen activator clearance in vivo. *J. Clin. Invest.* **92**, 937-944.

Wilnow, T. E., Hilpert, J., Armstrong, S. A., Rohlmann, A., Hammer, R. E., Burns, D. K. and Herz, J. (1996). Defective forebrain development in mice lacking gp330/megalin. *Proc. Natl. Acad. Sci. USA* **93**, 8460-8464.

Yepes, M., Sandkvist, M., Moore, E. G., Bugge, T. H., Strickland, D. K. and Lawrence, D. A. (2003). Tissue-type plasminogen activator induces opening of the blood-brain barrier via the LDL receptor-related protein. *J. Clin. Invest.* **112**, 1533-1540.

Zhang, W., Riedel, C., Carrasco, N. and Arvan, P. (2002). Polarized trafficking of thyrocyte proteins in MDCK cells. *Mol. Cell. Endocrinol.* **188**, 27-36.

Zheng, G., Bachinsky, D. R., Stamenkovic, I., Strickland, D. K., Brown, D., Andres, G. and McCluskey, R. T. (1994). Organ distribution in rats of two members of the low-density lipoprotein receptor gene family, gp330 and LRP/alpha 2MR, and the receptor-associated protein (RAP). *J. Histochem. Cytochem.* **42**, 531-542.

Zlokovic, B. V., Skundric, D. S., Segal, M. B., Lipovac, M. N., Mackic, J. B. and Davson, H. (1990). A saturable mechanism for transport of immunoglobulin G across the blood-brain barrier of the guinea pig. *Exp. Neurol.* **107**, 263-270.

Zlokovic, B. V., Martel, C. L., Matsubara, E., McComb, J. G., Zheng, G., McCluskey, R. T., Frangione, B. and Ghiso, J. (1996). Glycoprotein 330 /megalin: probable role in receptor-mediated transport of apolipoprotein J alone and in a complex with Alzheimer disease amyloid β at the blood-brain and blood-cerebrospinal fluid barriers. *Proc. Natl. Acad. Sci. USA* **93**, 4229-4234.

EXHIBIT E

Clearance of Alzheimer's amyloid-β_{1-40} peptide from brain by LDL receptor–related protein-1 at the blood-brain barrier

Masayoshi Shibata,[1] Shinya Yamada,[1] S. Ram Kumar,[1] Miguel Calero,[2] James Bading,[3] Blas Frangione,[2] David M. Holtzman,[4] Carol A. Miller,[5] Dudley K. Strickland,[6] Jorge Ghiso,[2] and Berislav V. Zlokovic[1,7]

[1]Department of Neurological Surgery, Keck School of Medicine of the University of Southern California, Los Angeles, California, USA
[2]Department of Pathology, New York University Medical Center, New York, New York, USA
[3]Department of Radiology, Keck School of Medicine of the University of Southern California, Los Angeles, California, USA
[4]Department of Neurology, Washington University School of Medicine, St. Louis, Missouri, USA
[5]Department of Pathology, Keck School of Medicine of the University of Southern California, Los Angeles, California, USA
[6]Department of Vascular Biology, Holland Laboratories, American Red Cross, Rockville, Maryland, USA
[7]Division of Neurovascular Biology, Center for Aging and Developmental Biology of the University of Rochester Medical School, Rochester, New York, USA

Address correspondence to: Berislav V. Zlokovic, Division of Neurovascular Biology, Aab Institute of Biomedical Sciences, Center for Aging and Developmental Biology, University of Rochester Medical School, 601 Elmwood Avenue, Box 645, Rochester, New York 14642, USA. Phone: (716) 273-3132; Fax: (716) 273-3133; E-mail: Berislav_Zlokovic@urmc.rochester.edu.

Received for publication June 5, 2000, and accepted in revised form November 6, 2000.

Elimination of amyloid-β peptide (Aβ) from the brain is poorly understood. After intracerebral microinjections in young mice, ^{125}I-Aβ_{1-40} was rapidly removed from the brain ($t_{1/2} \leq 25$ minutes), mainly by vascular transport across the blood-brain barrier (BBB). The efflux transport system for Aβ_{1-40} at the BBB was half saturated at 15.3 nM, and the maximal transport capacity was reached between 70 nM and 100 nM. Aβ_{1-40} clearance was substantially inhibited by the receptor-associated protein, and by antibodies against LDL receptor–related protein-1 (LRP-1) and α_2-macroglobulin (α_2M). As compared to adult wild-type mice, clearance was significantly reduced in young and old apolipoprotein E (apoE) knockout mice, and in old wild-type mice. There was no evidence that Aβ was metabolized in brain interstitial fluid and degraded to smaller peptide fragments and amino acids before its transport across the BBB into the circulation. LRP-1, although abundant in brain microvessels in young mice, was downregulated in older animals, and this downregulation correlated with regional Aβ accumulation in brains of Alzheimer's disease (AD) patients. We conclude that the BBB removes Aβ from the brain largely via age-dependent, LRP-1–mediated transport that is influenced by α_2M and/or apoE, and may be impaired in AD.

J. Clin. Invest. **106**:1489–1499 (2000).

Introduction

Deposition of amyloid-β peptide (Aβ) in the brain occurs during normal aging and is accelerated in patients with Alzheimer's disease (AD). Aβ is central to the pathology of AD, and is the main constituent of brain parenchymal and vascular amyloid (1–6). Aβ extracted from senile plaques contains mainly Aβ_{1-40} and Aβ_{1-42} (7), whereas vascular amyloid is predominantly Aβ_{1-39} and Aβ_{1-40} (8). Several sequences of Aβ were found in both lesions (9–11). A major soluble form of Aβ, which is present in the blood, cerebrospinal fluid (CSF) (12–14), and brain (15–16) is Aβ_{1-40}. In the circulation, CSF, and brain interstitial fluid (ISF), soluble Aβ may exist as a free peptide or be associated with different transport binding proteins such as apolipoproteins J (apoJ) (17–18) and E (apoE) (19), transthyretin (20), lipoproteins (21), albumin (22), and α_2-macroglobulin (α_2M) (23).

The neuronal theory argues that soluble brain-derived Aβ is a precursor of Aβ deposits. Neuronal cells secrete Aβ in culture (24), which supports this view. An increase in soluble Aβ in AD and Down syndrome brains precedes amyloid plaque formation (15, 25, 26) and correlates with the development of vascular pathology (27). Several cytosolic proteases that may degrade intracellular Aβ in vitro cannot degrade extracellular Aβ from brain ISF (28) or CSF (29) in vivo. An exception to this is enkephalinase, which may degrade Aβ_{1-42} from brain ISF (28). However, the physiological importance of this degradation in vivo remains unclear, because the peptide was studied at extremely high pharmacological concentrations (30).

It has been suggested that decreased clearance of Aβ from brain and CSF is the main cause of Aβ accumulation in sporadic AD (31). Because Aβ is continuously produced in the brain, we hypothesized that an effi-

cient clearance mechanism or mechanisms must exist at the blood-brain barrier (BBB) to prevent its accumulation and subsequent aggregation in the brain. Cell-surface receptors such as the receptor for advanced glycation end products (RAGE) (32–33), scavenger receptor type A (SR-A) (34), LDL receptor–related protein-1 (LRP-1) (35–38), and LRP-2 (39) bind Aβ at low (nanomolar) concentrations as free peptide (RAGE, SR-A) and/or in complex with α_2M, apoE, or apoJ (LRP-1, LRP-2). RAGE and SR-A regulate brain endothelial endocytosis and transcytosis of Aβ that is initiated at the luminal side of the BBB (33), whereas LRP-2 mediates BBB transport of plasma Aβ complexed to apoJ (39). The role of vascular receptors and BBB transport in the removal of brain-derived Aβ is unknown.

In this study, we developed a brain tissue clearance technique in mice based on a model used previously in the rabbit (40). This technique was used to determine in vivo the efflux rates of $A\beta_{1-40}$ from the CNS as a function of time and concentration of peptide, and to characterize vascular transport and/or any receptor-mediated efflux mechanisms involved in elimination of brain-derived Aβ across the BBB. The study focused on LRP-1 and its ligands, α_2M and apoE, first because they promote Aβ clearance in smooth muscle cells (35), neurons (36, 38), and fibroblasts (37); and second, because apoE4 is a definite risk factor, and α_2M is a possible risk factor for AD (41–42).

Methods

Synthetic peptide and radioiodination. Peptide DAEFRHDSGYEVHHQKLVFFAEDVGSNKGAIIGLMVGGVV ($A\beta_{1-40}$) homologous to residues 672–711 of Aβ-precursor protein 770 was synthesized at the W.M. Keck Facility at Yale University using *N-t*-butyloxycarbonyl chemistry. The peptide was purified by HPLC. Aliquots of the final products were lyophilized and stored at –20°C until use. Radioiodination was carried out with $Na^{125}I$ and IodoBeads (Pierce Chemical Co., Rockford, Illinois, USA), and the resulting components were resolved by HPLC (39). Aliquots of radiolabeled $A\beta_{1-40}$ were kept at –20°C for a maximum of 4 weeks before use. The HPLC analysis confirmed that more than 99% of radioactivity was present in the form of nonoxidized monomeric peptide.

Brain clearance model in mice. Experiments were performed on male C57BL/6 wild-type mice, 8–10 weeks old and 9–10 months old, and on male apoE knockout (apoE KO) mice on a C57BL/6 background (Taconic Farms, Germantown, New York, USA) that were also 8–10 weeks old and 9–10 months old. CNS clearance of radiolabeled $A\beta_{1-40}$ and the inert polar marker inulin was determined as described below (40, 43).

A stainless steel guide cannula was implanted stereotaxically into the right caudate nucleus of mice anesthetized with 60 mg/kg intraperitoneal sodium pentobarbital). Coordinates for the tip of the cannula were 0.9 mm anterior and 1.9 mm lateral to bregma, and 2.9 mm below the surface of the brain. The guide cannula and screw were fixed to the skull with methylmethacrylate (Plastics One Inc., Roanoke, Virginia, USA), and a stylet was introduced into the guide cannula. Animals were observed for 1 week before radiotracer studies.

For radioisotope injection, animals were reanesthetized, and an injector cannula (Plastics One Inc.) was attached to a 10-μl gas-tight microsyringe (Hamilton Co., Reno, Nevada, USA) using 24-gauge Teflon tubing (Small Parts Inc., Miami Lake, Florida, USA). The amount of injected tracer was determined accurately using a micrometer to measure linear displacement of the syringe plunger in the precalibrated microsyringe. Tracer fluid (0.5 μl) containing ^{125}I-$A\beta_{1-40}$ at concentrations varying from 0.05 nM to 120 nM was injected over a period of 5 minutes, along with [^{14}C]inulin. When the effect of different molecular reagents was tested, those were injected simultaneously with the radiolabeled peptides.

Time response was studied with ^{125}I-$A\beta_{1-40}$ from 10 minutes to 300 minutes; dose-dependent effects were determined at 30 minutes. The effects of different molecular reagents that may potentially inhibit ^{125}I-$A\beta_{1-40}$ clearance were studied at 30 minutes. Among the reagents studied was the rabbit anti–human LRP-1 Ab designated R777, which was affinity purified on a Sepharose–LRP-1 heavy-chain column as described (44). R777 immunoprecipitates mouse LRP-1, as we described (44), and blocks LRP-1–mediated uptake of amyloid β precursor protein (APP) and thrombospondin in murine fibroblasts (45, 46). Another studied reagent that may inhibit ^{125}I-$A\beta_{1-40}$ clearance is receptor-associated protein (RAP; kindly provided by G. Bu, Washington University). We also studied the rabbit anti–mouse α_2M Ab designated YNRMA2M, which is specific for mouse α_2M as demonstrated by radial immunodiffusion and immunoelectrophoresis (Accurate Chemical & Scientific Corp., Westbury, New York, USA); a rabbit anti–rat gp330 affinity-purified IgG designated Rb6286, which crossreacts with mouse LRP-2 as reported (47) (kindly provided by Scott Argraves, University of South Carolina Medical School, Charleston, South Carolina, USA); a rabbit anti-human RAGE Ab that crossreacts with mouse RAGE (32) (kindly provided by D. Stern, Columbia University, New York, New York, USA), and fucoidin (Sigma Chemical Co., St. Louis, Missouri, USA).

Tissue sampling and radioactivity analysis. Brain, blood, and CSF were sampled and prepared for radioactivity analysis. Degradation of ^{125}I-$A\beta_{1-40}$ was initially studied by trichloroacetic acid (TCA) precipitation assay. Previous studies with ^{125}I-$A\beta_{1-40}$ demonstrated an excellent correlation between TCA and HPLC methods (33, 48–51). Brain, plasma, and CSF samples were mixed with TCA (final concentration 10%) and centrifuged at 24,840 *g* at 4°C for 8–10 minutes. Radioactivity in the precipitate, water, and chloroform fractions was determined in a gamma counter (Wallac Finland Oy, Turku, Finland). The ^{125}I-$A\beta_{1-40}$ injected into the brain was more than 97% intact, according to TCA analysis.

Degradation of ^{125}I-$A\beta_{1-40}$ in the brain was further

studied by HPLC and SDS-PAGE analysis. After intracerebral injections of ^{125}I-Aβ_{1-40}, brain tissue was homogenized in PBS containing protease inhibitors (0.5 mM phenylmethylsulfonyl fluoride, 1 μg/ml leupeptin, and 1 mM *p*-aminobenzamidine), and then centrifuged at 100,000 *g* for 1 hour at 4°C. The supernatant was then lyophilized. The resulting material was dissolved in 0.005% trifluoroacetic acid (TFA) in water at pH 2 before injection onto a Vydac C4 column (The Separations Group, Hesperia, California, USA). The separation was achieved with a 30-minute linear gradient of 25–83% acetonitrile in 0.1% TFA at a flow rate of 1 ml/min, as we have described (51). Under these conditions, the Aβ_{1-40} standard eluted at 14.5 minutes. Column eluants were monitored at 214 nm. The eluted fractions were collected and counted. The ^{125}I-Aβ_{1-40} injected into the brain was greater than 97% intact according to HPLC analysis, confirming the results of TCA analysis.

For SDS-PAGE analysis, TCA-precipitated samples were resuspended in 1% SDS, vortexed, and incubated at 55°C for 5 minutes. Samples were then neutralized, boiled for 3 minutes, homogenized, and analyzed by electrophoresis in 10% Tris-tricine gels, followed by fluorography. Lyophilized HPLC fractions were resuspended in sample buffer, neutralized, boiled, and electrophoresed as we have reported (39).

Calculations of clearance rates. The analysis of curves of radioactivity disappearance from the brain was as reported (40, 43). The percentage of radioactivity remaining in the brain after microinjection was determined as

(Equation 1) $\%\ \text{Recovery in brain} = 100 \times (N_b/N_i)$

where N_b is the radioactivity remaining in the brain at the end of the experiment, and N_i is the radioactivity injected into the brain.

In all calculations, the dpm values for [^{14}C]inulin and the cpm values for TCA-precipitable ^{125}I radioactivity were used. Inulin was studied as a metabolically inert polar reference marker that is neither transported across the BBB nor retained by the brain (40); its clearance rate, k_{inulin}, provides a measure of the ISF bulk flow and is calculated as

(Equation 2) $N_{b(inulin)}/N_{i(inulin)} = \exp(-k_{inulin} \times t)$

In the case of Aβ, there are two possible physiological pathways of elimination: direct transport across the BBB into the bloodstream, and elimination via ISF bulk flow into the CSF and cervical lymphatics. It is also possible that Aβ is retained within the brain by binding to its cell-surface receptors directly as a free peptide, and/or by binding to different transport proteins. Thus, according to the model, the fraction of Aβ remaining in the brain can be expressed as

(Equation 3) $N_{b(A\beta)}/N_{i(A\beta)} = (a_1 + a_2) \times e^{-k_1 \times t}$

where $a_1 = k_2/(k_1 + k_2)$ and $a_2 = k_1/(k_1 + k_2)$, and k_1 and k_2 denote the fractional coefficients of total efflux from the brain and retention within the brain, respectively.

The fractional rate constant of Aβ efflux across the BBB from brain parenchyma can be calculated by knowing the fractional rate coefficient of total efflux of Aβ and inulin as

(Equation 4) $k_3 = k_1 - k_{(inulin)}$

i.e., as the difference between the fractional rate constant for total efflux of Aβ and the fractional rate constant of inulin. The half-saturation concentration for the elimination of Aβ via transport across the BBB, $k_{1/2}$, was calculated from the equation

(Equation 5) $[1 - (N_b/N_i)] \times 100 = Cl_{max}/(k_{1/2} + N_i)$

where Cl_{max} represents the maximal efflux capacity for the saturable component of Aβ clearance across the BBB, corrected for peptide clearance by the ISF flow. Cl_{max} is expressed as a percentage of the injected dose, $[1 - (N_b / N_i)] \times 100$, cleared from brain by saturable BBB transport over 30 minutes.

The MLAB mathematical modeling system (Civilized Software Inc., Silver Spring, Maryland, USA) was used to fit the compartmental model to the disappearance curves or percent recovery data with inverse square weight.

Immunocytochemical analysis in mice. Expression of LRP-1 and α_2M in mouse brain was studied by immunohistochemical analysis. Fresh-frozen, acetone-fixed brain sections of 2-month-old and 9-month-old wild-type and apoE KO mice were stained using anti-human LRP R777 Ab that crossreacts with mouse LRP-1 (44–46) (1.5 mg/ml; 1:300 dilution), and anti-mouse α_2M Ab (as described above, 1:250 dilution). R777 was affinity purified over a Sepharose–LRP-1 heavy-chain column, as described (44). The number of positive vessels was counted in ten random fields by two independent blinded observers, and was expressed as percentage per square millimeter of section. The extent and intensity of staining in cellular elements was quantitated using the ESECO Digimatic Universal Imaging System (Electronic Systems Engineering Co., West Chester, Pennsylvania, USA) and NIH imaging systems. Microvessels were carefully excluded from the quantitation by suitably varying the magnitudes of measurement. The relative intensity of cellular staining (excluding the microvasculature) in brain sections of young mice was arbitrarily normalized to 1 for purposes of comparison. Routine controls included sections prepared without primary Ab, without secondary Ab, and the use of an irrelevant primary Ab.

Neuropathological analysis in humans. Three AD patients and three neurologically normal, age-matched controls from the Alzheimer's Disease Research Center of the University of Southern California were evaluated clinically and were followed to autopsy. Included were three males and three females, ranging in age from 69 to 99 years.

Tissue blocks (1 cm^3) were obtained postmortem (range 4–7 hours; mean 5 hours.), fixed in 10% neutral buffered formalin (pH 7.3; Sigma Chemical Co.), and

embedded in paraffin or snap-frozen in liquid nitrogen–chilled isopentane. Tissues were sampled from the superior and middle frontal gyrus (Brodmann's area 10), and the cerebellar hemisphere.

Sections were stained with either hematoxylin and eosin or thioflavine S, in a modification of Bielschowsky's silver impregnation method (Gallyas stain). Thioflavine S–stained sections were viewed through a Zeiss fluorescence microscope with a narrow-band, blue/violet filter at 400–455 nm. Examination was performed by two independent observers. Diagnosis of AD was according to a modified protocol from the Consortium to Establish a Registry for Alzheimer's Disease (52).

For immunocytochemical analysis, we used cryostat sections (10 μm) of frontal cortex (Brodmann's area 10) that were air dried. Immunocytochemistry was performed using the avidin-biotin peroxidase complex method (Vector Laboratories Inc., Burlingame, California, USA). Antibodies included $A\beta_{1\text{-}40}$, rabbit anti-human, 1:1,000 (1 mg/ml; Chemicon International, Temecula, California, USA); $A\beta_{1\text{-}42}$, rabbit anti-human, 1:1,000 (1 mg/ml); the mouse mAb to the heavy chain of human LRP-1 designated 8G1, which is specific for human LRP-1 and recognizes an epitope on the 515-kDa subunit (53), 1:300 (1.5 mg/ml); and CD105 (clone SMG), mouse anti-human, 1:100 (0.1 mg/ml; Serotec Ltd., Oxford, United Kingdom). For single staining with CD105 and LRP, after incubation with primary Ab, sections were washed three times in PBS (pH 7.4), and treated with biotinylated anti-mouse IgG for 30 minutes. After three washes in PBS, slides were incubated with avidin-biotin–horseradish peroxidase complex for 30 minutes and washed three times in PBS. Binding was detected with an SG peroxidase detection kit (blue/gray; Vector Laboratories Inc.). For double labeling, after incubation with Aβ overnight at 4°C, sections were washed three times with PBS and treated with biotinylated anti-rabbit IgG. They were then washed again, and positivity was detected with NovaRED (Vector Laboratories Inc.). After three washes in PBS, the second primary Ab (LRP or CD-105) was applied, and staining was performed as described for single labeling. Imaging was accomplished using an Axiophot II microscope (Carl Zeiss Inc., Thornwood, New York, USA) equipped with a SPOT digital camera (Diagnostic Instruments Inc., Sterling Heights, Michigan, USA).

Results

Figure 1a illustrates brain radioactivity-disappearance curves of [^{14}C]inulin and ^{125}I-$A\beta_{1\text{-}40}$ (TCA-precipitable ^{125}I radioactivity) studied at a concentration of 60 nM. Clearance of inulin, a reference extracellular fluid (ECF) marker that is neither transported across the BBB nor retained by the brain (40, 43), approximated a single exponential decay, as expected from previous studies. The clearance curve reflecting total efflux of ^{125}I-$A\beta_{1\text{-}40}$ from brain was bi-exponential, and was much lower than that for inulin, indicating significant biological transport of $A\beta_{1\text{-}40}$ out of the brain. The two components of $A\beta_{1\text{-}40}$ efflux, rapid elimination by vascular transport across the BBB into the blood and slow elimination via the ISF flow, were computed from Figure 1a with equations 3 and 4 and are illustrated in Figure 1b. Figure 1b indicates significantly higher clearance of Aβ via BBB transport than via ISF bulk flow.

The half-time ($t_{1/2}$) for brain efflux of $A\beta_{1\text{-}40}$ and inulin calculated from Figure 1a and equations 2 and 3 were 25.5 ± 2.0 minutes and 239.0 ± 12.5 minutes, respectively, a 9.4-fold difference (Table 1). The half-time of efflux of $A\beta_{1\text{-}40}$ across the BBB was 34.6 ± 3.6 minutes, 6.9-fold faster than by ISF bulk flow. In addition to efflux, there was also a slow, time-dependent retention of $A\beta_{1\text{-}40}$ in brain parenchyma with a $t_{1/2}$ of 164.5 minutes. As shown in Table 1, the rate k (min^{-1}) of clearance of $A\beta_{1\text{-}40}$ from the brain was 7.9-fold higher than that for inulin. The relative contributions of $A\beta_{1\text{-}40}$ efflux at 60 nM, by transport across the BBB and by ISF bulk flow based on 5-

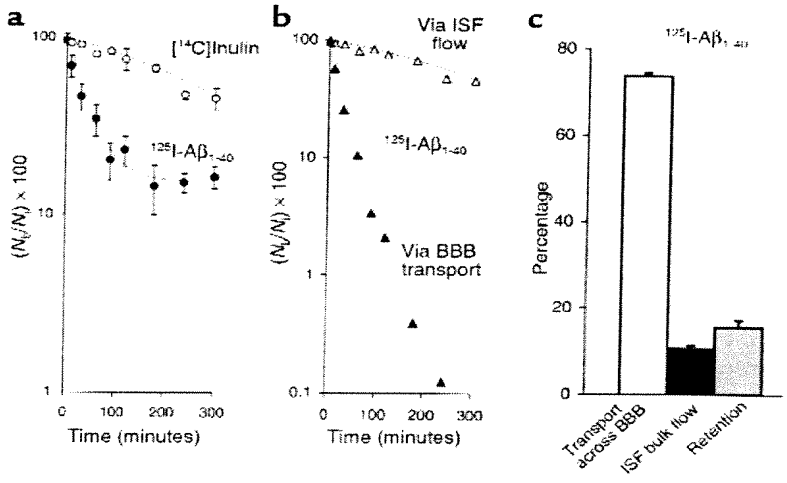

Figure 1
(**a**) Time-disappearance curves of [^{14}C]inulin (open circles) and ^{125}I-$A\beta_{1\text{-}40}$ (60 nM; TCA-precipitable ^{125}I radioactivity, filled circles) from the CNS after simultaneous microinjections of tracers into the caudate nucleus in mice. Each point represents the mean ± SD of three to seven animals. (**b**) Two components of ^{125}I-$A\beta_{1\text{-}40}$ efflux, vascular transport across the BBB (filled triangles) and transport via ISF bulk flow (open triangles), were computed with equations 3 and 4 using data from **a**. (**c**) Relative contributions to $A\beta_{1\text{-}40}$ efflux by its transport across the BBB (open bar), diffusion via ISF bulk flow (filled bar), and retention (gray bar) in the brain were studied at 60 nM concentrations and calculated from the fractional coefficients given in Table 1.

hour measurements, were 73.8% and 10.7% respectively, whereas 15.6% of the dose remained sequestered within the CNS (Figure 1c).

After CNS injection, both tracers reached the CSF; the CSF time-appearance curves are shown in Figure 2a. The amount of ^{125}I-Aβ_{1-40} (TCA-precipitable ^{125}I radioactivity) measured in the CSF was lower than that for inulin at each studied timepoint, possibly reflecting active clearance of Aβ_{1-40} from the CSF, as was suggested previously (28). It is noteworthy that at each studied timepoint, the ^{125}I-labeled material in the CSF was greater than 96% TCA-precipitable, indicating no degradation of the peptide. Both tracers also appeared in plasma (Figure 2b), and higher levels of TCA-precipitable ^{125}I-Aβ_{1-40} radioactivity than of [^{14}C]inulin radioactivity were consistent with active transport of Aβ_{1-40} out of the CNS across the BBB. The absolute amounts of both tracers in the CSF and plasma were low, however, due to relatively rapid clearance from the CSF in comparison to slow ISF bulk flow (29), and significant systemic body clearance (48), respectively.

Figure 3 (a and b) illustrates that ^{125}I-Aβ_{1-40} was not significantly degraded in brain ISF before its transport across the BBB, as determined by TCA, HPLC, and SDS-PAGE analysis of ^{125}I radioactivity in brains. The TCA analysis suggests that only 4.2–9.9% of ^{125}I radioactivity in brains was not TCA-precipitable at different timepoints within 270 minutes of intracerebral microinjection of ^{125}I-Aβ_{1-40} (Figure 3a). The HPLC analysis of brain radioactivity confirmed the TCA results by indicating that 93.7% of the peptide remains intact in brain ISF at 60 minutes (Figure 3b, right). It is noteworthy that ^{125}I-Aβ_{1-40} was more than 97% intact at the time of injection, as determined both by the HPLC and TCA analyses. The results were corroborated by SDS-PAGE analysis of lyophilized aliquots of HPLC peaks of brain homogenates at different timepoints after ^{125}I-Aβ_{1-40} injection, showing a single radioactive band at about 4 kDa (Figure 3b, left). The identity of the radioactive components on gels as Aβ_{1-40} peptide was confirmed by Western blot analysis using anti-Aβ Ab and enhanced chemiluminescence as a detection system (not shown). More than 96% of ^{125}I radioactivity in the CSF was TCA-precipitable at studied timepoints between 15 minutes and 270 minutes (not shown). In contrast, degradation products of ^{125}I-Aβ_{1-40} were found in plasma (Figure 3c); the amount of degraded ^{125}I-Aβ_{1-40} corresponding to non-TCA-precipitable ^{125}I radioactivity increased from 37.6% to 58.3% during the period from 15 minutes to 120 minutes after intracerebral microinjection of intact ^{125}I-Aβ_{1-40} (Figure 3c). It is noteworthy that the amount of radioactivity in plasma after 120 minutes was relatively small, and approached the limits of sensitivity of the TCA assay.

Table 1
Clearance rates (k) for ^{125}I-Aβ_{1-40} and [^{14}C]inulin

Parameter	^{125}I-Aβ_{1-40}		[^{14}C]inulin	
	k (min^{-1})	$t_{1/2}$ (min)	k (min^{-1})	$t_{1/2}$ (min)
Total efflux	0.0229 ± 0.0023[A]	25.5 ± 2.0[A]	0.0029 ± 0.0002	239.0 ± 12.5
Transport via BBB	0.0200 ± 0.0023	34.6 ± 3.6	None	None
Transport via ISF	0.0029 ± 0.0002	239.0 ± 12.5	0.0029 ± 0.0002	239.0 ± 12.5
Retention in brain	0.0042 ± 0.0005	164.5 ± 17.6	None	None

Data are mean ± SD from 38 individual experiments. Fractional rate (k) values were calculated using equations 3 and 4. [A]$P < 0.05$ by Student's t test.

Clearance of Aβ in young mice was concentration dependent (Figure 4a). The efflux transport system was half saturated ($K_{1/2}$) at 15.3 nM of Aβ_{1-40}. The plateau or maximal clearance capacity was reached between 70 nM and 100 nM, and further increases in Aβ concentration resulted in progressively greater retention of the peptide in the brain. In contrast, clearance of [^{14}C]inulin did not change with increasing concentrations of Aβ, suggesting a physiologically intact BBB (Figure 4a).

The next set of experiments was designed to characterize the BBB transport system responsible for the transcytosis of Aβ. Brains were loaded with ^{125}I-Aβ_{1-40} at either 12 nM (Figure 4b) or 60 nM (Figure 4c), and clearance was determined at 30 minutes in the absence and presence of several molecular reagents that may act as potential inhibitors of and/or competitors in export. Figure 4b indicates that both the LRP-1 Ab (60 μg/ml) and RAP (200 nM) produced significant (58% and 30%, respectively) reductions in Aβ clearance from the brain compared with vehicle-treated controls; increasing the concentration of RAP to 5 μM decreased Aβ clearance by 44%. A significant (25%) inhibition in Aβ clearance

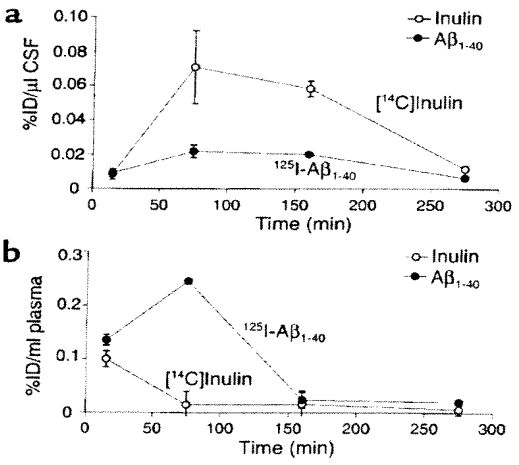

Figure 2
Time-appearance curves of [^{14}C]inulin (open circles) and ^{125}I-Aβ_{1-40} (60 nM; TCA-precipitable ^{125}I radioactivity, filled circles) in the CSF (**a**) and plasma (**b**) after simultaneous microinjections of tracers into the caudate nucleus in mice. Values are expressed as percentages of injected dose (%ID); each point is mean ± SD of three to seven animals.

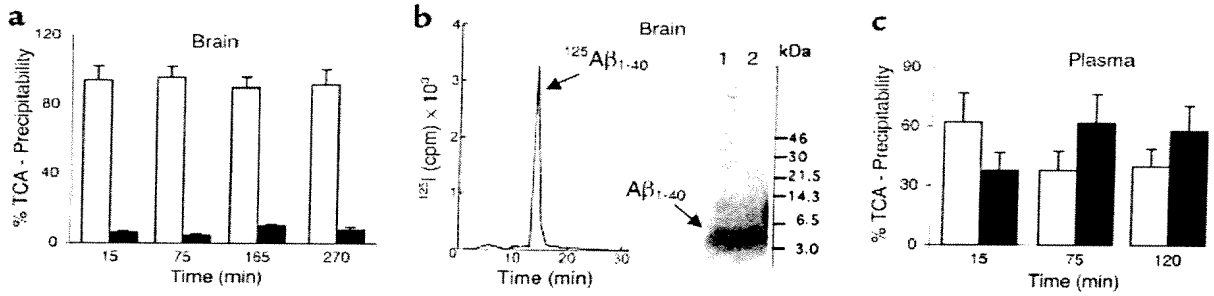

Figure 3

(**a**) Brain TCA-precipitable (open bars) and non-TCA-precipitable ^{125}I radioactivity (solid bars) after intracerebral microinjections of ^{125}I-$A\beta_{1-40}$ (60 nM) into the caudate nucleus in mice, expressed as a percentage of total ^{125}I radioactivity in the brain; mean ± SD of three to five animals. (**b**) Left panel shows HPLC elution profile of brain tissue 60 minutes after intracerebral microinjection of ^{125}I-$A\beta_{1-40}$ (60 nM). Separation was performed for 30 mg of brain tissue on a reverse-phase HPLC column, using a 30-minute linear gradient of 25–83% acetonitrile in 0.1% TFA, pH 2. ^{125}I-$A\beta_{1-40}$ eluted at 52%, corresponding to the elution time of $A\beta_{1-40}$ standard. Right panel shows SDS-PAGE analysis of brain tissue supernatant at 30 minutes (lane 1) and 60 minutes (lane 2) after intracerebral microinjection of ^{125}I-$A\beta_{1-40}$ (60 nM). The radioactivity in the brain eluted as a single peak on HPLC, with the same retention time as the $A\beta_{1-40}$ standard (data not shown). Aliquots of lyophilized sample were subjected to 10% Tris-tricine SDS-PAGE, transferred to a nitrocellulose membrane, and exposed to x-ray film. (**c**) Plasma TCA-precipitable (open bars) and non-TCA-precipitable ^{125}I radioactivity (filled bars) after intracerebral microinjections of ^{125}I-$A\beta_{1-40}$ (60 nM) into the caudate nucleus in mice, expressed as a percentage of total ^{125}I radioactivity in plasma; mean ± SD of three to five animals.

was also obtained in the presence of anti-α_2M Ab (20 μg/ml). In contrast, anti-LRP-2 Ab (Figure 4b) and anti-RAGE Ab (Figure 4c) did not affect Aβ clearance. Fucoidin, a specific ligand for SR-A, produced a modest increase in clearance, possibly by blocking the binding of Aβ to parenchymal SR-A receptors, thereby allowing more peptide to be available for clearance. At higher Aβ loads (Figure 4c), anti-LRP-1 Ab produced a 53% decrease in clearance, similar to that observed at a lower load (Figure 4b), but Aβ recovery approached that of [^{14}C]inulin, suggesting drainage of the peptide almost exclusively via ISF bulk flow. Clearance of [^{14}C]inulin was not affected by any of the studied molecular reagents. We also demonstrated that BCH, a

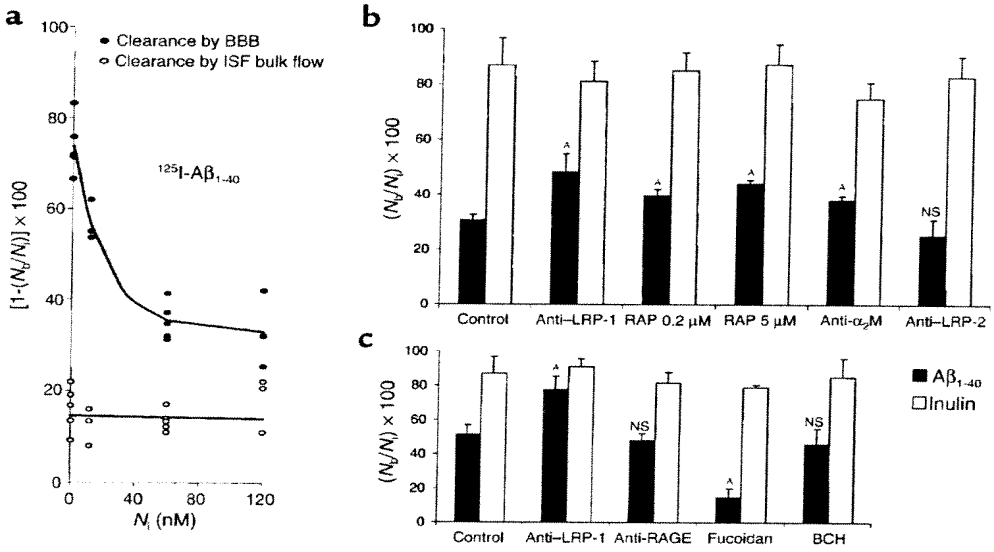

Figure 4

(**a**) Concentration-dependent clearance of $A\beta_{1-40}$ from mouse brain. Clearance via BBB transport (filled circles) is shown separately from clearance via ISF bulk flow (open circles). Clearance was determined 30 minutes after simultaneous microinjection of ^{125}I-$A\beta_{1-40}$ at increasing concentrations (0.05–120 nM) along with [^{14}C]inulin into the caudate nucleus. (**b**) Effects of anti-LRP-1 Ab R777 (60 μg/ml), RAP (0.2 and 5 μM), anti-α_2M Ab (20 μg/ml), and anti-LRP-2 Ab Rb6286 (60 μg/ml) on brain clearance of ^{125}I-$A\beta_{1-40}$ at 12 nM, determined 30 minutes after simultaneous microinjection of ^{125}I-$A\beta_{1-40}$ and [^{14}C]inulin. (**c**) Effects of anti-LRP-1 Ab R777 (60 μg/ml), anti-RAGE Ab (60 μg/ml), fucoidin (100 μg/ml), and 2-amino-bicyclo[2.2.1]heptane-2-carboxylic acid (BCH; 10 mM) on brain clearance of ^{125}I-$A\beta_{1-40}$ at a higher load of 60 nM, determined 30 minutes after simultaneous microinjection of ^{125}I-$A\beta_{1-40}$ and [^{14}C]inulin. Mean ± SD of three to four animals. $^AP < 0.05$; NS, not significant.

substrate that specifically blocks the L system for amino acids, does not affect clearance of Aβ across the BBB. This excludes the possibility that ^{125}I-Aβ_{1-40} is degraded to ^{125}I-tyrosine that is then transported out of the CNS instead of ^{125}I-Aβ_{1-40}.

Next, we studied the effect of apoE and aging by determining Aβ clearance in 2-month-old and 9-month-old apoE KO mice and wild-type mice, using two different loads of ^{125}I-Aβ_{1-40}, 12 nM (Figure 5a) and 60 nM (Figure 5b). Figure 5a shows that the clearance of Aβ was reduced by 30% in young apoE KO mice, and by about 55% and 40% in 9-month-old wild-type and apoE KO mice, respectively. These results were confirmed at a higher load of Aβ; the observed decrease in clearance was 46% in 9-month-old apoE KO mice (Figure 5b).

Immunocytochemical studies confirmed abundant expression of LRP-1 in brain microvessels (including capillaries, small venules, and arterioles) in 2-month-old mice (Figure 6a, upper panel; and Figure 6b, upper panel), in addition to significant parenchymal cellular (including neuronal) staining (Figure 6a, upper panel). As shown in the lower panels of Figures 6a and 6b, there was a significant reduction in LRP-1–positive vessels in 9-month-old mice compared with 2-month-old mice; the number of LRP-1–positive vessels dropped from 94% in 2-month-old mice to 52% in 9-month-old mice (Figure 6d, upper panel). Quantitative analysis of LRP-1–positive parenchymal cells (excluding blood vessels) showed a trend toward reduced staining in older animals, though the difference was not statistically significant (Figure 6d, lower panel). Similarly, there was no difference between young and old mice in the number of α_2M-positive microvessels or parenchymal cells in the brain (Figure 6c, upper and lower panels, respectively; Figure 6d, lower panel). It is noteworthy that staining for α_2M was not able to distinguish between circulating α_2M and α_2M expressed on microvessels.

Frontal cortex of all AD patients revealed moderate to marked neuritic plaques and Aβ deposits; two of the three showed parenchymal and vascular amyloid. Controls revealed no neuritic plaques or Aβ in the parenchyma, and only meningeal vascular Aβ in one of the three patients. As seen in Figure 7a, staining for LRP-1 in the frontal cortex of control patients revealed moderate vascular staining in capillaries and arterioles, as well as neuronal staining. There was reduced LRP-1 staining in AD tissues, including regions with Aβ_{1-40}-positive or Aβ_{1-42}-positive plaques and vessels (Figure 7b). However, the immediate subcortical white matter showed more robust vascular staining for LRP-1, and absence of staining for Aβ, in both AD patients and controls (not shown). Anti-CD105, which identifies vascular endothelium, revealed ample staining of capillaries and arterioles of frontal cortex in controls, and moderately reduced numbers of stained vessels in AD tissues. Cerebellum revealed equivalent vascular staining with anti–LRP-1 and anti-CD105 in AD and control sections (not shown). No anti-Aβ_{1-40}–positive or Aβ_{1-42}–positive staining was seen in either AD or control tissues.

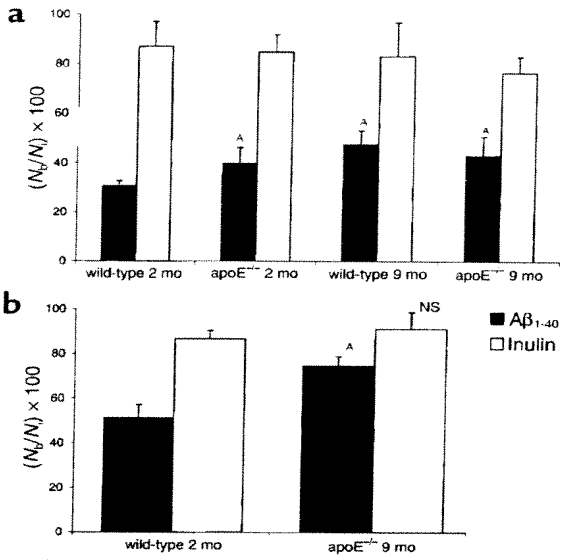

Figure 5

(**a**) Effect of apoE genotype and age on brain clearance of ^{125}I-Aβ_{1-40}. Brain clearance of ^{125}I-Aβ_{1-40} in 2-month-old and 9-month-old wild-type mice and apoE KO mice studied at the lower load of 12 nM ^{125}I-Aβ_{1-40} (**a**) and a higher load of 60 nM (**b**). In all studies, ^{125}I-Aβ_{1-40} and [^{14}C]inulin were injected simultaneously, and clearance was determined after 30 minutes. Mean ± SD of three to four animals. $^{A}P < 0.05$; NS, not significant compared with 2-month-old wild-type mice.

Discussion

This study demonstrates the importance of vascular transport across the BBB in clearing Aβ from the brain into the circulation. Moreover, we provide evidence that this transport mechanism is mediated mainly via LRP-1 in brain microvascular endothelium, and suggest that transport of brain-derived Aβ out of the CNS may be influenced by the LRP-1 ligands α_2M and apoE. This vascular clearance mechanism for Aβ is age dependent, and lower clearance rates in older animals correlate with decreased vascular abundance of LRP-1.

The capability of BBB to remove Aβ was significant in younger animals. The elimination time, $t_{1/2}$, for Aβ_{1-40} at 60 nM was 25 minutes, or 9.4-fold faster than for inulin, an ECF marker used to determine the ISF bulk flow rate (40). The major component of the CNS efflux of Aβ was transport across the BBB into the vascular system. The clearance of Aβ across the BBB was dependent on both time and concentration. At very low concentrations, i.e., less than 2 nM as found normally in mouse brain (54–55), Aβ_{1-40} was eliminated from brain at a rate that was on average 3.5-fold faster than when it was present at a load of 60 nM. This may be comparable to concentrations of Aβ_{1-40} found in the brains of transgenic APP animals at 3–4 months of age (54–55). The efflux transport system was half saturated at 15.3 nM of Aβ_{1-40}, and appears to be fully saturated at concentrations between 70 nM and 100 nM.

Thus, this efflux transporter may be completely saturated by higher levels of Aβ, as are found in the brains of older transgenic APP animals (54–55), which in turn may lead to vascular accumulation of Aβ and development of prominent deposits of cerebrovascular amyloid, as recently described (56–57).

In this study, we did not observe significant metabolism or degradation of $A\beta_{1-40}$ within 5 hours, in contrast to a recent report suggesting that $A\beta_{1-42}$ is degraded by enkephalinase (neprilysin) in the brain within minutes (28). It may be that $A\beta_{1-40}$ and $A\beta_{1-42}$ are processed differently in the brain. However, the physiological relevance of the proposed degradation mechanism for $A\beta_{1-42}$ (28) remains unclear, because the peptide was studied at extremely high concentrations (~240 μM) that are not found even in brains with severe β-amyloidosis (30). As shown by pharmacological studies, these high concentrations of Aβ may impair local BBB integrity (58–59), which in turn may contaminate brain ISF with blood and/or plasma that possesses Aβ-degrading activity (48), as confirmed in this study.

Consistent with the hypothesis that cytosolic peptidases have little access to Aβ peptides secreted or injected into brain ISF (28) or CSF (29), it has been reported recently that insulin-degrading enzyme (IDE) cannot not degrade Aβ in the brain in vivo after intracerebral injection of radiolabeled peptide (28). This is in contrast to in vitro degradation of ^{125}I-$A\beta_{1-40}$ by IDE from brain and liver cytosol fractions (60). Because IDE is an intracellular protease, it is not surprising that IDE may not be able to process Aβ from brain ISF, particularly if peptide clearance is faster than its cellular uptake, as suggested by our data and a previous study (28). It is noteworthy that brain endothelial cells in vitro (33) and astrocytes (61) do not catabolize Aβ, in contrast to activated microglial cells that secrete a specific metalloproteinase that degrades Aβ in vitro (61). Neuronal cells in vitro metabolize Aβ via an LRP-1–dependent mechanism that may require apoE or α_2M (38). The rate of this degradation, however, is about 50- to 100-fold slower than that occurring via transport across the BBB in vivo.

Transport of Aβ out of the CSF was not associated with significant degradation of peptide in the CSF (29). Lower levels of $A\beta_{1-40}$ than inulin in the CSF may suggest active transport of Aβ from the CSF to the blood, possibly across the choroid plexus or leptomeningeal vessels, as shown previously (29). Higher levels of radiolabeled Aβ in the plasma relative to inulin confirm vascular transport of the peptide out of the CNS. Although our results indicate that brain-derived Aβ could contribute to the pool of circulating peptide, its degradation in plasma, systemic metabolism, and body clearance tend to reduce the levels of circulating peptide, as shown previously (48). Under our experimental con-

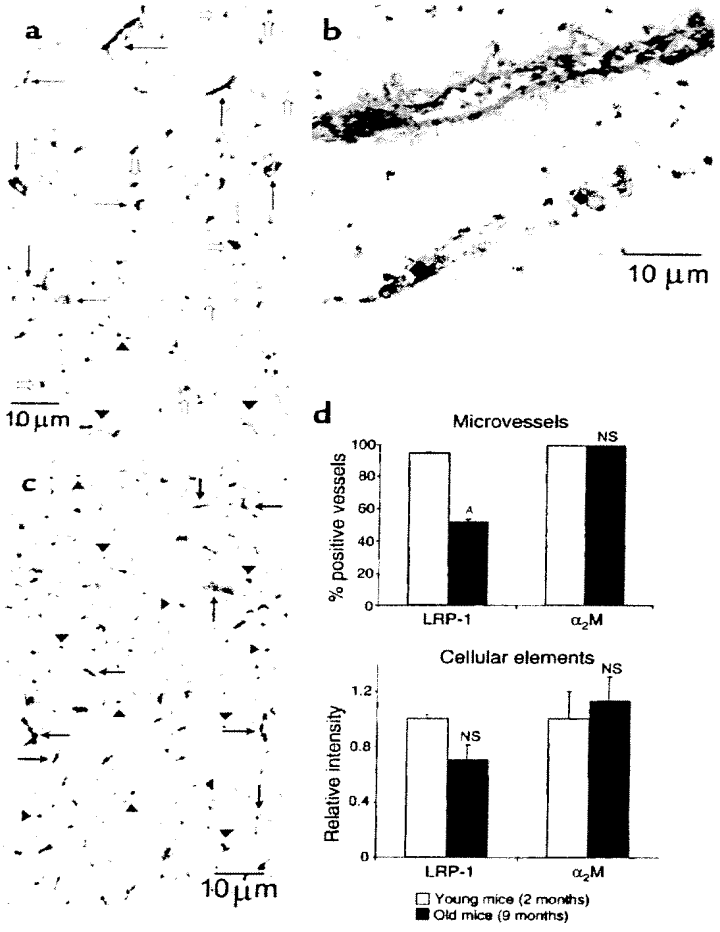

Figure 6

(**a**) LRP-1 immunoreactivity in brain microvessels of young (2-month-old; upper panel) and old (9-month-old; lower panel) wild-type mice. Many vessels in young mice stained positive for LRP-1, detected with anti–LRP-1 Ab R777 (5 μg/ml; arrows). There were relatively fewer positive vessels in old mice (arrows), and many weakly positive- or negative-staining vessels (arrowheads). There was no significant difference in the staining of parenchymal cellular elements (open arrows) between the young and old mice. Vessels in young mice stained strongly positive (**b**, upper panel) compared with the faint staining seen in old mice (**b**, lower panel). In contrast, there was no difference in staining for α_2M in brain cells (arrowheads) or microvessels (arrows) between young (**c**, upper panel) and old (**c**, lower panel) mice. (**d**) Comparison of LRP-1 and α_2M immunoreactivity in brain microvessels (upper panel) and parenchymal cellular elements (lower panel) in young and old wild-type mice. $^AP < 0.05$; NS, not significant.

Figure 7
LRP-1 expression in human frontal cortex. Brain sections (Brodmann's area 10) of controls (**a** and **c**) reveal well-defined staining of capillaries (arrowheads) and arterioles (arrows) by LRP-1, detected with anti-LRP-1 mAb 8G1 (5 μg/ml) (**a**) and CD105 (**c**). No Aβ staining was present in double-labeled or serially labeled sections (not shown). In contrast, double-labeled sections from AD patients show vessels and plaque cores stained positive with anti-$A\beta_{1-40}$ (brown stain), reduced numbers and intensity of LRP-1 staining of vessels (**b**), and reduced numbers of CD105-labeled vessels (**d**).

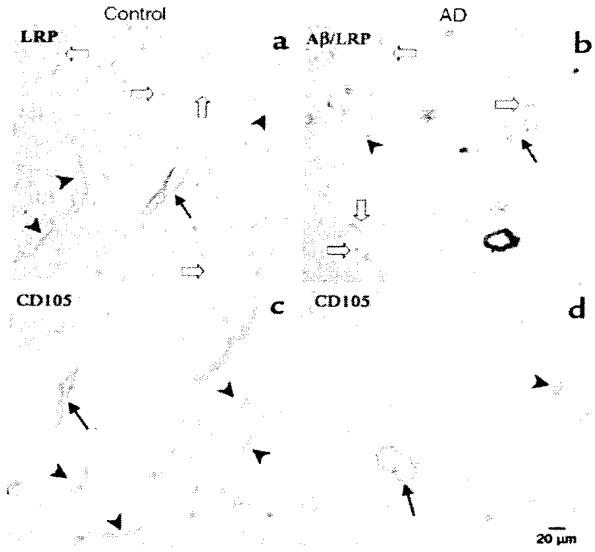

ditions, the levels of radiolabeled Aβ in the circulation were two to three orders of magnitude lower than the brain levels. This makes re-entry of radiolabeled Aβ into the brain very unlikely, because the blood-to-brain transport of Aβ normally operates down the concentration gradient (39, 62–65). In addition, the apoJ system that transports blood-borne Aβ into the brain is saturated under the physiological conditions (64) that may facilitate the efflux of Aβ from the brain. Previous studies have shown that circulating free Aβ is also metabolized during its transport across the BBB (48, 49, 65, 66), possibly by pericytes, which represent a major enzymatic barrier for the transport of several peptides and proteins across the BBB (67).

The affinity of neprilysin for its physiological substrates (e.g., enkephalins, tachykinins, atrial natriuretic peptide) and/or different synthetic peptides is in the low millimolar range (68). In contrast, the levels of Aβ in the brain are normally in the low nanomolar range, and in transgenic mouse models of brain amyloidosis they vary from 40 nM to 250 nM/kg from 3 to 12 months of age (54). Thus, under physiological and/or pathological conditions, Aβ will likely bind to its high-affinity cell-surface receptors (such as RAGE and/or SR-A), and/or high-affinity transport binding proteins (α_2M, apoE, and apoJ), which all react with low nanomolar levels of peptide corresponding to their K_D values.

In this study, anti–LRP-1 antibodies inhibited $A\beta_{1-40}$ clearance by about 55%, both at lower (12 nM) and higher loads (60 nM) of the peptide, suggesting the involvement of LRP-1 in vascular elimination of Aβ from the brain. RAP, a chaperone protein that facilitates proper folding and subsequent trafficking of LRP-1 and LRP-2 (69), also inhibited Aβ clearance. RAP binds to multiple sites on LRP and antagonizes binding of all known LRP ligands to both LRP-1 and LRP-2 in vitro (69), as well as to LRP-2 in vivo at the blood side of the BBB (39). In this study, RAP at higher concentrations produced inhibition of Aβ clearance comparable to that produced by an anti–LRP-1 Ab. It is interesting that anti–LRP-1 Ab inhibited vascular transport of Aβ almost completely at higher concentrations of peptide, which may indicate that LRP-1 could be of primary importance in eliminating the peptide from the brain. At a lower load of the peptide (i.e., 12 nM), neither of the molecular reagents was able to abolish clearance of Aβ, which suggests that in addition to LRP-1, there may be an alternative, highly sensitive BBB transport mechanism (or mechanisms) that eliminates the peptide from the brain at very low concentrations. The molecular nature of this putative second transport system is not presently known, although data from this study suggest that RAGE and LRP-2 are unlikely to be involved in rapid elimination of Aβ from brain. The fact that fucoidin, an SR-A ligand, moderately increased clearance of Aβ suggests that inhibition of SR-A receptors in the brain may decrease CNS sequestration of the peptide, thus allowing more peptide to be available for enhanced clearance across the BBB.

A role for LRP-1 in promoting Aβ clearance in vitro in smooth muscle cells, neurons, and fibroblasts via α_2M and apoE has been suggested (35–38), although at significantly slower rates than the Aβ transport across the BBB demonstrated in this study. High-affinity in vitro binding of Aβ to α_2M and to lipidated apoE3 and apoE4, and a lower-affinity binding to delipidated apoE isoforms has been well documented (23, 70). Binding/uptake studies in mouse embryonic fibroblasts (wild type and deficient in LRP-1), confirmed that free Aβ is not a ligand for LRP-1 (37, 45). The possible role of the two LRP-1 ligands in elimination of Aβ via vascular transport is suggested by inhibition of Aβ clearance with anti-α_2M antibodies and by significantly reduced clearance in apoE KO animals (by 30% and 46% at 2 months and 9 months of age, respectively, compared with young wild-type controls). In relation to these findings, it is interesting to note that recent studies have indicated that lack of endogenous mouse apoE in both the APP^{V717F} and APPsw mouse models of AD results in less Aβ deposition and no fibrillar Aβ deposits in the brain (57, 71). This suggests that mouse apoE strongly facilitates Aβ fibrillogenesis. It is possible that mouse apoE also plays a role in clearance of

soluble Aβ across the BBB, as suggested by the current study, but that its ability to influence Aβ aggregation in APP transgenic mice is dominant. In contrast to the effects of mouse apoE, a recent study demonstrates that human apoE isoforms suppress early Aβ deposition in APP^{V717F} mice (72). Further studies in this model will be useful to determine whether this suppressive effect of human apoE isoforms on early Aβ deposition is secondary to effects on facilitating Aβ transport across the BBB. Although our study does not rule out the possibility that Aβ clearance by neurons, vascular smooth muscle cells, and fibroblasts shown in vitro (35–38) may also occur in vivo, vascular transport across the BBB seems to be of primary importance for rapid elimination of Aβ from brain in vivo.

Because normal aging is associated with Aβ accumulation in the brain (1), and there is a significant, time-dependent, and progressive accumulation of the peptide with age in transgenic APP animals (54, 55), we postulated that Aβ clearance mechanisms might be impaired in older animals, and are also possibly impaired in elderly humans. Our findings of about 55–65% inhibition of Aβ clearance in 9-month-old wild-type animals compared with young (2-month-old) animals confirmed this hypothesis. Immunocytochemical studies indicated a significant reduction in the number of LRP-1–positive cerebral blood vessels, from 94% in 2-month-old mice to 52% in 9-month-old mice, which correlated well with the observed reductions in the clearance capacities in the two age groups. Interestingly, downregulation of vascular LRP-1 correlated well with regional parenchymal and vascular accumulation of Aβ in brains of Alzheimer's patients compared with age-matched controls. In brain areas where LRP-1 vascular expression remains prominent, such as in the white matter, no accumulation of Aβ was found in Alzheimer's brains.

In conclusion, our data support the concept that the vascular system plays an important role in regulating the levels of Aβ in the brain. Our findings further suggest that if the levels of Aβ in brain extracellular space exceed the transport capacity of the clearance mechanism across the BBB, or if the vascular transport of the peptide were impaired, for example by downregulation of LRP-1, this would result in accumulation of Aβ in the brain, and possibly formation of amyloid plaques. Previous studies from our laboratory and others have demonstrated a major role of the BBB in determining the concentrations of Aβ in the CNS by regulating transport of circulating Aβ (33, 39, 49–51, 62–66). This study extends this hypothesis by showing that vascular transport out of the brain across the BBB may represent a major physiological mechanism that prevents accumulation of Aβ and amyloid deposition in the brain.

Acknowledgments

This work was supported in part by NIH grants AG-16223 and NS-33466 (to B.V. Zlokovic), AG-05891 (to B. Frangione), AG-05142 (to C. Finch and C.A. Miller), AG-13956 (to D.M. Holtzman), NS-38777 (to J. Ghiso), and HL-50784 (to D.K. Strickland). We acknowledge the excellent technical assistance of Celia Williams.

1. Wisniewski, T., Ghiso, J., and Frangione, B. 1997. Biology of Aβ amyloid in Alzheimer's disease. *Neurobiol. Dis.* **4**:311–328.
2. Selkoe, D.J. 1997. Alzheimer's disease: genotype, phenotype, and treatments. *Science.* **275**:630–631.
3. Selkoe, D.J. 1998. The cell biology of β-amyloid precursor protein and presenilin in Alzheimer's disease. *Trends Cell Biol.* **8**:447–453.
4. Younkin, S.G. 1998. The role of Aβ42 in Alzheimer's disease. *J. Physiol. (Paris).* **92**:289–292.
5. Roses, A.D. 1998. Alzheimer disease: a model of gene mutations and susceptibility polymorphisms for complex psychiatric diseases. *Am. J. Med. Genet.* **81**:49–57.
6. Hardy, J., Duff, K., Hardy, K.G., Perez-Tur, J., and Hutton, M. 1998. Genetic dissection of Alzheimer's disease and related dementias: amyloid and its relationship to tau. *Nat. Neurosci.* **1**:355–358.
7. Masters, C.L., et al. 1985. Amyloid plaque core protein in Alzheimer disease and Down syndrome. *Proc. Natl. Acad. Sci. USA.* **82**:4245–4249.
8. Prelli, F., Castano, E.M., Glenner, G.G., and Frangione, B. 1988. Differences between vascular and plaque core amyloid in Alzheimer's disease. *J. Neurochem.* **51**:648–651.
9. Roher, A.E., et al. 1993. β-amyloid (1–42) is a major component of cerebrovascular amyloid deposits: implications for the pathology of Alzheimer disease. *Proc. Natl. Acad. Sci. USA.* **90**:10836–10840.
10. Shinkai, Y., et al. 1995. Amyloid β-proteins 1-40 and 1-42(43) in the soluble fraction of extra- and intracranial blood vessels. *Ann. Neurol.* **38**:421–428.
11. Castaño, E.M., et al. 1996. The length of amyloid-β in hereditary cerebral hemorrhage with amyloidosis, Dutch type. Implications for the role of amyloid-β 1-42 in Alzheimer's disease. *J. Biol. Chem.* **271**:32185–32191.
12. Seubert, P., et al. 1992. Isolation and quantification of soluble Alzheimer's amyloid-β peptide from biological fluids. *Nature.* **359**:325–327.
13. Shoji, M., et al. 1996. Production of the Alzheimer amyloid-β protein by normal proteolytic processing. *Science.* **258**:126–129.
14. Vigo-Pelfrey, C., Lee, D., Keim, P., Lieberburg, I., and Schenk, D.B. 1993. Characterization of β-amyloid peptide from human cerebrospinal fluid. *J. Neurochem.* **61**:965–968.
15. Tabaton, M., et al. 1994. Soluble amyloid β-protein is a marker of Alzheimer amyloid in brain but not in cerebrospinal fluid. *Biochem. Biophys. Res. Commun.* **200**:1598–1603.
16. Kuo, Y.M., et al. 1996. Water-soluble Aβ (N-40, N-42) oligomers in normal and Alzheimer disease brains. *J. Biol. Chem.* **271**:4077–4081.
17. Ghiso, J., et al. 1993. The cerebrospinal-fluid soluble form of Alzheimer's amyloid-β is complexed to SP-40, 40 (apolipoprotein J), and inhibitor of the complement membrane-attack complex. *Biochem. J.* **293**:27–30.
18. Matsubara, E., Frangione, B., and Ghiso, J. 1995. Characterization of apolipoprotein J-Alzheimer's Aβ interaction. *J. Biol. Chem.* **270**:7563–7567.
19. Yang, D.S., Smith, J.D., Zhou, Z., Gandy, S.E., and Martins, R.N. 1997. Characterization of the binding of amyloid-β peptide to cell culture-derived native apolipoprotein E2, E3, and E4 isoforms and to isoforms from human plasma. *J. Neurochem.* **68**:721–725.
20. Schwarzman, A.L., et al. 1994. Transthyretin sequesters amyloid β-protein and prevents amyloid formation. *Proc. Natl. Acad. Sci. USA.* **91**:8368–8372.
21. Matsubara, E., et al. 1999. Lipoprotein-free amyloidogenic peptides in plasma are elevated in patients with sporadic Alzheimer's disease and Down's syndrome. *Ann. Neurol.* **45**:537–541.
22. Biere, A.L., et al. 1996. Amyloid β-peptide is transported on lipoproteins and albumin in human plasma. *J. Biol. Chem.* **271**:32916–32922.
23. Du, Y., et al. 1997. β2-Macroglobulin as a β-amyloid peptide-binding plasma protein. *J. Neurochem.* **69**:299–305.
24. Busciglio, J., Gabuzda, D.H., Matsudaira, P., and Yanker, B.A. 1993. Generation of β-amyloid in the secretory pathway in neuronal and non-neuronal cells. *Proc. Natl. Acad. Sci. USA.* **90**:2092–2096.
25. Naslund, J., et al. 1994. Relative abundance of Alzheimer Aβ amyloid peptide variants in Alzheimer disease and normal aging. *Proc. Natl. Acad. Sci. USA.* **91**:8378–8382.
26. Teller, J.K., et al. 1996. Presence of soluble amyloid β-peptide precedes amyloid plaque formation in Down's syndrome. *Nat. Med.* **2**:93–95.
27. Suzuki, N., et al. 1994. High tissue content of soluble amyloid-β 1-40 is linked to cerebral amyloid angiopathy. *Am. J. Pathol.* **145**:452–460.
28. Iwata, N., et al. 2000. Identification of the major $Aβ_{1-42}$-degrading catabolic pathway in brain parenchyma: suppression leads to biochemical and pathological deposition. *Nat. Med.* **6**:143–150.

29. Ghersi-Egea, J.F., et al. 1996. Fate of cerebrospinal fluid-borne amyloid β-peptide: rapid clearance into blood and appreciable accumulation by cerebral arteries. *J. Neurochem.* **67**:880–883.
30. Zlokovic, B.V., Yamada, S., Holtzman, D., Ghiso, J., and Frangione, B. 2000. Clearance of amyloid β-peptide from brain: transport or metabolism? *Nat. Med.* **6**:718–719.
31. Rosenberg, R.N. 2000. The molecular and genetic basis of AD: the end of the beginning. *Neurology.* **54**:2045–2054.
32. Yan, S.D., et al. 1996. RAGE and amyloid-β peptide neurotoxicity in Alzheimer's disease. *Nature.* **382**:685–691.
33. Mackic, J.B., et al. 1998. Human blood-brain barrier receptors for Alzheimer's amyloid-β_{1-40}: asymmetrical binding, endocytosis and transcytosis at the apical side of brain microvascular endothelial cell monolayer. *J. Clin. Invest.* **102**:734–743.
34. Paresce, D.M., Ghosh, R.N., and Maxfield, F.R. 1996. Microglial cells internalize aggregates of the Alzheimer's disease amyloid β-protein via a scavenger receptor. *Neuron.* **17**:553–565.
35. Urmoneit, B., et al. 1997. Cerebrovascular smooth muscle cells internalize Alzheimer amyloid β-protein via a lipoprotein pathway: implications for cerebral amyloid angiopathy. *Lab. Invest.* **77**:157–166.
36. Jordan, J., et al. 1998. Isoform-specific effect of apolipoprotein E on cell survival and β-amyloid-induced toxicity in rat hippocampal pyramidal neuronal cultures. *J. Neurosci.* **18**:195–204.
37. Narita, M., Holtzman, D.M., Schwartz, A.L., and Bu, G. 1997. α_2-macroglobulin complexes with and mediates the endocytosis of β-amyloid peptide via cell surface low-density lipoprotein receptor-related protein. *J. Neurochem.* **69**:1904–1911.
38. Qiu, Z., Strickland, D.K., Hyman, B.T., and Rebeck, G.W. 1999. α_2-macroglobulin enhances the clearance of endogenous soluble β-amyloid peptide via low-density lipoprotein receptor-related protein in cortical neurons. *J. Neurochem.* **73**:1393–1398.
39. Zlokovic, B.V., et al. 1996. Glycoprotein 330/megalin: probable role in receptor-mediated transport of apolipoprotein J alone and in a complex with Alzheimer's disease amyloid β at the blood-brain and blood-cerebrospinal fluid barriers. *Proc. Natl. Acad. Sci. USA.* **93**:4229–4236.
40. Yamada, S., dePasquale, M., Patlak, C.S., and Cserr, H.F. 1991. Albumin outflow into deep cervical lymph from different regions of rabbit brain. *Am. J. Physiol.* **261**:H1197–H1204.
41. Strittmater, W., and Roses, A. 1996. Apolipoprotein E and Alzheimer's disease. *Annu. Rev. Neurosci.* **19**:53–77.
42. Blacker, D., et al. 1998. α2-macroglobulin is genetically associated with Alzheimer's disease. *Nat. Gen.* **19**:357–360.
43. Zlokovic, B.V., Davson, H., Preston, J.E., and Segal, M.B. 1987. Effects of aluminum on cerebrospinal fluid secretion. *Exp. Neurol.* **98**:436–452.
44. Kounnas, M.Z., et al. 1992. The α_2-macroglobulin receptor/low density lipoprotein receptor-related protein binds and internalizes *Pseudomonas* exotoxin A. *J. Biol. Chem.* **267**:12420–12423.
45. Kounnas, M.Z., et al. 1995. LDL receptor-related protein, a multifunctional ApoE receptor, binds secreted β-amyloid precursor protein an mediates its degradation. *Cell.* **82**:331–340.
46. Mikhailenko, I., Kounnas, M.Z., and Strickland, D.K. 1995. Low density lipoprotein receptor-related protein/α 2-macroglobulin receptor mediates the cellular internalization and degradation of thrombospondin. A process facilitated by cell-surface proteoglycans. *J. Biol. Chem.* **270**:9543–9549.
47. Kounnas, M.Z., Haudenschild, C.C., Strickland, D.K., and Argraves, W.S. 1994. Immunological localization of glycoprotein 330, low density lipoprotein receptor related protein and 39 kDa receptor associated protein in embryonic mouse tissues. *In Vivo.* **8**:343–351.
48. Mackic, J.B., et al. 1998. Cerebrovascular accumulation and increased blood-brain barrier permeability to circulating Alzheimer's amyloid β-peptide in aged squirrel monkey with cerebral amyloid angiopathy. *J. Neurochem.* **70**:210–215.
49. Maness, L.M., Banks, W.A., Podlisny, M.B., Selkoe, D.J., and Kastin, A.J. 1994. Passage of human amyloid-β protein 1-40 across the murine blood-brain barrier. *Life Sci.* **55**:1643–1650.
50. Poduslo, J.F., Curran, G.L., Haggard, J.J., Biere, A.L., and Selkoe, D.J. 1997. Permeability and residual plasma volume of human, Dutch variant, and rat amyloid β-protein 1-40 at the blood-brain barrier. *Neurobiol. Dis.* **4**:27–34.
51. Martel, C.L., et al. 1997. Isoform-specific effects of apolipoproteins E2, E3, E4 on cerebral capillary sequestration and blood brain barrier transport of circulating Alzheimer's amyloid β. *J. Neurochem.* **69**:1995–2004.
52. Hyman, B.T., and Trojanowski, J.Q. 1997. Consensus recommendations for the postmortem diagnosis of Alzheimer disease from the National Institute on Aging and the Reagan Institute Working Group on diagnostic criteria for the neuropathological assessment of Alzheimer disease. *J. Neuropathol. Exp. Neurol.* **56**:1095–1097.
53. Strickland, D.K., et al. 1990. Sequence identity between the α_2-macroglobulin receptor and low density lipoprotein receptor-related protein suggests that this molecule is a multifunctional receptor. *J. Biol. Chem.* **265**:17401–17404.
54. Hsiao, K., et al. 1996. Correlative memory deficits, Aβ elevation, and amyloid plaques in transgenic mice. *Science.* **274**:99–102.
55. Holcomb, L., et al. 1998. Accelerated Alzheimer-type phenotype in transgenic mice carrying both mutant amyloid precursor protein and presenilin 1 transgenes. *Nat. Med.* **4**:97–100.
56. Calhoun, M.E., et al. 1999. Neuronal overexpression of mutant amyloid precursor protein results in prominent deposition of cerebrovascular amyloid. *Proc. Natl. Acad. Sci. USA.* **96**:14088–14093.
57. Holtzman, D.M., et al. 2000. ApoE facilitates neuritic and cerebrovascular plaque formation in the APPsw mouse model of Alzheimer's disease. *Ann. Neurol.* **47**:739–747.
58. Blanc, E.M., Toborek, M., Mark, R.J., Hennig, B., and Mattson, M.P. 1997. Amyloid β-peptide induces cell monolayer albumin permeability, impairs glucose transport, and induces apoptosis in vascular endothelial cells. *J. Neurochem.* **68**:1870–1881.
59. Thomas, T., Thomas, G., McLendon, C., Sutton, T., and Mullan, M. 1996. β-amyloid mediated vasoactivity and vascular endothelial damage. *Nature.* **380**:168–171.
60. Kurochkin, I.V., and Goto, S. 1994. Alzheimer's β-amyloid peptide specifically interacts with and is degraded by insulin degrading enzyme. *FEBS Lett.* **345**:33–37.
61. Mentlein, R., Ludwig, R., and Martensen, I. 1998. Proteolytic degradation of Alzheimer's disease amyloid β-peptide by a metalloproteinase from microglia cells. *J. Neurochem.* **70**:721–726.
62. Zlokovic, B.V., et al. 1993. Blood-brain barrier transport of circulating Alzheimer's amyloid-β. *Biochem. Biophys. Res. Commun.* **197**:1034–1040.
63. Ghilardi, J.R., et al. 1996. Intra-arterial infusion of [^{125}I]$A\beta_{1-40}$ labels amyloid deposits in the aged primate brain in vivo. *Neuroreport.* **7**:2607–2611.
64. Shayo, M., McLay, R.N., Kastin, A.J., and Banks, W.A. 1997. The putative blood-brain barrier transporter for the β-amyloid binding protein apolipoprotein J is saturated at physiological concentrations. *Life Sci.* **60**:L115–L118.
65. Martel, C.L., Mackic, J.B., McComb, J.G., Ghiso, J., and Zlokovic, B.V. 1996. Blood-brain barrier uptake of the 40 and 42 amino acid sequences of circulating Alzheimer's amyloid-β in guinea pigs. *Neurosci. Lett.* **206**:157–160.
66. Saito, Y., Buciak, J., Yang, J., and Pardridge, W.M. 1995. Vector-mediated delivery of ^{125}I-labeled β-amyloid peptide Aβ 1-40 through the blood-brain barrier and binding to Alzheimer's disease amyloid to the $A\beta_{1-40}$ vector complex. *Proc. Natl. Acad. Sci. USA.* **92**:10227–10231.
67. Krause, D., Kunz, J., and Dermietzel, R. 1993. Cerebral pericytes: a second line of defense in controlling blood-brain barrier peptide metabolism. *Adv. Exp. Med. Biol.* **331**:149–152.
68. Hersh, L.B., and Morihara, K. 1986. Comparison of subsite specificity of the mammalian neutral endopeptidase 24.11 (enkephalinase) to the bacterial neutral endopeptidase thermolysin. *J. Biol. Chem.* **261**:6433–6437.
69. Bu, G., and Rennke, S. 1996. Receptor-associated protein is a folding chaperone for low-density lipoprotein receptor-related protein. *J. Biol. Chem.* **271**:22218–22224.
70. Tokuda, T., et al. 2000. Lipidation of apolipoprotein E influences its isoform-specific interaction with Alzheimer's amyloid β-peptides. *Biochem. J.* **348**:359–365.
71. Bales, K.R., et al. 1999. Apolipoprotein E is essential for amyloid deposition in the APP(V717F) transgenic mouse model of Alzheimer's disease. *Proc. Natl. Acad. Sci. USA.* **96**:15233–15238.
72. Holtzman, D.M., et al. 1999. In vivo expression of apolipoprotein E reduces amyloid β deposition in a mouse model of Alzheimer's disease. *J. Clin. Invest.* **103**:R15–R21.